DESIGN CONSIDERATION AND STEADY STATE STUDY OF THRUST BEARINGS IN HIGH SPEED SUBSONIC APPLICATIONS.

by

ARVIND PRABHAKAR

Presented to the Faculty of the Graduate School of

The University of Texas at Arlington in Partial Fulfillment

of the Requirements

for the Degree of

MASTER OF SCIENCE IN MECHANICAL ENGINEERING

THE UNIVERSITY OF TEXAS AT ARLINGTON

MAY 2016

ACKNOWLEDGEMENTS

I would like to thank my advisor Dr. Daejong Kim for his able guidance, support and constant encouragement throughout the course of this research. Dr. Kim's passion and dedication have been extremely inspirational and his vision has motivated me while working at the Turbomachinery and Energy Systems Laboratory. I would also like to thank Dr. Brian Dennis and Dr. Rajeev Kumar for many valuable suggestions.

I would also like to express my gratitude to Dr. Hyejin Moon and Dr. Ankur Jain for kindly accepting to be members of the supervising committee.

I am greatly indebted to my colleagues at Turbomachinery and Energy Systems Laboratory, for all their support and guidance.

Last but not least, I would like to specially thank my parents and my brother for their support, patience and continuous encouragement during my studies.

April 25, 2016

ABSTRACT

DESIGN CONSIDERATION AND STEADY STATE STUDY OF THRUST BEARINGS IN HIGH SPEED SUBSONIC APPLICATIONS.

ARVIND PRABHAKAR, M.S.

The University of Texas at Arlington, 2016

Supervising Professor: Daejong Kim

Thrust bearings are required to perform at high speeds in various turbomachinery applications causing the nature of fluid flow within the bearings to be in high subsonic as well as supersonic regimes. The motivation of this research is to develop a bearing performance prediction model tailored for high subsonic speeds and large Reynolds numbers.

The prime fluid characteristics studied in the thin film for predicting the bearing performance has been achieved by carefully considering inertial, viscous as well as compressible effects within the thin film fluid flow.

Fluid inertia is a vital physical phenomenon that plays an important role in prediction of thrust bearing performance at high speeds. Conventional lubrication modelling of fluid flow by Reynolds equation for high speed applications has limitations due to the assumption of non-inertial nature of flow. Hence, the investigation of high speed performance of thrust bearing requires computational fluid dynamics (CFD) modelling of three dimensional (3D) thin film Navier-Stokes equations.

For the purpose of this research thesis an in house computational solver has been developed that solves three dimensional thin film Navier-Stokes equations to investigate

effects of fluid inertia, viscosity and compressibility on performance of thrust bearings in high speed isothermal flow conditions.

The geometrical structure of thin film studied is essentially a 3D fluid volume formed by two rigid sliding surfaces consisting of an inlet region converging with a constant slope and an exit region of constant gap.

A density based segregated solver is adopted to solve the Momentum and continuity Navier-Stokes equations. The comparison of results from the solutions of 3D thin film Navier-Stokes equations with Reynolds equation show that there is a substantial difference between prediction of bearing performance as Reynolds number increases and inertial effects become predominant.

TABLE OF CONTENTS

LIST OF ILLUSTRATIONS

LIST OF TABLES

Chapter 1

INTRODUCTION

1.1 Background

Foil Thrust bearing is a vital component of oil free turbomachinery. The potential of thrust bearings has been realised in the past few years for applications in high speed turbomachinery on account of the fact that foil thrust bearings are self-acting hydrodynamic bearings making use of air as a working fluid [1]. They are of increasing interest in turbomachinery and other applications from many points of view. Gas lubricants have a much wider temperature range than oils (both lower and higher), better cleanliness, and are better for the environment [2]

Implementation of gas foil bearing (GFB) technology into turboshaft engines of rotorcraft propulsion systems gives oil-free compact units with extended maintenance intervals and increased life [3]

The air film develops as a result of viscous air flow driven by the moving surface (the shaft for journal bearings, the thrust runner for thrust bearings). [1]

Air-lubricated foil bearings with compliant bearing surface have been used for decades in small gas turbines [4] and air handling turbomachinery [5], where the rotor weight is much smaller than load capacity of the foil bearings. [6]

As demand for load carrying capacity of thrust bearing has increased over the years the design considerations for thrust bearings which were initially designed for low to medium speed applications are also required to be reconsidered if they are to be successfully designed for high speed applications.

Reynolds equation has been widely used in modelling lubrication flow and performance of thrust bearings for a number of years However, The underlying assumption of negligible fluid inertia is not reasonable to make as the regime of fluid flow within thrust

bearings becomes substantially high. While Reynolds equation models lubrication for a good estimation of bearing performance its inability to predict performance of thrust bearing in high speed applications is a major drawback. This can be overcome by solving thin film Navier-Stokes equations.

Florence Dupuy and Benyebka Bou-Saïd [7] investigated the effects of fluid inertia on bearing performance of a one dimensional bearing in both subsonic and supersonic flow regimes. The authors point out the performance prediction of a thrust bearing by comparing results from modified Reynolds equation and thin Film Naiver-Stokes equations.

This thesis comprises of investigation of effects of inertia on performance of a 3 dimensional bearing by solving the 3 dimensional thin film Navier-Stokes equations for laminar, compressible, viscous flow and comparing the results with those of compressible Reynolds equation. Comparison of simulated results are made for a thin film at varying Reynolds numbers, varying clearances to film length ratios. Ng and Pan [8] have developed a linearized turbulent lubrication theory for modelling high speed turbulent flows accurately however, for low clearances to Film length ratios and subsonic speeds the flow Reynolds number is not substantially high to observe turbulent behaviour in thin films hence, Laminar flow modelling was selected for the purpose of this thesis.

1.1.1 Hydrodynamic Thin Film Lubrication

Hydrodynamic thin film lubrication is a hydrodynamic phenomenon where a lubricant flows in between the narrow gap of two closely spaced surfaces. One surface is usually fixed while the other surface moves relative to the fixed one. The pressure generation i.e. the load carrying capacity comes from the nature of shape of the two surfaces. The surfaces usually form a converging gap. In case

of bearings the stationary surface is the bearing surface, top foil in case of foil bearings. The moving surface is the surface of shaft (in case of journal bearings) or thrust runner (in case of thrust bearings). The film thickness between these two surfaces could vary only along film length or could vary along the direction of leakage flow as well. Film thickness can also be a transient function and may vary in time. In the cartesian coordinate representation of thin films. ‘x’ axis usually indicates the direction of length, ‘y’ axis indicates the direction of film thickness and ‘z’ direction indicates direction of leakage flow. ‘u’ velocity usually refers to velocity along ‘x’ direction, ‘v’ velocity refers to velocity along ‘y’ direction and ‘w’ velocity refers to velocity along ‘z’ direction.

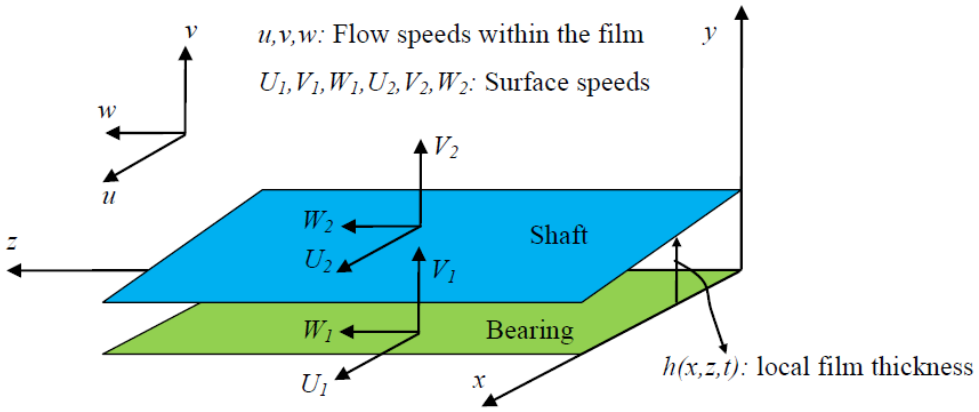

Figure 1 Illustration of hydrodynamic thin film

In figure 1, for general analysis purpose U2, V2, W2 denote velocities of moving surface in x, y and z directions, respectively. U1, V1, W1 denote velocities of stationary surface in x, y and z directions, respectively.

Hydrodynamic thin film lubrication is characterized by a thin layer of fluid film which has an average thickness much lower in magnitude compared to the length of the thin film.

For the classical lubrication theory considerations, an analysis of the order of magnitude indicates that the pressure does not vary across film thickness of the thin film hence, one momentum transport equation can be neglected while deriving governing equation for pressure for such films.

Fluid inertia is a phenomenon which has been found to be not significant for extremely thin films or low speed configurations of such films hence, inertia is neglected while deriving governing equation for pressure for such films which is also known as Reynolds equation. At high speeds the effect of inertia cannot be neglected. High speed configurations of thin films thus, require extensive computational modelling of Navier-Stokes momentum equations.

1.1.2 Application Of Thin Film Lubrication In Bearings

The two main applications of thin film lubrication is in thrust bearings and Journal bearings these are discussed as follows:

1) Thrust Bearing: Thrust bearings make use of hydrodynamic thin film lubrication as a load supporting mechanism. A fluid wedge thin film is formed by relative surface motion of the thrust runner over the respective bearing surfaces [7]. For the external load to be supported it is required that there exist a separation between the thrust runner and bearing surface i.e. top foil. This separation can only be achieved if the fluid pressure forces balance the bearing load and maintain equilibrium. For this to work the fluid must be continuously introduced into and pressurized in the film space [8]. It is

this thin film space which is the fluid thin film formed by a hydrodynamic action. Figure 2 shows a thrust bearing without a thrust runner.

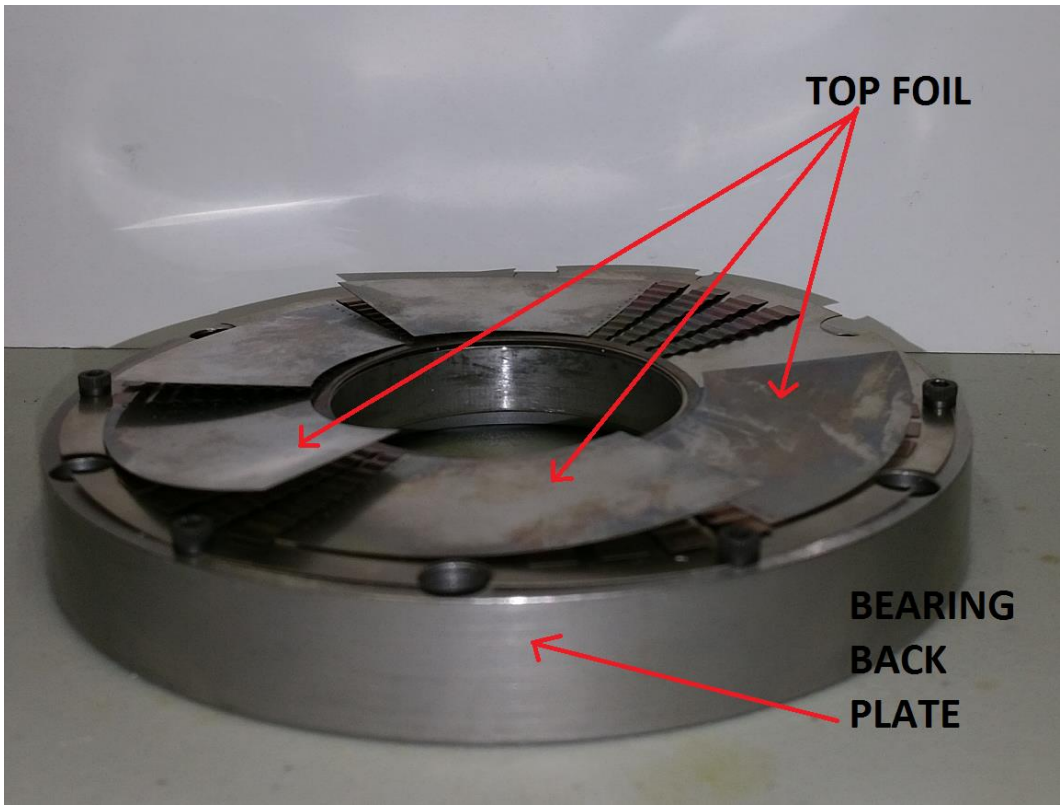

Figure 2 A thrust bearing

2) Journal Bearing: Thin films are formed under similar conditions in journal bearings as thrust bearings i.e. by viscous effects and wedge effects. The thin lubrication film in journal bearings is created by the relative motion of the sliding surfaces and the shape. The journal bearing consists of a shaft that is supported by a compliant foil. The high speed rotation of the shaft and viscosity of the air allows air to be pulled in between the high speed rotating shaft and foil. The entrapped air then separates physical contact between the shaft and bearing while taking up the weight of the shaft plus the load on it. This entrapped air forms a thin fluid lubrication film between the rotating shaft and the foil.

Figure 3 shows a journal bearing without a shaft.

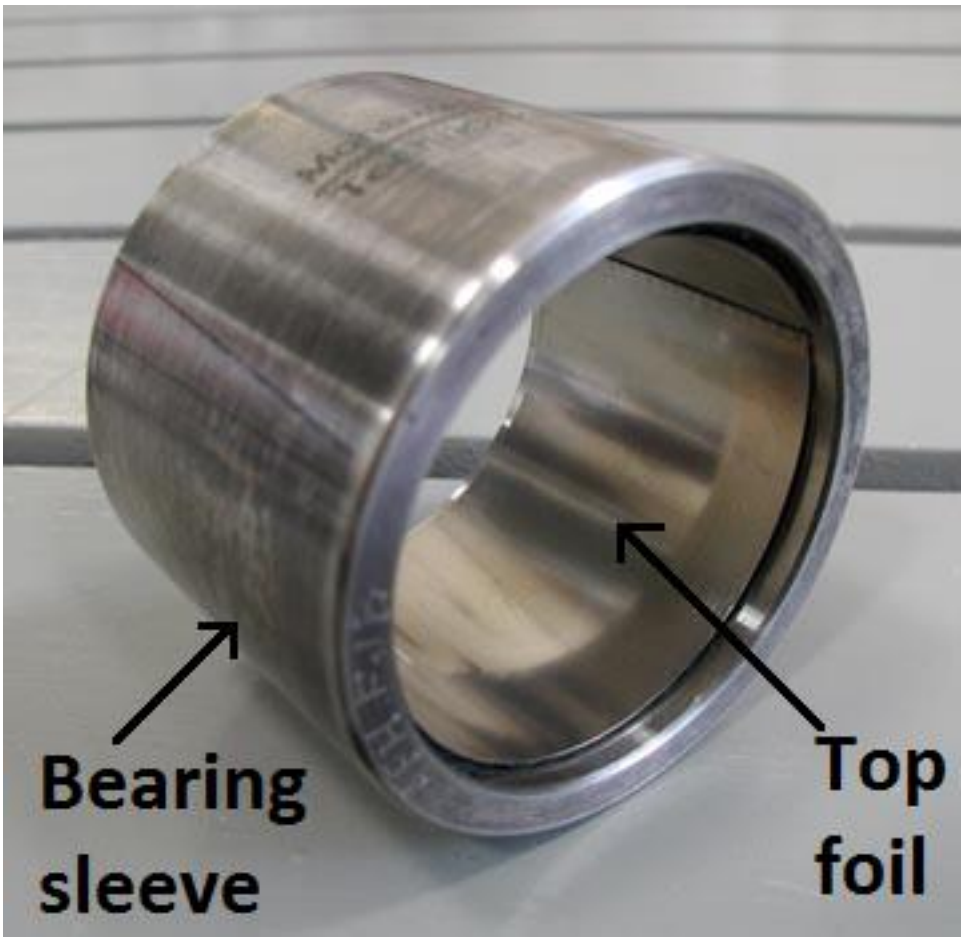

Figure 3 A journal bearing

1.1.3 Structure Of Foil Thrust Bearings

A typical foil thrust bearing is shown in the Figure 2. A smooth foil constitutes the bearing surface (top foil) and that is supported by a corrugated sheet of metal foil (bump foil) beneath it which provides structural stiffness. The top foil and the bump foil retract under the action of hydrodynamic forces created by the movement of the runner and form the compliant structure which is encased on a rigid stationary bearing back plate [9]. The

top foil and the bump foil are fixed at one end and free at the other. Due to rotation of runner fluid element is drawn into the converging wedge between the runner and the top foil. After a certain minimum velocity of the runner is achieved (Lift off speed) the runner is separated from the top foil by forming a thin fluid film. It is due to this viscous effect and converging wedge effect that a hydrodynamic pressure is generated which supports the load of the rotating runner. The load that can be sustained by the fluid film without breaking is called the load capacity of the bearing [9]. The compliant structure formed by the foil thrust bearing components allows foil thrust bearings to accommodate Thermal, as well as mechanical distortions much better than their rigid bearing counterparts. Journal bearings have a similar design to thrust foil bearings however, arrangement is different than that of thrust bearings and leakage flows are somewhat confined. It is notable that in contrast to journal bearings, typical thrust bearing configurations result in large differences between runner surface velocities at the inner and outer diameters of the thrust pads.[10] The hydrodynamic equation applicable to lubrication was first published by Osborne Reynolds in 1886 and is eponymously called the Reynolds equation [11].

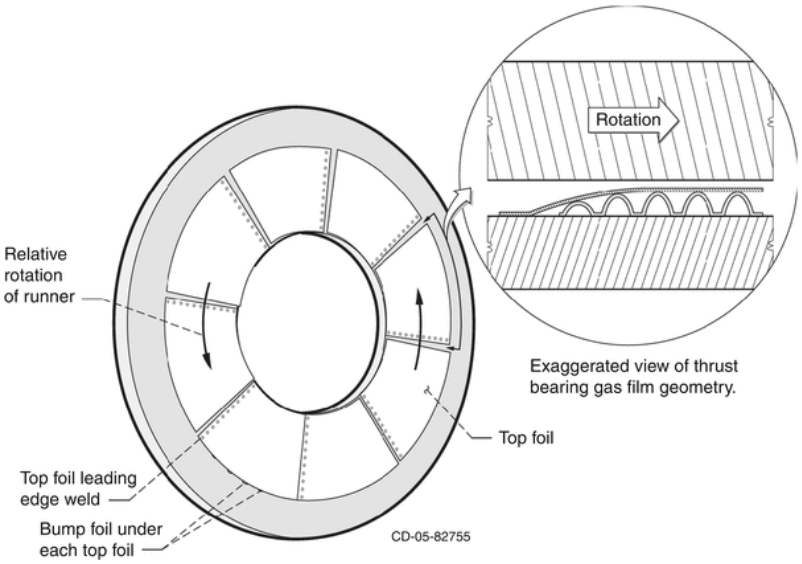

Figure 4 schematic of thrust bearing

1.1.4 Principle Of Operation Of Foil Thrust Bearing

As discussed in section 1.1.3 The Thrust foil bearing consists of multiple pads of compliant smooth surfaces called top foil. As the runner rotates the top foil forms a wedge shaped axial clearance with the runner surface. This clearance is so small that it is not visible to naked eye. The order of this clearance is in microns. Figure 5 shows a stationary thrust runner resting over bearing. The runner and top foil have physical contact in the beginning however after a certain speed the runner lifts off from the top foil. The load carrying capacity of the foil thrust bearing comes from the hydrodynamic pressure which is generated as the thrust runner moving over top foil drags gas into the converging area due to viscous nature of gas. The hydrodynamic pressure creates physical separation between the runner surface and top foil, and hence the runner becomes fully airborne and the friction loss becomes negligible [8]

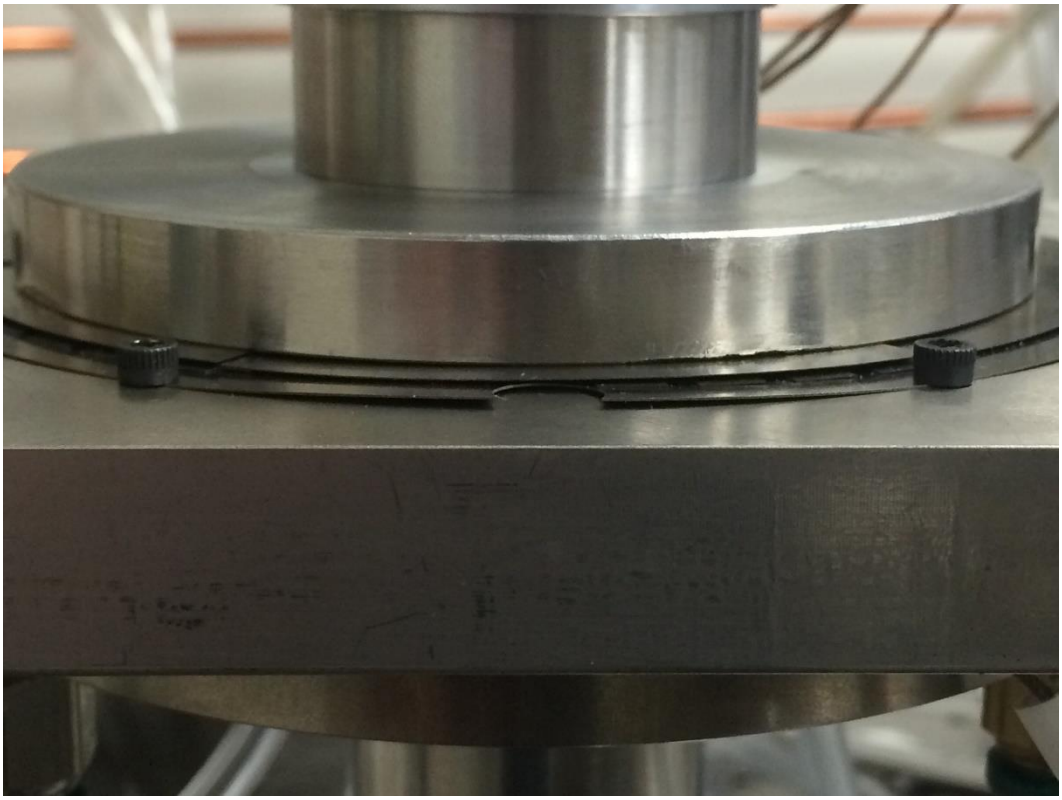

Figure 5 stationary runner over thrust bearing

1.2 Classical Lubrication Theory

Thin Film lubrication is governed as well as modelled based on the classical lubrication theory which was first derived by Osborne Reynolds in the 1886. The theory was derived based on fundamental assumptions of negligible fluid flow inertia therefore, limiting the application of the theory to low Reynolds numbers flows. Other important assumptions made by classical lubrication theory are:

1. The fluid film is extremely thin therefore the effect of curvature is negligible. Classical lubrication theory provides a good estimation for thin films having low film clearance to length ratio.

2. Fluid flow in thin films is assumed to be incompressible.
3. Fluid flow is assumed to be laminar in most cases as Reynolds number is fairly low on account of small value of clearance and low speeds.

1.2.1 Postulates Of Reynolds Equation

The Reynolds equation is a partial differential equation based on the classical lubrication theory. Reynolds equation governs the pressure distribution within thin viscous fluid films. This equation is derived from momentum transport and continuity equations with the assumption of negligible inertia. Therefore, a single partial differential equation with just two dependent variables (pressure, channel height) represents all the three momentum equations and the continuity equation [9]. The following assumptions or postulates are common in the derivation of Reynolds equation [12]:

- Continuum flow of newtonian fluid with constant viscosity
- Isothermal flow because of thin film and metallic boundaries
- Pressure variation across the film is not a dominant factor
- Viscous forces dominate over gravity and inertia.

The Reynolds equation is an elliptic partial differential equation, whose analytical solution can be obtained for specific applications after laborious mathematical derivations [13,14]. For this reason, the most common and practical way of solving the Reynolds equation is through numerical methods, despite the implicit errors of such methods. For the purpose of this research thesis the Reynolds equation has been solved using the finite volume method.

The Reynolds equation governing pressure field for the three dimensional thin cartesian coordinate film is given by:

$$\frac{\partial}{\partial x}\left(\frac{\rho h^3}{12\mu}\frac{\partial p}{\partial x}\right)+\frac{\partial}{\partial z}\left(\frac{\rho h^3}{12\mu}\frac{\partial p}{\partial z}\right)=\frac{1}{2}\frac{\partial}{\partial x}\left(\rho h U\right) \quad (1.1)$$

1.3 Viscous Flow Theory

Viscous flow in fluids is governed by the partial differential equations known as the Navier-stokes equations. These equations were first introduced by Claude Naiver in the year 1822 for incompressible flows. The equations proposed by Claude Naiver were extended in a more advanced fashion by George stokes in the year 1845. These equations describe behavior of large class of fluids. In section 1.2.1 Reynolds equation was derived from the simplification of incompressible Navier-Stokes and continuity equation by neglecting inertia terms. The nature of fluid flow in thrust bearings is both viscous as well as compressible this requires the solution of compressible Navier-stokes momentum equations. Inviscid flows are described using the Euler equations. Inviscid theory is widely applicable in a number of cases however, it fails in case of thin film lubrication. The very application of no slip boundary conditions in bearing analysis requires detailed viscous modelling. Viscosity has a major role in thin film pressure generation hence, requiring detailed modelling of highly non-linear Navier-Stokes momentum equations. The Non-Linearity of Navier-stokes equations makes it highly challenging to solve. Approximate solutions of Navier-stokes equations are possible to achieve by implementing an effective numerical discretization scheme such as Finite Volume method to convert the highly non-linear equations into algebraic equations and applying Computational Fluid Dynamics iterative Algorithms. The Navier-stokes equations are among the very few equations of mathematical physics for which nonlinearity arises not from the physical attributes of the system but rather from the mathematical (Kinematical) aspects of the problem [15].

The x-momentum Navier-Stokes equation is:

$$\left(\frac{\partial}{\partial x}\rho uu+\frac{\partial}{\partial y}\rho uv+\frac{\partial}{\partial z}\rho uw\right)=-\frac{\partial p}{\partial x}+\frac{\partial}{\partial x}\left(-\frac{2}{3}\mu\left(\nabla.V\right)+2\mu\frac{\partial u}{\partial x}\right)+\frac{\partial}{\partial y}\left(\mu\left(\frac{\partial v}{\partial x}+\frac{\partial u}{\partial y}\right)\right)+\frac{\partial}{\partial z}\left(\mu\left(\frac{\partial u}{\partial z}+\frac{\partial w}{\partial x}\right)\right) \tag{1.2}$$

The y-momentum Navier-Stokes equation is:

$$\left(\frac{\partial}{\partial x}\rho uv+\frac{\partial}{\partial y}\rho vv+\frac{\partial}{\partial z}\rho vw\right)=-\frac{\partial p}{\partial y}+\frac{\partial}{\partial x}\left(\mu\left(\frac{\partial v}{\partial x}+\frac{\partial u}{\partial y}\right)\right)+\frac{\partial}{\partial y}\left(-\frac{2}{3}\mu\left(\nabla.V\right)+2\mu\frac{\partial v}{\partial y}\right)+\frac{\partial}{\partial z}\left(\mu\left(\frac{\partial w}{\partial y}+\frac{\partial v}{\partial z}\right)\right) \tag{1.3}$$

The z-momentum Navier-Stokes equation is:

$$\left(\frac{\partial}{\partial x}\rho uw+\frac{\partial}{\partial y}\rho vw+\frac{\partial}{\partial z}\rho ww\right)=-\frac{\partial p}{\partial z}+\frac{\partial}{\partial x}\left(\mu\left(\frac{\partial u}{\partial z}+\frac{\partial w}{\partial x}\right)\right)+\frac{\partial}{\partial y}\left(\mu\left(\frac{\partial w}{\partial y}+\frac{\partial v}{\partial z}\right)\right)+\frac{\partial}{\partial z}\left(-\frac{2}{3}\mu\left(\nabla.V\right)+2\mu\frac{\partial w}{\partial z}\right) \tag{1.4}$$

The Navier-Stokes momentum equations have been discussed more in detail and have been non-dimensionalized in section 3.3 using a conventional lubrication scaling to adapt them to thin films. The mixed terms in the Navier-stokes equations lead to complex correlations compared to heat conduction or diffusion problems. For simple Flow some terms can be neglected, and analytical solutions can be given for Navier-Stokes equations. [15] However, analytical solutions for more complicated physical problems cannot be obtained for the naiver-stokes equations. For high speed viscous flows in thin fluid films as in the case of thrust bearings a more detailed modelling of

Navier-stokes equations is necessary thus, requiring robust numerical methods. Advances in CFD methods have inspired the numerical solution of full naiver-stokes equations. A combination of a well posed discretization scheme along with an iterative method can provide a reasonable numerical solution of Navier-Stokes equations. Finite Volume scheme is one of the most popular methods for discretization of Navier-Stokes equations. Finite volume scheme has been discussed in section 4.3.1 in detail.

1.4 Thesis Objective

The objective of this thesis is to develop a computational solver for simulating steady state performance of a 3 dimensional Thin film in a gas thrust bearing for High Flow Reynolds numbers. This has been achieved by computationally solving the compressible 3 dimensional Thin Film Navier-Stokes equations for a Laminar flow using the finite volume discretization. The thesis aims at studying effect of inertia in thin film lubrication which is a dominating factor in high speed flows. The computational Solver stands as an accurate prediction model for thrust bearings operating in high speed subsonic regimes. The computational solver can be used as a standalone prediction model for bearing performance or it can be integrated into a more detailed bearing performance program to model interactions between deformable structural performance and fluid performance. The thesis aims at comparing thin film lubrication performance predicted by classical lubrication theory with solutions of thin film Navier-stokes equations. At higher flow Reynolds number the computational solver is an indicator of bearing under design or an over design.

1.5 Organization of Thesis

The organization of this thesis is based on the following outline. Chapter 1 presents an Introduction and background to the concept and application of thin film

lubrication in thrust bearings. Chapter 2 is a review of literature relevant to previous attempts at understanding effects of fluid inertia in thin film lubrication. Chapter 2 is followed by chapter 3 which discusses fundamental governing equations pertaining to thin films that describe compressible and viscous flow with or without inertia effects. Chapter 4 describes numerical modelling of governing thin film equations. The beginning of chapter 4 discusses solution methodology adopted by the CFD solver developed for the purpose of this thesis. The finite volume method approach and general convection diffusion equation used in modelling the governing equations is described in chapter 4. Chapter 4 also details discretization approach adopted in this thesis. Chapter 5 presents the results of the current study along with detailed discussion. Conclusions from the research are discussed in Chapter 6. Chapter 7 presents information on future areas of research.

Chapter 2

LITERATURE REVIEW

Thrust foil bearings have received much attention in the past three decades on account of their robust performance for high speed oil free turbomachinery. Some of the advantages that the thrust foil bearings offer include: high rotational speed capability, no auxiliary lubrication system, non-contacting high speed operation, and improved damping as compared to rigid hydrodynamic bearings [16]. The application of thrust foil bearings in high speed applications have drawn attention towards development of detailed and accurate predictive models in comparison to existing classical lubrication theory models. Focus of much of the research has been on including effect of inertia in performance prediction of thin film lubrication in bearings and seals. In this section some of the works done in this area have been reviewed and cited. The literature review presented in this section facilitates justification in comparison between previously evaluated thin film performances by consideration of inertial effects. This also provides guidance in developing the prediction model by considering all possible physical and governing phenomena.

It was pointed out by Frêne et al. [10] that the study of non-laminar and inertial phenomena in fluid film lubrication was initiated more than 50 years ago, but it remains of interest because of the continuing emergence of challenging problems.

One of the earliest available works on effect of fluid inertia on bearing performance was by simulation of Unsteady Navier-Stokes equations for hydrodynamic bearings done by Henry A. putre in the article computer solution of unsteady Navier-Stokes equations For an Infinite hydrodynamic Step Bearing [17]. In this work velocity and pressure distribution was solved for an infinite hydrodynamic step bearing with no side leakage using the two dimensional incompressible Navier-Stokes equations. The study was compared with

original inertia less prediction of the step bearing by Lord Rayleigh [18]. It was pointed out that fluid inertia has significant effect in bearing performance hence, it should not be neglected in performance prediction models. John Tichy et al. [1] have investigated performance of a thin film in a high speed subsonic compressible lubrication regime using a one-dimensional (1D) approximation. They observed that for a compressible flow the effect of Mach number is small up to M=0.5 but not negligible However, the effect of heat transfer is huge. They point out that the bearings designed by the classical lubrication theory are likely over-designed.

Noël Brunetière and Bernard Tournerie [19] in their paper have developed an efficient numerical model for analysing inertia-influenced flows in thin fluid films. The finite element model was applied to thin films in misaligned hydrostatic seal. The effect of inertia on leakage flow in the seals was analysed. Significant differences were observed. The authors point out the importance of including inertia for modelling lubrication thin film flows in high speeds.

Gandjalikhan S. A. Nassab [20] presents a study where Inertia Effect on the thermohydrodynamic characteristics of journal bearings was studied. The authors applied a computational fluid dynamics (CFD) technique to solve The exact governing equations without applying simplifying assumptions of lubrication. Numerical solutions of the full three-dimensional Navier-Stokes equations with and without inertia terms, coupled with the energy equation in the lubricant flow and the heat conduction equations in the bearing and the shaft were obtained. They clearly point out effect of Inertia on the thermohydrodynamic characteristics of journal bearings.

Constantinescu [21] has studied the influence of inertia forces in turbulent as well as laminar self-Acting films. The obtained results show that for steady films, convective inertia forces lead basically to Bernoulli effects, while for unsteady films inertia forces

may influence both damping and stiffness characteristics of the bearing. At the same time it is pointed out that when Bernoulli effects are important, similar effects may occur in the inlet region of the film.

The accuracy of the compressible Reynolds equation for predicting the local pressure in gas-lubricated textured parallel slider bearings was studied by Bart Raeymaekers [22]. It was pointed out that deviation between the local bearing pressure obtained with the Reynolds equation and the Navier-Stokes equations increases with increasing texture aspect ratio of the parallel slider bearings. While this study indicated that inertia was found to be negligible, significant cross-film pressure gradient and a large velocity gradient in the sliding direction in the lubricant film was found. This is a phenomena that the classical lubrication theory fails to explain.

Hu and Leutheusser [23] studied parallel slider bearings with sinusoidal grooves on one of the surfaces. They suggested that for large Reynolds numbers inertia is important when defining the limits of applicability of the Reynolds equation from classical lubrication theory. Further, it was also suggested by Arghir et al. [24] that when calculating the hydrodynamic pressure for a large Reynolds number fluid inertia becomes increasingly important.

Chien-Hsin Chen and Cha'o-Kuang Chen [25] from their research on Influence of fluid Inertia on the operating characteristics of finite journal bearings concluded that the effect of inertia appears to be small for low Reynolds numbers however, the inertia plays a significant role in influencing the side flow rate.

Chapter 3

THIN FILM MODEL OVERVIEW

The thin film is essentially a dual profile fluid geometry that is formed when the fluid is entrained between the high speed rotating runner and the stationary top foil. Figure 6 shows a picture of thrust bearing assembly along with the runner.

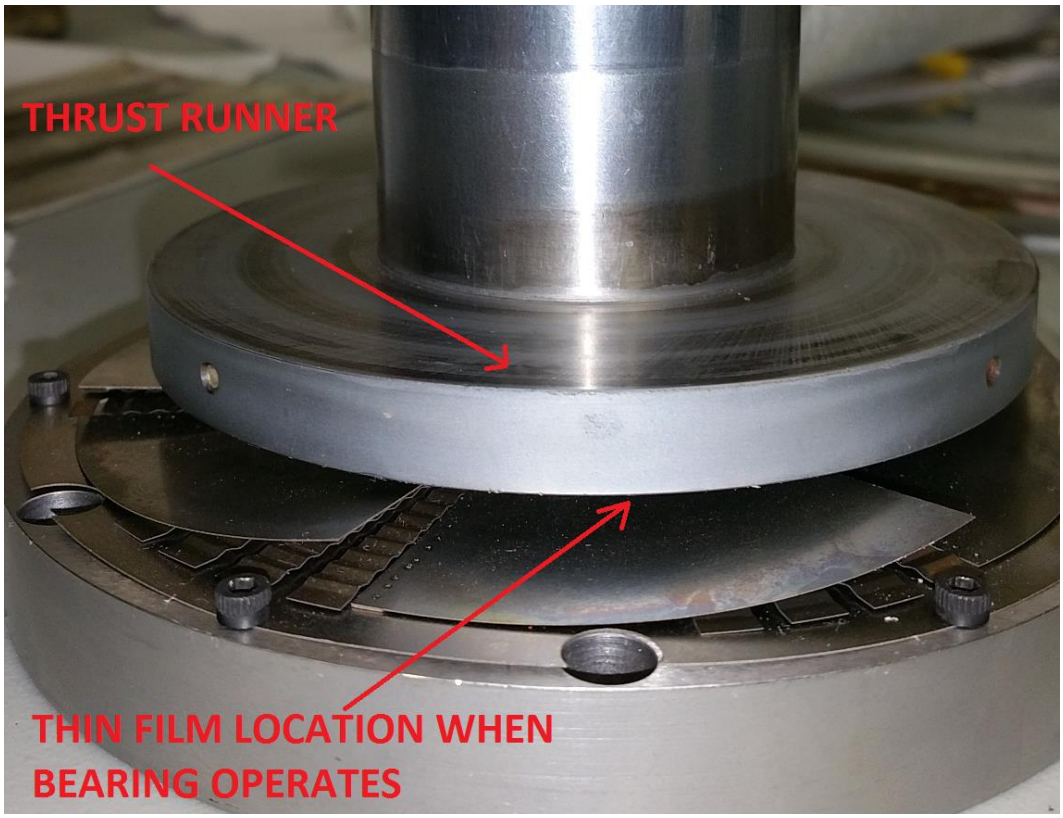

Figure 6 thin film shape estimation

For illustration purpose the clearance shown between top foil and thrust runner is highly enlarged in the picture however, in operation this gap reduces to the order of microns and it is in this gap where the dual profile thin film is formed. Figure 7 shows the shape and the nomenclature generally applicable to thin films. This thin film profile is a direct consequence of shape estimation of fluid film from working condition of the thrust

bearing. For computational ease the pie shaped computational fluid domain is often assumed to be of rectangular geometry. The thin film is a wedge plus flat shaped lubrication film between the stationary top foil surface and a high speed moving wall i.e. the runner. The thin film model considered for this thesis is a three dimensional taper fluid film with a constant slope up to the extent of taper region of the top foil and a flat film of constant thickness beyond the taper region. The inlet and outlet is formed by the wedge taper and the flat region respectively. The beginning of the wedge taper is the location of inlet. The end of flat is the location of outlet. The inlet is the location of maximum film thickness and the outlet is the location of minimum film thickness. The film thickness has a linear taper along the direction of the runner surface velocity. The computational domain of the three dimensional thin film considers that the thin film is fully developed and there is some leakage flow. The Cartesian coordinate for the thin film is assigned with x-axis in the direction of the thin film length, y-axis along the direction of film thickness, and z- axis along the direction of leakage flow.

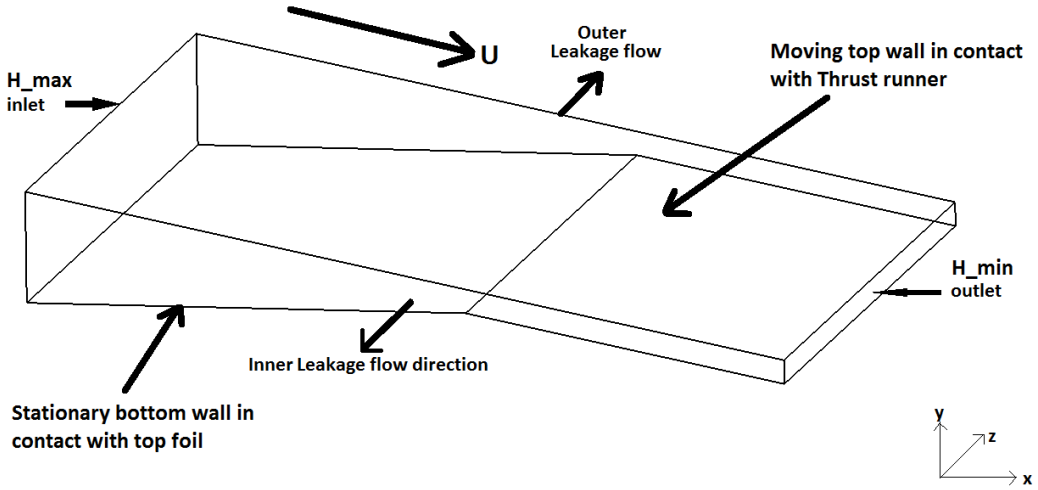

Figure 7 shape and the nomenclature of thin film.

3.1 Governing Equations

The 3 dimensional compressible, viscous thin film fluid flow is primarily governed by the Navier-stokes equations. The fundamental governing Navier-Stokes equations for the three dimensional compressible, viscous flow for an isothermal gas in a thin film are as follows:

Mass Continuity equation:

$$\left(\frac{\partial}{\partial x} \rho u + \frac{\partial}{\partial y} \rho v + \frac{\partial}{\partial z} \rho w \right) = 0 \tag{3.1}$$

Momentum conservation:

The x-Momentum Navier-Stokes equation from (1.2) is:

$$\begin{aligned} &\left(\frac{\partial}{\partial x} \rho uu + \frac{\partial}{\partial y} \rho uv + \frac{\partial}{\partial z} \rho uw \right) = -\frac{\partial p}{\partial x} + \frac{\partial}{\partial x}\left(-\frac{2}{3} \mu \left(\nabla . V \right) + 2\mu \frac{\partial u}{\partial x} \right) \\ &+ \frac{\partial}{\partial y}\left(\mu \left(\frac{\partial v}{\partial x} + \frac{\partial u}{\partial y} \right) \right) + \frac{\partial}{\partial z}\left(\mu \left(\frac{\partial u}{\partial z} + \frac{\partial w}{\partial x} \right) \right) \end{aligned} \tag{3.2}$$

The y-Momentum Navier-Stokes equation from (1.3) is:

$$\left(\frac{\partial}{\partial x}\rho uv+\frac{\partial}{\partial y}\rho vv+\frac{\partial}{\partial z}\rho vw\right)=-\frac{\partial p}{\partial y}+\frac{\partial}{\partial x}\left(\mu\left(\frac{\partial v}{\partial x}+\frac{\partial u}{\partial y}\right)\right)$$
$$+\frac{\partial}{\partial y}\left(-\frac{2}{3}\mu\left(\nabla.V\right)+2\mu\frac{\partial v}{\partial y}\right)+\frac{\partial}{\partial z}\left(\mu\left(\frac{\partial w}{\partial y}+\frac{\partial v}{\partial z}\right)\right) \quad (3.3)$$

The z-Momentum Navier-Stokes equation from (1.4) is:

$$\left(\frac{\partial}{\partial x}\rho uw+\frac{\partial}{\partial y}\rho vw+\frac{\partial}{\partial z}\rho ww\right)=-\frac{\partial p}{\partial z}+\frac{\partial}{\partial x}\left(\mu\left(\frac{\partial u}{\partial z}+\frac{\partial w}{\partial x}\right)\right)$$
$$+\frac{\partial}{\partial y}\left(\mu\left(\frac{\partial w}{\partial y}+\frac{\partial v}{\partial z}\right)\right)+\frac{\partial}{\partial z}\left(-\frac{2}{3}\mu\left(\nabla.V\right)+2\mu\frac{\partial w}{\partial z}\right) \quad (3.4)$$

The left-hand side terms of the Navier-Stokes momentum equations represent fluid inertia (momentum swept along the film), and the two right-hand side terms are pressure gradient and viscous forces, respectively. [2]. the isothermal boundaries and isothermal thin film temperature assumption of the model does not necessitate the solution of energy equation for temperature field. Hence, Energy equation is not included as one of the governing equations for the isothermal, compressible, viscous fluid flow model of the thin film.

Chapter 4

NUMERICAL MODELLING OF THE THIN FILM EQUATIONS

4.1 Solution Methodology: A General Look

Over the years many suitable solution methodologies have been proposed for the computational fluid dynamics solution of the governing fluid dynamics equations.

The two broad categories of solution methods for the solution of governing fluid dynamics equations are density Based Solvers and pressure Based Solvers.

4.1.1 Density Based Solvers

The density based solver is traditionally suited for high compressible flow problems. The momentum equations are solved in order to obtain the velocity field. In the density-based approach, the continuity equation is used to obtain the density field while the pressure field is determined from the equation of state. Density based solvers tend to be a suitable choice for flows involving greater compressibility or shock waves (Discontinuities). [26]

4.1.2 Pressure Based Solvers

The pressure based solvers solve the momentum equations for velocity field and then a pressure correction equation for pressure. Pressure based solvers tend to be better for incompressible flows and still perform reasonably well for weakly or moderately compressible flows. [26]

At highly compressible flow regimes the continuity balance is affected by density changes as well as velocity changes. This is on account of the pressure changes that not only affect the velocity but also density. Thus, a pressure based solver is required to account for both these changes at high speeds and high compressibility.

4.2 Solution Methodology Applied To Thin Film Governing Equations

The fundamental governing fluid dynamics equations of thin film discussed in section 3.1 are solved using the density based solver approach. Programming language used to develop the solver is C++. The IDE used is Visual Studio 2015. Post-processing is performed using MATLAB R2013A. The run time for code till convergence criteria is reached is couple of hours and varies based on grid size however, a good initial guess pressure field available from solution of Reynolds equation and velocity guess fields from solution of analytical velocities of Reynolds equation assists the density based solver to reach a faster convergence. The solution methodology for the developed thin film computational solver is outlined by the flowchart given in Figure 8.

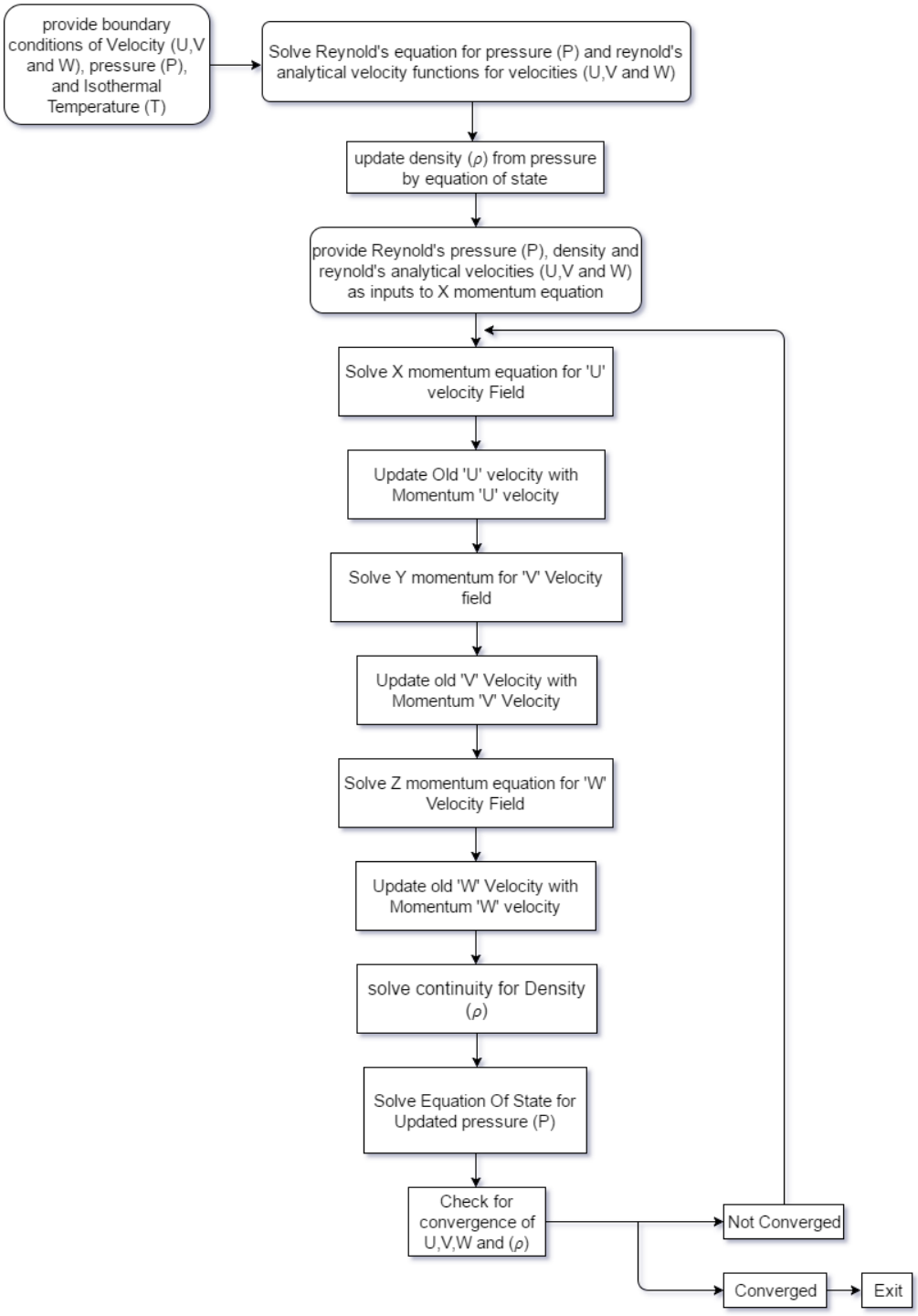

Figure 8 Solving methodology

4.2 Finite Volume Method: Some Fundamentals

The finite volume method (FVM) is one of the most versatile techniques for discretization that is used in the field of computational fluids dynamics (CFD). It is based on the Control volume Formulation of analytical fluid dynamics. The most suitable advantage of finite volume method is its ability to be applied to structured as well as unstructured grids with robust schemes. The first well documented use of the finite volume method was by Harlow (1957) at Los Alamos and Gentry, Martin and Daley (1966).

The ability of finite volume scheme to conserve the local numerical fluxes is an additional feature that is the numerical flux is conserved from one discretization cell to its neighbor. This last feature makes the finite volume method quite attractive when modelling problems for which the flux is of importance, such as in fluid mechanics, semi-conductor device simulation, heat and mass transfer [27].

Many commercial CFD codes make use of finite volume method as a discretization scheme applied to unstructured Grids.

The control volume approach of the Finite volume scheme ensures that it is locally conservative because a local balance is written on each discretization cell within the grid. Using divergence formula, an integral formulation of fluxes over boundary of the control volume is obtained. The fluxes on the boundary are discretized with respect to discrete unknowns. To describe how the concerned variable varies between cell centroids of neighbouring cells interpolation profiles are assumed.

FVM is one of the ideal methods for application in computations of discontinuous solutions arising in compressible flow problems.

Discontinuities are required to satisfy Rankine-Hugoniot Jump condition which is a consequence of conservation [28,29].

The basic finite volume method consists of the following steps:

1) The Flow domain is divided into a number of small control volumes.

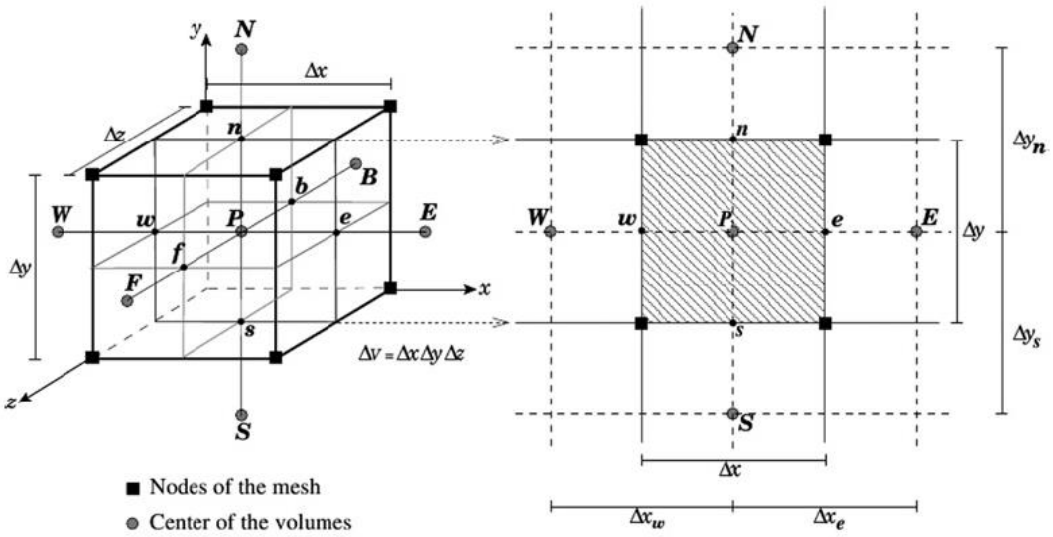

Figure 9 three and two Dimensional Finite Volume cells

2) The grid points where variables are stored are typically defined as centre of each control volume within the fluid domain.

3) The transport equation(s) are then integrated over each control volume within the fluid domain.

4) The divergence theorem is applied to the integrated transport equation(s).

5) In order to evaluate derivative terms, the values at control volume faces are needed. Interpolation techniques decide the variation of the property.

6) Extra boundary nodes are often added for suitability of problem definition.

7) The result is a set of linear algebraic equations, one for each control volume.

5) The linear algebraic equations are solve iteratively or simultaneously using suitable numerical methods such as Gauss-seidel or Runge-kutta .

4.3 The Convection-Diffusion Equation

Convection diffusion equation is an equation that describes general physical phenomena of convection and diffusion in nature. This equation is also commonly referred to as Advection-Diffusion equation. It is an equation that models phenomena where both convection and diffusion occur simultaneously. Diffusion refers to a generalized sense. It is not restricted only to diffusion of a chemical species by concentration gradients. The diffusion flux due to the gradient of the variable ϕ is $-\Gamma\frac{\partial\phi}{\partial x}$,

Which, for specific meanings of ϕ , would represent chemical-species diffusion flux, heat flux, viscous stress, etc. [13]

A general convection diffusion equation is given by:

$$\frac{\partial(\rho\phi)}{\partial t}+\nabla.(\rho V\phi)=\nabla.(\Gamma\nabla\phi)+S \qquad (4.1)$$

The four terms are ‘unsteady term’, ‘convection term’, ‘diffusion term’ and ‘source term’.

In general, $\phi=\phi(x,y,z,t)$

Γ is the diffusion coefficient corresponding to the particular property ϕ .

As ϕ takes different values, we get conservation equations for different quantities.

$\phi=1$: conservation of mass

$\phi = \mathrm{u}$: conservation of momentum

$\phi = \mathrm{h}$: conservation of energy

4.3.1 Finite Volume Method Applied to a General Advection-Diffusion Equation

The basic finite volume method begins with the generic scalar transport equation governing the transport of mass, momentum, energy, and other transported scalars [13]. This equation is the generic convection-diffusion equation which has been discussed in section 4.3. consider the general convection diffusion equation (4.1) given in section 4.3 as:

$$\frac{\partial(\rho\phi)}{\partial t} + \nabla.(\rho V\phi) = \nabla.(\Gamma\nabla\phi) + S$$

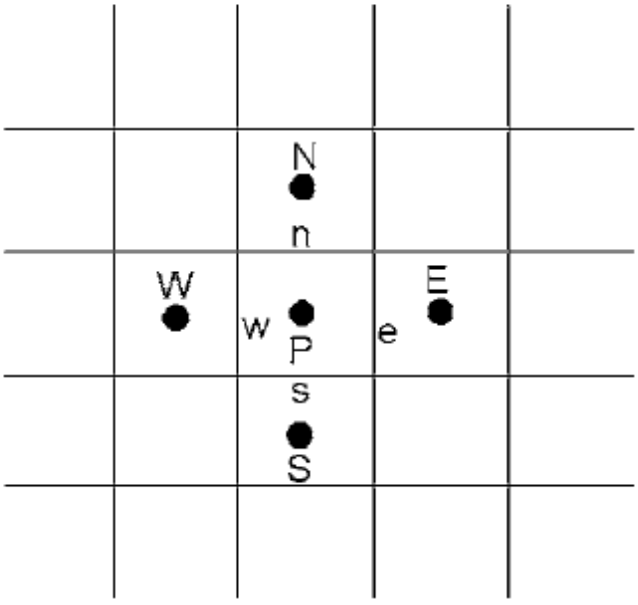

Figure 10 Grid scheme for a two dimensional finite volume scheme

In a finite volume discretization scheme the value of the equation variables are stored at the cell centroids. Consider the grid scheme in Figure 10. The geometry for consideration is divided into number of small control volumes or cells as shown. The centre of each cell in the figure is a centroid and this is where the information pertaining to the equation variables are stored. The convection diffusion equation is integrated over the control volume associated with the cell 'P'. The discretization yields:

$$\frac{\partial(\rho\phi)}{\partial t}+\left(\rho u\phi-\Gamma\frac{\partial\phi}{\partial x}\right)_e A_e-\left(\rho u\phi-\Gamma\frac{\partial\phi}{\partial x}\right)_w A_w + \left(\rho v\phi-\Gamma\frac{\partial\phi}{\partial y}\right)_n A_n-\left(\rho v\phi-\Gamma\frac{\partial\phi}{\partial y}\right)_s A_s=S_\phi\Delta V \tag{4.2}$$

The above equation is the general discretized convection diffusion equation using the finite volume scheme. The terms A_e,A_w, A_n , A_s represent the cell face areas.

The face values and the face derivatives of the transported property ϕ is calculated by a number of available schemes. These schemes relate the face values and face gradients to the cell centred values of the transported quantity. Convective and diffusive fluxes are evaluated at the cell-face centroids *e*, *w, n* and *s.* [25]. The evaluation of the gradient as well as the value of property ϕ at faces in terms of the cell centered values casts the discretized equation into the standard finite volume form given as:

$$a_P\phi_P=a_E\phi_E+a_W\phi_W+a_N\phi_N+a_S\phi_S+b \tag{4.3}$$

4.3.1.1. Finite Volume Schemes for evaluating Face values of Transported quantities in general convection diffusion equations

Over the years much research has been done on devising interpolation schemes which give accurate estimation for face values of the transported quantity Φ. In this section some of the common schemes have been discussed.

1) The Upwind Scheme:

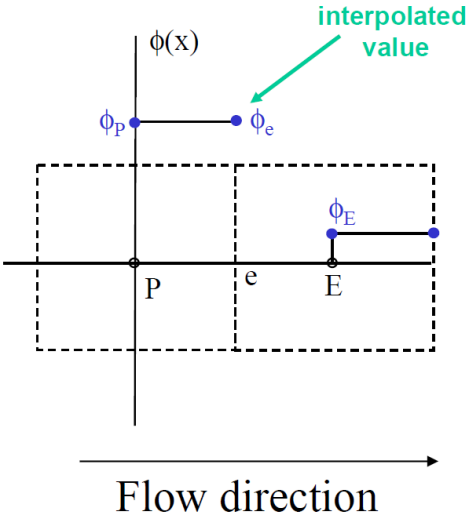

Figure 11 the Upwind Scheme

The upwind scheme recognizes that the weak point in the preliminary formulation is the assumption that the convected transport property ϕ at a face is an average of the values of property ϕ at nodes exactly upstream and downstream of the face. Thus, the upwind scheme works by assuming the value of convected property ϕ at the interface as equal to ϕ at the grid point on the upwind side of the face. The upwind scheme formulation leaves the diffusion term unchanged however, the convection term 'F' is calculated from the above mentioned assumption. [13]

For a convected property ϕ_e at the east face mathematically, The upwind scheme can be interpreted as:

$$\phi_e = \phi_P \text{ If } F_e > 0$$

$$\phi_e = \phi_E \text{ if } F_e < 0$$

The upwind scheme always makes the solution physically realistic, satisfying the scarborough criterion. Upwind scheme is said to be based on the 'tank-and-tube' model. [13]

2) The Exponential Scheme:

The exponential scheme derives inspiration from the exact solution of the general convection diffusion equation. It tries to replicate the behaviour of transported quantity ϕ, which can be derived as an exact solution of the general convection diffusion equation only when the diffusion coefficient is considered to be constant. Instead of assuming piecewise linear distribution of ϕ as in the case of central differencing scheme or assuming ϕ at the face of the control volume is equal to the value of ϕ at the upwind side in the upwind scheme, the distribution of ϕ between grid points is taken as that obtained from the exact solution. While the exponential scheme is quite accurate the computational time is much longer than that of upwind scheme. Patankar [13] proposed a scheme called power law scheme that has almost the same accuracy as exponential scheme yet had a much shorter computational time. In the finite volume discretization scheme used for the governing equations in this thesis. Power law scheme has been used.

3) The Hybrid Scheme:

The hybrid scheme was developed by Brian Spalding (1972). Hybrid scheme combines upwind difference scheme with central difference scheme. The choice between two schemes is based on absolute value of peclet number.

The hybrid scheme recognizes that if the peclet number is less than 2, it is suitable to use central difference scheme. For large peclet numbers i.e. greater than 2 it uses the upwind difference scheme. The larger value of convection causes an augmentation of peclet number. Although, the upwind scheme is first order accurate it is a useful scheme for highly convective flows.

4) Power Law Scheme:

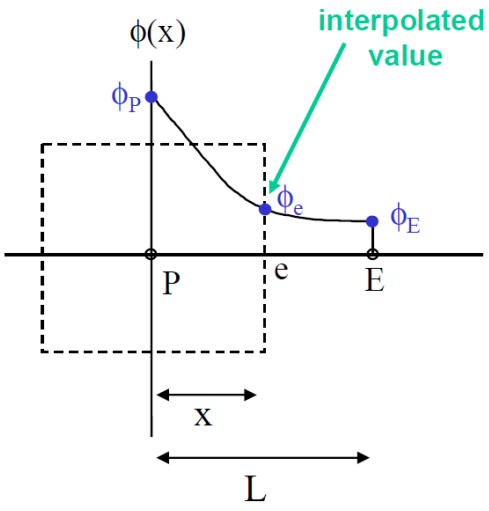

Figure 12 Power Law Scheme

This scheme is based on the analytical solution of one-dimensional advection-diffusion equation. The face value is determined from an exponential profile fitted through cell values. The exponential profile is approximated using following power law equation.

$$\phi_e = \phi_P - \frac{(1 - 0.1\,Pe)^5}{Pe}(\phi_E - \phi_P)$$

For values of Pe greater than 10, diffusion is ignored and first order upwind scheme is used.[30]

5) QUICK Scheme:

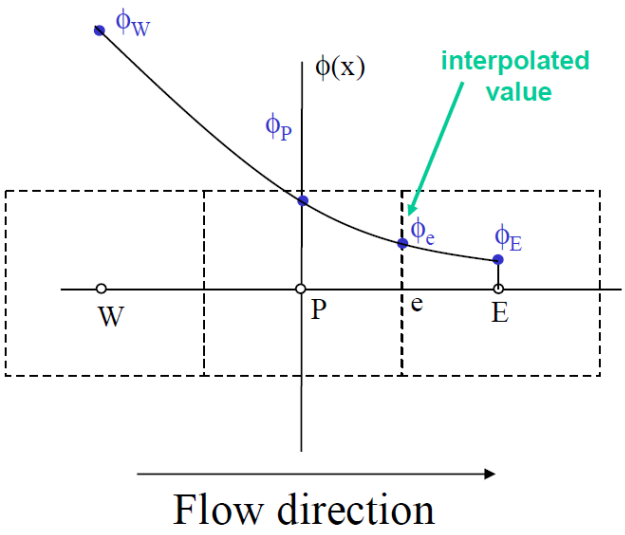

Figure 13 QUICK Scheme

QUICK stands for Quadratic Upwind Interpolation for Convective Kinetics. A quadratic curve is fitted through two upstream nodes and one downstream node. This is a very accurate scheme, but in regions with strong gradients, overshoots and undershoots can occur. This can lead to stability problems in the calculation. [30]

Finally we get an equation of the form,

$$a_P\phi_P = a_W\phi_W + a_E\phi_E + b$$

We solve iteratively for ϕ_P.

4.4 The Reynolds Equation

the Reynolds equation (1.1) governing pressure field for the three dimensional thin Cartesian coordinate film is repeated here and is given by:

$$\frac{\partial}{\partial x}\left(\frac{\rho h^3}{12\mu}\frac{\partial p}{\partial x}\right)+\frac{\partial}{\partial z}\left(\frac{\rho h^3}{12\mu}\frac{\partial p}{\partial z}\right)=\frac{1}{2}\frac{\partial}{\partial x}(\rho hU)$$

For an ideal gas we know that pressure, density and temperature are related by the ideal gas law, which is given by

$$p = \rho RT$$

Substituting density as: $\rho = \frac{P}{RT}$ into the compressible Reynolds equation and rearranging the Reynolds equation we get:

$$\frac{\partial}{\partial x}\left(\frac{Ph^3}{RT12\mu}\frac{\partial p}{\partial x}\right)+\frac{\partial}{\partial z}\left(\frac{Ph^3}{RT12\mu}\frac{\partial p}{\partial z}\right)=\frac{1}{2}\frac{\partial}{\partial x}\left(\frac{PhU}{RT}\right) \quad (4.4)$$

Further, for an isothermal gas we know that temperature ‘T’ and specific gas constant ‘R’ are constant, this allows elimination of ‘RT’ from the Reynolds equation. This gives:

$$\frac{\partial}{\partial x}\left(\frac{ph^3}{12\mu}\frac{\partial p}{\partial x}\right)+\frac{\partial}{\partial z}\left(\frac{ph^3}{12\mu}\frac{\partial p}{\partial z}\right)=\frac{1}{2}\frac{\partial}{\partial x}(phU) \quad (4.5)$$

Since, U is a fixed velocity therefore, the right hand side of the above equation can be taken out of the derivative and simplified as:

$$\frac{\partial}{\partial x}\left(\frac{ph^3}{\mu}\frac{\partial p}{\partial x}\right)+\frac{\partial}{\partial z}\left(\frac{ph^3}{\mu}\frac{\partial p}{\partial z}\right)=6U\frac{\partial}{\partial x}(ph) \quad (4.6)$$

This is the isothermal compressible Reynolds equation.

4.4.1.Non Dimensionalization Of Reynolds Equation

The Reynolds equation is non-dimensionalized by applying a conventional non-dimensional lubrication scaling to the isothermal compressible form of Reynolds equation, the lubrication scaling is:-

$$\bar{u} = \frac{u}{u_0}, \bar{v} = \left(\frac{v}{u_0}\right)\left(\frac{L}{C}\right), \bar{w} = \frac{w}{u_0}, \bar{p} = \frac{p}{p_a}, \bar{\mu} = \frac{\mu}{\mu_0}, \bar{\rho} = \frac{\rho}{\rho_0},$$

$$\bar{x} = \frac{x}{L}, \bar{y} = \frac{y}{C}, \bar{z} = \frac{z}{R}$$

Where u, v, w denote the fluid velocities along x, y and z directions respectively, we denote thin film length L, Film width R, Film inlet height h_{max}, Film outlet height, h_{min}, clearance of thin film ($C = \frac{h_{max} + h_{min}}{2}$), runner linear speed u_0,pressure p, atmospheric pressure p_a, density ρ, viscosity μ. The reference value of density and viscosity (with subscript 0) are at $T = 298K$. Which has been assumed as the isothermal temperature.

Substituting non dimensional quantities into (4.6) and converting into non-dimensional form we get:

$$\frac{\partial}{\partial(\bar{x}L)}\left(\frac{\bar{p}p_a\bar{H}^3C^3}{\bar{\mu}\mu_0}\frac{\partial\bar{p}p_a}{\partial(\bar{x}L)}\right) + \frac{\partial}{\partial(\bar{z}R)}\left(\frac{\bar{p}p_a\bar{H}^3C^3}{\bar{\mu}\mu_0}\frac{\partial p}{\partial(\bar{z}R)}\right) = 6U\frac{\partial}{\partial(\bar{x}L)}\left(\bar{p}p_a\bar{H}C\right) \quad (4.7)$$

Dividing the above equation (4.7) throughout by '$\frac{{p_a}^2 C^3}{\mu_0 L^2}$' i.e. coefficient of derivative of 'x' term. We get:

$$\frac{\partial}{\partial \bar{x}}\left(\frac{\bar{p}\bar{H}^3}{\bar{\mu}}\frac{\partial \bar{p}}{\partial \bar{x}}\right)+\frac{L^2}{R^2}\frac{\partial}{\partial \bar{z}}\left(\frac{\bar{p}\bar{H}^3}{\bar{\mu}}\frac{\partial \bar{p}}{\partial \bar{z}}\right) = \frac{\mu_0 L^2}{{p_a}^2 C^3} * 6U p_a C \frac{\partial}{\partial(\bar{x}L)}\left(\bar{p}\bar{H}\right) \tag{4.8}$$

This can be further simplified as:

$$\frac{\partial}{\partial \bar{x}}\left(\frac{\bar{p}\bar{H}^3}{\bar{\mu}}\frac{\partial \bar{p}}{\partial \bar{x}}\right)+\frac{L^2}{R^2}\frac{\partial}{\partial \bar{z}}\left(\frac{\bar{p}\bar{H}^3}{\bar{\mu}}\frac{\partial \bar{p}}{\partial \bar{z}}\right) = \left(\frac{6U\mu_0 L}{p_a C^2}\right) * \frac{\partial}{\partial(\bar{x})}\left(\bar{p}\bar{H}\right) \tag{4.9}$$

Including constant coefficients within the derivative on the left hand side and denoting the constant coefficient of the term on the right hand side of the above equation, we get:

$$\frac{\partial}{\partial \bar{x}}\left(\frac{\bar{p}\bar{H}^3}{\bar{\mu}}\frac{\partial \bar{p}}{\partial \bar{x}}\right)+\frac{\partial}{\partial \bar{z}}\left(\frac{\bar{p}\bar{H}^3 L^2}{\bar{\mu}R^2}\frac{\partial \bar{p}}{\partial \bar{z}}\right) = \Lambda \frac{\partial}{\partial(\bar{x})}\left(\bar{p}\bar{H}\right) \tag{4.10}$$

Where, $\Lambda = \left(\frac{6U\mu_0 L}{p_a C^2}\right)$, is known as the bearing compressibility number

The above equation is the non-dimensionalized isothermal, compressible Reynolds equation.

4.5 The Navier-Stokes Equations

The Navier-stokes equations are fluid equations that describe fluid behavior in a viscous flow. The Navier-Stokes equations are derived based on certain assumptions of fluid

flow. The main assumption in the derivation of Navier-stokes equation is that the fluid, at the scale of interest, is a continuum, in other words is not made up of discrete particles but rather a continuous substance. Another necessary assumption is that all the fields of interest like pressure, velocity, density, temperature and so on are differentiable, weakly at least. [31]. For a thin fluid film the entire Navier-stokes simplifies into thin film Navier-Stokes equations which have been discussed in sections 4.5.1.1, 4.5.2.1 and 4.5.3.1. This is a direct consequence of Conventional lubrication scaling applied to these equations. Some Non-dimensional coefficients appear with many terms which cause the relative magnitude of such terms to be negligible hence, such terms are carefully neglected to reduce the system of equations into simpler equations thereby, reducing computational overhead. The Navier-Stokes equations are highly Non-linear for most cases except in limiting cases such as one-dimensional flow and stokes flow (creeping flow), in such cases it is possible to reduce the Non-Linear equations into simplified linear equations. The nonlinearity is due to convective acceleration, which is an acceleration associated with the change in velocity over position. Hence, any convective flow, whether turbulent or not, will involve nonlinearity, an example of convective but laminar (nonturbulent) flow would be the passage of a viscous fluid (for example, oil) through a small converging nozzle [12]. The flow of gas into converging wedge of thin film geometry is another example of non-linear Navier-Stokes equations modeling.

4.5.1 The X-Momentum Navier-Stokes Equation

The general compressible three dimensional X-Momentum Navier-stokes equation as briefly mentioned in section 1.3 is given by:

$$\left(\frac{\partial}{\partial x}\rho uu+\frac{\partial}{\partial y}\rho uv+\frac{\partial}{\partial z}\rho uw\right)=-\frac{\partial p}{\partial x}+\frac{\partial}{\partial x}\left(-\frac{2}{3}\mu\left(\nabla.V\right)+2\mu\frac{\partial u}{\partial x}\right)$$
$$+\frac{\partial}{\partial y}\left(\mu\left(\frac{\partial v}{\partial x}+\frac{\partial u}{\partial y}\right)\right)+\frac{\partial}{\partial z}\left(\mu\left(\frac{\partial u}{\partial z}+\frac{\partial w}{\partial x}\right)\right)$$

Simplifying further by expanding dilation term, we get:

$$\left(\frac{\partial}{\partial x}\rho uu+\frac{\partial}{\partial y}\rho uv+\frac{\partial}{\partial z}\rho uw\right)=-\frac{\partial p}{\partial x}$$
$$+\frac{\partial}{\partial x}\left(-\frac{2}{3}\mu\left(\frac{\partial u}{\partial x}+\frac{\partial v}{\partial y}+\frac{\partial w}{\partial z}\right)+2\mu\frac{\partial u}{\partial x}\right) \quad (4.11)$$
$$+\frac{\partial}{\partial y}\left(\mu\left(\frac{\partial v}{\partial x}+\frac{\partial u}{\partial y}\right)\right)+\frac{\partial}{\partial z}\left(\mu\left(\frac{\partial u}{\partial z}+\frac{\partial w}{\partial x}\right)\right)$$

$$\left(\frac{\partial}{\partial x}\rho uu+\frac{\partial}{\partial y}\rho uv+\frac{\partial}{\partial z}\rho uw\right)=-\frac{\partial p}{\partial x}$$
$$+\frac{\partial}{\partial x}\left(\frac{4}{3}\mu\frac{\partial u}{\partial x}-\frac{2}{3}\mu\frac{\partial v}{\partial y}-\frac{2}{3}\mu\frac{\partial w}{\partial z}\right) \quad (4.12)$$
$$+\frac{\partial}{\partial y}\left(\mu\left(\frac{\partial v}{\partial x}+\frac{\partial u}{\partial y}\right)\right)+\frac{\partial}{\partial z}\left(\mu\left(\frac{\partial u}{\partial z}+\frac{\partial w}{\partial x}\right)\right)$$

Expanding the Derivatives on the Right Hand side, we get:

$$\left(\frac{\partial}{\partial x}\rho uu+\frac{\partial}{\partial y}\rho uv+\frac{\partial}{\partial z}\rho uw\right)=-\frac{\partial p}{\partial x}+\frac{\partial}{\partial x}\left(\frac{4}{3}\mu\frac{\partial u}{\partial x}\right)$$
$$-\frac{\partial}{\partial x}\left(\frac{2}{3}\mu\frac{\partial v}{\partial y}\right)-\frac{\partial}{\partial x}\left(\frac{2}{3}\mu\frac{\partial w}{\partial z}\right)+\frac{\partial}{\partial y}\left(\mu\frac{\partial v}{\partial x}\right) \quad (4.13)$$
$$+\frac{\partial}{\partial y}\left(\mu\frac{\partial u}{\partial y}\right)+\frac{\partial}{\partial z}\left(\mu\frac{\partial w}{\partial x}\right)+\frac{\partial}{\partial z}\left(\mu\frac{\partial u}{\partial z}\right)$$

The above equation can be simplified as:

$$\left(\frac{\partial}{\partial x}\rho uu+\frac{\partial}{\partial y}\rho uv+\frac{\partial}{\partial z}\rho uw\right)=-\frac{\partial p}{\partial x}+\frac{\partial}{\partial x}\left(\mu\frac{\partial u}{\partial x}\right)$$
$$+\frac{\partial}{\partial y}\left(\mu\frac{\partial u}{\partial y}\right)+\frac{\partial}{\partial z}\left(\mu\frac{\partial u}{\partial z}\right)+\frac{\partial}{\partial x}\left(\frac{1}{3}\mu\frac{\partial u}{\partial x}\right) \quad (4.14)$$
$$-\frac{\partial}{\partial x}\left(\frac{2}{3}\mu\frac{\partial v}{\partial y}\right)-\frac{\partial}{\partial x}\left(\frac{2}{3}\mu\frac{\partial w}{\partial z}\right)+\frac{\partial}{\partial y}\left(\mu\frac{\partial v}{\partial x}\right)+\frac{\partial}{\partial z}\left(\mu\frac{\partial w}{\partial x}\right)$$

Now, consider the last two terms in equation i.e. $\frac{\partial}{\partial y}\left(\mu\frac{\partial v}{\partial x}\right)+\frac{\partial}{\partial z}\left(\mu\frac{\partial w}{\partial x}\right)$ if a continuous differentiability is assumed then the partial derivatives on these last two terms can be interchanged. This gives:

$$\left(\frac{\partial}{\partial x}\rho uu+\frac{\partial}{\partial y}\rho uv+\frac{\partial}{\partial z}\rho uw\right)=-\frac{\partial p}{\partial x}+\frac{\partial}{\partial x}\left(\mu\frac{\partial u}{\partial x}\right)$$
$$+\frac{\partial}{\partial y}\left(\mu\frac{\partial u}{\partial y}\right)+\frac{\partial}{\partial z}\left(\mu\frac{\partial u}{\partial z}\right)+\frac{\partial}{\partial x}\left(\frac{1}{3}\mu\frac{\partial u}{\partial x}\right) \quad (4.15)$$
$$-\frac{\partial}{\partial x}\left(\frac{2}{3}\mu\frac{\partial v}{\partial y}\right)-\frac{\partial}{\partial x}\left(\frac{2}{3}\mu\frac{\partial w}{\partial z}\right)+\frac{\partial}{\partial x}\left(\mu\frac{\partial v}{\partial y}\right)+\frac{\partial}{\partial x}\left(\mu\frac{\partial w}{\partial z}\right)$$

$$\left(\frac{\partial}{\partial x}\rho uu+\frac{\partial}{\partial y}\rho uv+\frac{\partial}{\partial z}\rho uw\right)=-\frac{\partial p}{\partial x}+\frac{\partial}{\partial x}\left(\mu\frac{\partial u}{\partial x}\right)$$
$$+\frac{\partial}{\partial y}\left(\mu\frac{\partial u}{\partial y}\right)+\frac{\partial}{\partial z}\left(\mu\frac{\partial u}{\partial z}\right) \quad (4.16)$$
$$+\frac{\partial}{\partial x}\left[\left(\frac{1}{3}\mu\frac{\partial u}{\partial x}\right)-\left(\frac{2}{3}\mu\frac{\partial v}{\partial y}\right)-\left(\frac{2}{3}\mu\frac{\partial w}{\partial z}\right)+\left(\mu\frac{\partial v}{\partial y}\right)+\left(\mu\frac{\partial w}{\partial z}\right)\right]$$

Further, combining terms together we get:

$$\left(\frac{\partial}{\partial x}\rho uu+\frac{\partial}{\partial y}\rho uv+\frac{\partial}{\partial z}\rho uw\right)=-\frac{\partial p}{\partial x}+\frac{\partial}{\partial x}\left(\mu\frac{\partial u}{\partial x}\right)$$
$$+\frac{\partial}{\partial y}\left(\mu\frac{\partial v}{\partial y}\right)+\frac{\partial}{\partial z}\left(\mu\frac{\partial w}{\partial z}\right)+\frac{\partial}{\partial x}\left(\frac{1}{3}\mu\nabla.\vec{V}\right) \quad (4.17)$$

The above Equation, is the simplified x-momentum Navier-stokes equation.

4.5.1.1 Non dimensionalization of x-momentum Navier-Stokes equation

We apply a conventional non-dimensional lubrication scaling to the x-Momentum Navier-Stokes equation, the lubrication scaling is:-

$$\bar{u}=\frac{u}{u_0},\ \bar{v}=\left(\frac{v}{u_0}\right)\left(\frac{L}{C}\right),\ \bar{w}=\frac{w}{u_0},\ \bar{p}=\frac{p}{p_a},\ \bar{\mu}=\frac{\mu}{\mu_0},\ \bar{\rho}=\frac{\rho}{\rho_0},$$

$$\bar{x}=\frac{x}{L},\ \bar{y}=\frac{y}{C},\ \bar{z}=\frac{z}{R}$$

Where u, v, w denote the fluid velocities along x, y and z directions respectively, we denote thin film length L, clearance of thin film C, runner linear speed u_0,pressure p, atmospheric pressure P_a, density ρ, viscosity μ. The reference value of density and viscosity (with subscript 0) are at $T=298\ K$. Which has been assumed as the isothermal temperature.

Substituting the non-dimensional quantities into simplified x-momentum Navier-stokes equation and converting into non-dimensional form we get:

$$\frac{\partial}{\partial(\bar{x}L)}(\bar{\rho}\rho_0\bar{u}u_0\bar{u}u_0)+\frac{\partial}{\partial(\bar{y}C)}\left(\bar{\rho}\rho_0\bar{v}u_0\left(\frac{C}{L}\right)\bar{u}u_0\right)+\frac{\partial}{\partial(\bar{z}R)}(\bar{\rho}\rho_0\bar{w}u_0\bar{u}u_0)$$
$$=-\frac{\partial(\bar{p}P_a)}{\partial(\bar{x}L)}+\frac{\partial}{\partial(\bar{x}L)}\left(\bar{\mu}\mu_0\frac{\partial(\bar{u}u_0)}{(\bar{x}L)}\right)+\frac{\partial}{\partial(\bar{y}C)}\left(\bar{\mu}\mu_0\frac{\partial(\bar{u}u_0)}{(\bar{y}C)}\right)$$
$$+\frac{\partial}{\partial(\bar{z}R)}\left(\bar{\mu}\mu_0\frac{\partial(\bar{u}u_0)}{(\bar{z}R)}\right) \qquad (4.18)$$
$$+\frac{\partial}{\partial(\bar{x}L)}\left(\frac{1}{3}\bar{\mu}\mu_0\left(\frac{\partial\bar{U}U_0}{\partial\bar{X}L}+\frac{\partial\bar{v}u_0\left(\frac{C}{L}\right)}{\partial(\bar{y}C)}+\frac{\partial\bar{w}u_0}{\partial\bar{z}R}\right)\right)$$

Taking constants out of derivatives we get:

$$\left(\frac{\rho_0u_0u_0}{L}\right)*\frac{\partial(\bar{\rho}\bar{u}\bar{u})}{\partial\bar{x}}+\left(\frac{\rho_0u_0u_0}{L}\right)*\frac{\partial(\bar{\rho}\bar{v}\bar{u})}{\partial\bar{y}}+\left(\frac{\rho_0u_0u_0}{R}\right)*\frac{\partial(\bar{\rho}\bar{w}\bar{u})}{\partial\bar{z}}=$$
$$-\left(\frac{P_a}{L}\right)*\frac{\partial\bar{p}}{\partial\bar{x}}+\left(\frac{\mu_0u_0}{L*L}\right)*\frac{\partial}{\partial\bar{x}}\left(\bar{\mu}\frac{\partial\bar{u}}{\partial\bar{x}}\right)+\left(\frac{\mu_0u_0}{C*C}\right)*\frac{\partial}{\partial\bar{y}}\left(\bar{\mu}\frac{\partial\bar{u}}{\partial\bar{y}}\right)$$
$$+\left(\frac{\mu_0u_0}{R*R}\right)*\frac{\partial}{\partial\bar{z}}\left(\bar{\mu}\frac{\partial\bar{u}}{\partial\bar{z}}\right) \qquad (4.19)$$
$$+\frac{1}{3}\left(\frac{\mu_0u_0}{L*L}\right)\frac{\partial}{\partial\bar{x}}\left\{\bar{\mu}\left[\left(\frac{\partial\bar{u}}{\partial\bar{x}}\right)+\left(\frac{\partial\bar{v}}{\partial\bar{y}}\right)+\left(\frac{L}{R}\right)\left(\frac{\partial\bar{w}}{\partial\bar{z}}\right)\right]\right\}$$

Dividing the above equation throughout by '$\left(\frac{\rho_0u_0u_0}{L}\right)$' i.e. coefficient of derivative of 'x' term. We get:

$$\frac{\partial\left(\bar{\rho}\overline{uu}\right)}{\partial\bar{x}}+\frac{\partial\left(\bar{\rho}\overline{vu}\right)}{\partial\bar{y}}+\left(\frac{L}{R}\right)*\frac{\partial\left(\bar{\rho}\overline{wu}\right)}{\partial\bar{z}}=-\left(\frac{P_a}{\rho_0 u_0 u_0}\right)*\frac{\partial\bar{p}}{\partial\bar{x}}$$
$$+\left(\frac{\mu_0}{\rho_0 u_0 L}\right)*\frac{\partial}{\partial\bar{x}}\left(\bar{\mu}\frac{\partial\bar{u}}{\partial\bar{x}}\right)+\left(\frac{\mu_0 L}{\rho_0 u_0 C*C}\right)*\frac{\partial}{\partial\bar{y}}\left(\bar{\mu}\frac{\partial\bar{u}}{\partial\bar{y}}\right)$$
$$+\left(\frac{\mu_0 L}{\rho_0 u_0 R*R}\right)*\frac{\partial}{\partial\bar{z}}\left(\bar{\mu}\frac{\partial\bar{u}}{\partial\bar{z}}\right) \qquad (4.20)$$
$$+\frac{1}{3}\left(\frac{\mu_0}{\rho_0 u_0 L}\right)\frac{\partial}{\partial\bar{x}}\left\{\bar{\mu}\left[\left(\frac{\partial\bar{u}}{\partial\bar{x}}\right)+\left(\frac{\partial\bar{v}}{\partial\bar{y}}\right)+\left(\frac{L}{R}\right)\left(\frac{\partial\bar{w}}{\partial\bar{z}}\right)\right]\right\}$$

From the above equation it can be observed that the magnitude of the terms, $\frac{\mu_0}{\rho_0 u_0 L}, \frac{\mu_0 L}{\rho_0 u_0 R*R}$ are quite small thus, the terms appearing as coefficients with these terms can be neglected. This reduces the X-Momentum Navier-Stokes equation to:

$$\frac{\partial\left(\bar{\rho}\overline{uu}\right)}{\partial\bar{x}}+\frac{\partial\left(\bar{\rho}\overline{vu}\right)}{\partial\bar{y}}+\left(\frac{L}{R}\right)*\frac{\partial\left(\bar{\rho}\overline{wu}\right)}{\partial\bar{z}}=\frac{\mu_0 L}{\rho_0 u_0 *C*C}*\frac{\partial}{\partial\bar{y}}\left(\bar{\mu}\frac{\partial\bar{u}}{\partial\bar{y}}\right)$$
$$-\frac{P_a}{\rho_0 u_0 u_0}*\frac{\partial\bar{p}}{\partial\bar{x}} \qquad (4.21)$$

This is the thin film X-momentum Navier-stokes equation.

4.5.2 The Y-Momentum Navier-Stokes Equation

The general compressible three dimensional Y-Momentum Navier-Stokes equation as briefly mentioned in section 1.3 is given by:

$$\left(\frac{\partial}{\partial x}\rho uv+\frac{\partial}{\partial y}\rho vv+\frac{\partial}{\partial z}\rho vw\right)=-\frac{\partial p}{\partial y}+\frac{\partial}{\partial x}\left(\mu\left(\frac{\partial v}{\partial x}+\frac{\partial u}{\partial y}\right)\right)$$
$$+\frac{\partial}{\partial y}\left(-\frac{2}{3}\mu\left(\nabla.V\right)+2\mu\frac{\partial v}{\partial y}\right)+\frac{\partial}{\partial z}\left(\mu\left(\frac{\partial w}{\partial y}+\frac{\partial v}{\partial z}\right)\right) \quad (4.22)$$

Simplifying further by expanding dilation term, we get:

$$\left(\frac{\partial}{\partial x}\rho uv+\frac{\partial}{\partial y}\rho vv+\frac{\partial}{\partial z}\rho vw\right)=-\frac{\partial p}{\partial y}$$
$$+\frac{\partial}{\partial y}\left(-\frac{2}{3}\mu\left(\frac{\partial u}{\partial x}+\frac{\partial v}{\partial y}+\frac{\partial w}{\partial z}\right)+2\mu\frac{\partial v}{\partial y}\right) \quad (4.23)$$
$$+\frac{\partial}{\partial x}\left(\mu\left(\frac{\partial v}{\partial x}+\frac{\partial u}{\partial y}\right)\right)+\frac{\partial}{\partial z}\left(\mu\left(\frac{\partial w}{\partial y}+\frac{\partial v}{\partial z}\right)\right)$$

Further, simplification gives:

$$\left(\frac{\partial}{\partial x}\rho uv+\frac{\partial}{\partial y}\rho vv+\frac{\partial}{\partial z}\rho vw\right)=-\frac{\partial p}{\partial y}+\frac{\partial}{\partial y}\left(\frac{4}{3}\mu\frac{\partial u}{\partial x}-\frac{2}{3}\mu\frac{\partial v}{\partial y}-\frac{2}{3}\mu\frac{\partial w}{\partial z}\right)$$
$$+\frac{\partial}{\partial x}\left(\mu\left(\frac{\partial v}{\partial x}+\frac{\partial u}{\partial y}\right)\right)+\frac{\partial}{\partial z}\left(\mu\left(\frac{\partial w}{\partial y}+\frac{\partial v}{\partial z}\right)\right) \quad (4.24)$$

Expanding the Derivatives on Right hand side of the above equation we get:

$$\left(\frac{\partial}{\partial x}\rho uv+\frac{\partial}{\partial y}\rho vv+\frac{\partial}{\partial z}\rho vw\right)=-\frac{\partial p}{\partial y}+\frac{\partial}{\partial y}\left(\frac{4}{3}\mu\frac{\partial u}{\partial x}\right)-\frac{\partial}{\partial y}\left(\frac{2}{3}\mu\frac{\partial v}{\partial y}\right)$$
$$-\frac{\partial}{\partial y}\left(\frac{2}{3}\mu\frac{\partial w}{\partial z}\right)+\frac{\partial}{\partial x}\left(\mu\frac{\partial v}{\partial x}\right)+\frac{\partial}{\partial x}\left(\mu\frac{\partial u}{\partial y}\right)+\frac{\partial}{\partial z}\left(\mu\frac{\partial w}{\partial y}\right) \quad (4.25)$$
$$+\frac{\partial}{\partial z}\left(\mu\frac{\partial v}{\partial z}\right)$$

This equation can be simplified as:

$$\left(\frac{\partial}{\partial x}\rho uv+\frac{\partial}{\partial y}\rho vv+\frac{\partial}{\partial z}\rho vw\right)=-\frac{\partial p}{\partial y}+\frac{\partial}{\partial x}\left(\mu\frac{\partial u}{\partial x}\right)$$
$$+\frac{\partial}{\partial y}\left(\mu\frac{\partial v}{\partial y}\right)+\frac{\partial}{\partial z}\left(\mu\frac{\partial v}{\partial z}\right)+\frac{\partial}{\partial y}\left(\frac{1}{3}\mu\frac{\partial v}{\partial y}\right) \quad (4.26)$$
$$-\frac{\partial}{\partial y}\left(\frac{2}{3}\mu\frac{\partial u}{\partial y}\right)-\frac{\partial}{\partial y}\left(\frac{2}{3}\mu\frac{\partial w}{\partial z}\right)+\frac{\partial}{\partial x}\left(\mu\frac{\partial u}{\partial y}\right)+\frac{\partial}{\partial z}\left(\mu\frac{\partial w}{\partial y}\right)$$

Now, consider the last two terms in equation i.e. $\frac{\partial}{\partial x}\left(\mu\frac{\partial u}{\partial y}\right),\frac{\partial}{\partial z}\left(\mu\frac{\partial w}{\partial y}\right)$. If a continuous differentiability is assumed then the partial derivatives on these last two terms can be interchanged. This gives:

$$\left(\frac{\partial}{\partial x}\rho uv+\frac{\partial}{\partial y}\rho vv+\frac{\partial}{\partial z}\rho vw\right)=-\frac{\partial p}{\partial y}+\frac{\partial}{\partial x}\left(\mu\frac{\partial u}{\partial x}\right)$$
$$+\frac{\partial}{\partial y}\left(\mu\frac{\partial v}{\partial y}\right)+\frac{\partial}{\partial z}\left(\mu\frac{\partial v}{\partial z}\right)+\frac{\partial}{\partial y}\left(\frac{1}{3}\mu\frac{\partial v}{\partial y}\right) \quad (4.27)$$
$$-\frac{\partial}{\partial y}\left(\frac{2}{3}\mu\frac{\partial u}{\partial y}\right)-\frac{\partial}{\partial y}\left(\frac{2}{3}\mu\frac{\partial w}{\partial z}\right)+\frac{\partial}{\partial y}\left(\mu\frac{\partial v}{\partial x}\right)+\frac{\partial}{\partial y}\left(\mu\frac{\partial w}{\partial z}\right)$$

Further, simplifying:

$$\left(\frac{\partial}{\partial x}\rho uv+\frac{\partial}{\partial y}\rho vv+\frac{\partial}{\partial z}\rho vw\right)=-\frac{\partial p}{\partial y}+\frac{\partial}{\partial x}\left(\mu\frac{\partial u}{\partial x}\right)$$
$$+\frac{\partial}{\partial y}\left(\mu\frac{\partial v}{\partial y}\right)+\frac{\partial}{\partial z}\left(\mu\frac{\partial v}{\partial z}\right) \quad (4.28)$$
$$+\frac{\partial}{\partial y}\left[\left(\frac{1}{3}\mu\frac{\partial v}{\partial y}\right)-\left(\frac{2}{3}\mu\frac{\partial u}{\partial x}\right)-\left(\frac{2}{3}\mu\frac{\partial w}{\partial z}\right)+\left(\mu\frac{\partial u}{\partial x}\right)+\left(\mu\frac{\partial w}{\partial z}\right)\right]$$

Further, simplifying:

$$\left(\frac{\partial}{\partial x}\rho uv+\frac{\partial}{\partial y}\rho vv+\frac{\partial}{\partial z}\rho vw\right)=-\frac{\partial p}{\partial y}+\frac{\partial}{\partial x}\left(\mu\frac{\partial u}{\partial x}\right)$$
$$+\frac{\partial}{\partial y}\left(\mu\frac{\partial v}{\partial y}\right)+\frac{\partial}{\partial z}\left(\mu\frac{\partial v}{\partial z}\right)+\frac{\partial}{\partial y}\left[\left(\frac{1}{3}\mu\frac{\partial v}{\partial y}\right)+\left(\frac{1}{3}\mu\frac{\partial u}{\partial x}\right)+\left(\frac{1}{3}\mu\frac{\partial w}{\partial z}\right)\right] \quad (4.29)$$

$$\left(\frac{\partial}{\partial x}\rho uv+\frac{\partial}{\partial y}\rho vv+\frac{\partial}{\partial z}\rho vw\right)=-\frac{\partial p}{\partial y}+\frac{\partial}{\partial x}\left(\mu\frac{\partial u}{\partial x}\right)$$
$$+\frac{\partial}{\partial y}\left(\mu\frac{\partial v}{\partial y}\right)+\frac{\partial}{\partial z}\left(\mu\frac{\partial v}{\partial z}\right)+\frac{\partial}{\partial y}\left[\frac{1}{3}\mu\left(\frac{\partial v}{\partial y}+\frac{\partial u}{\partial x}+\frac{\partial w}{\partial z}\right)\right] \quad (4.30)$$

Further, combining terms together we get:

$$\left(\frac{\partial}{\partial x}\rho uv+\frac{\partial}{\partial y}\rho vv+\frac{\partial}{\partial z}\rho vw\right)=-\frac{\partial p}{\partial y}+\frac{\partial}{\partial x}\left(\mu\frac{\partial u}{\partial x}\right)$$
$$+\frac{\partial}{\partial y}\left(\mu\frac{\partial v}{\partial y}\right)+\frac{\partial}{\partial z}\left(\mu\frac{\partial v}{\partial z}\right)+\frac{\partial}{\partial y}\left(\frac{1}{3}\mu\nabla.\vec{V}\right) \quad (4.31)$$

Equation, is the Y-momentum Navier-stokes equation.

4.5.2.1 Non dimensionalization of Y-momentum Navier-Stokes equation

We non-dimensionalize the 3d Y-momentum Navier-Stokes equation to carry out a scaling analysis in order to reduce the 3d Y-momentum Navier-Stokes equation into a simplified thin film 3d Y-Momentum Navier-Stokes equation.

Consider the 3d Y-momentum Navier-Stokes equation simplified in section 4.3.2. Which is given as:

$$\left(\frac{\partial}{\partial x}\rho uv+\frac{\partial}{\partial y}\rho vv+\frac{\partial}{\partial z}\rho wv\right)=-\frac{\partial p}{\partial y}$$
$$+\frac{\partial}{\partial x}\left(\mu\frac{\partial v}{\partial x}\right)+\frac{\partial}{\partial y}\left(\mu\frac{\partial v}{\partial y}\right)+\frac{\partial}{\partial z}\left(\mu\frac{\partial v}{\partial z}\right)+\frac{\partial}{\partial y}\left(\frac{1}{3}\mu\nabla.\vec{V}\right) \quad (4.32)$$

We apply the same non-dimensional lubrication scaling as applied to X-momentum Navier-stokes equation. This gives:

$$\frac{\partial}{\partial(\bar{x}L)}\left(\bar{\rho}\rho_0\bar{u}u_0\bar{v}u_0\left(\frac{C}{L}\right)\right)+\frac{\partial}{\partial(\bar{y}C)}\left(\bar{\rho}\rho_0\bar{v}u_0\left(\frac{C}{L}\right)\bar{v}u_0\left(\frac{C}{L}\right)\right)$$
$$+\frac{\partial}{\partial(\bar{z}R)}\left(\bar{\rho}\rho_0\bar{w}u_0\bar{v}u_0\left(\frac{C}{L}\right)\right)=-\frac{\partial(\bar{p}P_a)}{\partial(\bar{y}C)}+\frac{\partial}{\partial(\bar{x}L)}\left(\bar{\mu}\mu_0\frac{\partial\left(\bar{v}u_0\left(\frac{C}{L}\right)\right)}{(\bar{x}L)}\right)$$
$$+\frac{\partial}{\partial(\bar{y}C)}\left(\bar{\mu}\mu_0\frac{\partial\left(\bar{v}u_0\left(\frac{C}{L}\right)\right)}{(\bar{y}C)}\right)+\frac{\partial}{\partial(\bar{z}R)}\left(\bar{\mu}\mu_0\frac{\partial\left(\bar{v}u_0\left(\frac{C}{L}\right)\right)}{(\bar{z}R)}\right) \quad (4.33)$$
$$+\frac{\partial}{\partial(\bar{y}C)}\left(\frac{1}{3}\bar{\mu}\mu_0\left(\frac{\partial\bar{U}U_0}{\partial\bar{X}L}+\frac{\partial\bar{v}u_0\left(\frac{C}{L}\right)}{\partial(\bar{y}C)}+\frac{\partial\bar{w}u_0}{\partial\bar{z}R}\right)\right)$$

By Taking constants out of derivatives we get:

$$\left(\frac{\rho_0u_0u_0}{L}\frac{C}{L}\right)*\frac{\partial(\bar{\rho}\bar{u}\bar{v})}{\partial\bar{x}}+\left(\frac{\rho_0u_0u_0}{L}\frac{C}{L}\right)*\frac{\partial(\bar{\rho}\bar{v}\bar{v})}{\partial\bar{y}}$$
$$+\left(\frac{\rho_0u_0u_0}{R}\frac{C}{L}\right)*\frac{\partial(\bar{\rho}\bar{w}\bar{v})}{\partial\bar{z}}=-\left(\frac{P_a}{C}\right)*\frac{\partial\bar{p}}{\partial\bar{y}}+\left(\frac{\mu_0u_0}{L*L}\frac{C}{L}\right)*\frac{\partial}{\partial\bar{x}}\left(\bar{\mu}\frac{\partial v}{\partial\bar{x}}\right)$$
$$+\left(\frac{\mu_0u_0}{C*L}\right)*\frac{\partial}{\partial\bar{y}}\left(\bar{\mu}\frac{\partial\bar{v}}{\partial\bar{y}}\right)+\left(\frac{\mu_0u_0}{R*R}\frac{C}{L}\right)*\frac{\partial}{\partial\bar{z}}\left(\bar{\mu}\frac{\partial\bar{v}}{\partial\bar{z}}\right) \quad (4.34)$$
$$+\frac{1}{3}\left(\frac{\mu_0u_0}{C*L}\right)\frac{\partial}{\partial\bar{y}}\left\{\bar{\mu}\left[\left(\frac{\partial\bar{u}}{\partial\bar{x}}\right)+\left(\frac{\partial\bar{v}}{\partial\bar{y}}\right)+\left(\frac{L}{R}\right)\left(\frac{\partial\bar{w}}{\partial\bar{z}}\right)\right]\right\}$$

Dividing the above equation throughout by $(\frac{\rho_0 u_0 u_0}{L}\frac{C}{L})$ i.e. coefficient of derivative of 'x' term. We get:

$$\begin{aligned}
&\frac{\partial(\bar{\rho}\bar{u}\bar{v})}{\partial\bar{x}}+\frac{\partial(\bar{\rho}\bar{v}\bar{v})}{\partial\bar{y}}+\left(\frac{L}{R}\right)*\frac{\partial(\bar{\rho}\bar{w}\bar{v})}{\partial\bar{z}}=-\left(\frac{P_a}{C}*\frac{L*L}{\rho_0 u_0 u_{0*} C}\right)*\frac{\partial\bar{p}}{\partial\bar{y}}\\
&+\left(\frac{\mu_0}{\rho_0 u_0 L}\right)*\frac{\partial}{\partial\bar{x}}\left(\bar{\mu}\frac{\partial v}{\partial\bar{x}}\right)+\left(\frac{\mu_0 L}{\rho_0 u_0 *C*C}\right)*\frac{\partial}{\partial\bar{y}}\left(\bar{\mu}\frac{\partial\bar{v}}{\partial\bar{y}}\right)\\
&+\left(\frac{\mu_0 L}{\rho_0 u_0 *R*R}\right)*\frac{\partial}{\partial\bar{z}}\left(\bar{\mu}\frac{\partial\bar{v}}{\partial\bar{z}}\right)\\
&+\frac{1}{3}\left(\frac{\mu_0 L}{\rho_0 u_0 *C*C}\right)\frac{\partial}{\partial\bar{y}}\left\{\bar{\mu}\left[\left(\frac{\partial\bar{u}}{\partial\bar{x}}\right)+\left(\frac{\partial\bar{v}}{\partial\bar{y}}\right)+\left(\frac{L}{R}\right)\left(\frac{\partial\bar{w}}{\partial\bar{z}}\right)\right]\right\}
\end{aligned} \tag{4.35}$$

From the above equation it can be observed that similar terms appear as coefficients in X-momentum equation. The magnitude of the terms $\frac{\mu_0}{\rho_0 u_0 L}$, $\frac{\mu_0 L}{\rho_0 u_0 R*R}$ are quite small thus, the terms appearing as coefficients with these terms can be neglected.

Further, for a thin film the gradient of pressure along film height is nearly negligible. This assumption allows to neglect the term: $-\left(\frac{P_a}{C}*\frac{L*L}{\rho_0 u_0 u_{0*} C}\right)*\frac{\partial\bar{p}}{\partial\bar{y}}$

These assumptions reduce the Y-momentum Navier-Stokes equation to :

$$\begin{aligned}
&\frac{\partial(\bar{\rho}\bar{u}\bar{v})}{\partial\bar{x}}+\frac{\partial(\bar{\rho}\bar{v}\bar{v})}{\partial\bar{y}}+\left(\frac{L}{R}\right)*\frac{\partial(\bar{\rho}\bar{w}\bar{v})}{\partial\bar{z}}=\frac{\mu_0 L}{\rho_0 u_0 *C*C}*\frac{\partial}{\partial\bar{y}}\left(\bar{\mu}\frac{\partial\bar{v}}{\partial\bar{y}}\right)\\
&+\frac{1}{3}\left(\frac{\mu_0 L}{\rho_0 u_0 C*C}\right)\frac{\partial}{\partial\bar{y}}\left\{\bar{\mu}\left[\left(\frac{\partial\bar{u}}{\partial\bar{x}}\right)+\left(\frac{\partial\bar{v}}{\partial\bar{y}}\right)+\frac{L}{R}\left(\frac{\partial\bar{w}}{\partial\bar{z}}\right)\right]\right\}
\end{aligned} \tag{4.36}$$

This is the thin film Y-momentum Navier-stokes equation.

4.5.3 The Z-Momentum Navier-Stokes Equation

The general compressible three dimensional Z-momentum Navier-stokes equation as briefly mentioned in section 1.3 is given by:

$$\left(\frac{\partial}{\partial x}\rho uw+\frac{\partial}{\partial y}\rho vw+\frac{\partial}{\partial z}\rho ww\right)=-\frac{\partial p}{\partial z}+\frac{\partial}{\partial x}\left(\mu\left(\frac{\partial u}{\partial z}+\frac{\partial w}{\partial x}\right)\right)+\frac{\partial}{\partial y}\left(\mu\left(\frac{\partial w}{\partial y}+\frac{\partial v}{\partial z}\right)\right)+\frac{\partial}{\partial z}\left(-\frac{2}{3}\mu\left(\nabla.V\right)+2\mu\frac{\partial w}{\partial z}\right) \tag{4.37}$$

Simplifying further by expanding dilation term, we get:

$$\left(\frac{\partial}{\partial x}\rho uw+\frac{\partial}{\partial y}\rho vw+\frac{\partial}{\partial z}\rho ww\right)=-\frac{\partial p}{\partial z}+\frac{\partial}{\partial z}\left(-\frac{2}{3}\mu\left(\frac{\partial u}{\partial x}+\frac{\partial v}{\partial y}+\frac{\partial w}{\partial z}\right)+2\mu\frac{\partial w}{\partial z}\right)+\frac{\partial}{\partial x}\left(\mu\left(\frac{\partial u}{\partial z}+\frac{\partial w}{\partial x}\right)\right)+\frac{\partial}{\partial y}\left(\mu\left(\frac{\partial w}{\partial y}+\frac{\partial v}{\partial z}\right)\right) \tag{4.38}$$

Simplifying, we get:

$$\left(\frac{\partial}{\partial x}\rho uw+\frac{\partial}{\partial y}\rho vw+\frac{\partial}{\partial z}\rho ww\right)=-\frac{\partial p}{\partial z}+\frac{\partial}{\partial z}\left(\frac{4}{3}\mu\frac{\partial w}{\partial z}-\frac{2}{3}\mu\frac{\partial u}{\partial x}-\frac{2}{3}\mu\frac{\partial v}{\partial y}\right)+\frac{\partial}{\partial x}\left(\mu\left(\frac{\partial u}{\partial z}+\frac{\partial w}{\partial x}\right)\right)+\frac{\partial}{\partial y}\left(\mu\left(\frac{\partial w}{\partial y}+\frac{\partial v}{\partial z}\right)\right) \tag{4.39}$$

Expanding the right hand side derivatives we get:

$$\left(\frac{\partial}{\partial x}\rho uw+\frac{\partial}{\partial y}\rho vw+\frac{\partial}{\partial z}\rho ww\right)=-\frac{\partial p}{\partial z}+\frac{\partial}{\partial z}\left(\frac{4}{3}\mu\frac{\partial w}{\partial z}\right)$$
$$+\frac{\partial}{\partial x}\left(\mu\frac{\partial w}{\partial x}\right)+\frac{\partial}{\partial y}\left(\mu\frac{\partial w}{\partial y}\right)-\frac{\partial}{\partial z}\left(\frac{2}{3}\mu\frac{\partial u}{\partial x}\right)-\frac{\partial}{\partial z}\left(\frac{2}{3}\mu\frac{\partial v}{\partial y}\right) \quad (4.40)$$
$$+\frac{\partial}{\partial x}\left(\mu\frac{\partial u}{\partial z}\right)+\frac{\partial}{\partial y}\left(\mu\frac{\partial v}{\partial z}\right)$$

This can be simplified as:

$$\left(\frac{\partial}{\partial x}\rho uw+\frac{\partial}{\partial y}\rho vw+\frac{\partial}{\partial z}\rho ww\right)=-\frac{\partial p}{\partial z}+\frac{\partial}{\partial x}\left(\mu\frac{\partial w}{\partial x}\right)+\frac{\partial}{\partial y}\left(\mu\frac{\partial w}{\partial y}\right)$$
$$+\frac{\partial}{\partial z}\left(\mu\frac{\partial w}{\partial z}\right)+\frac{\partial}{\partial z}\left(\frac{1}{3}\mu\frac{\partial w}{\partial z}\right)-\frac{\partial}{\partial z}\left(\frac{2}{3}\mu\frac{\partial u}{\partial x}\right)-\frac{\partial}{\partial z}\left(\frac{2}{3}\mu\frac{\partial v}{\partial y}\right) \quad (4.41)$$
$$+\frac{\partial}{\partial x}\left(\mu\frac{\partial u}{\partial z}\right)+\frac{\partial}{\partial y}\left(\mu\frac{\partial v}{\partial z}\right)$$

Now, consider the last two terms in equation i.e. $\frac{\partial}{\partial x}\left(\mu\frac{\partial u}{\partial z}\right)$, $\frac{\partial}{\partial y}\left(\mu\frac{\partial v}{\partial z}\right)$ if a continuous differentiability is assumed then the partial derivatives on these last two terms can be interchanged. This gives:

$$\left(\frac{\partial}{\partial x}\rho uw+\frac{\partial}{\partial y}\rho vw+\frac{\partial}{\partial z}\rho ww\right)=-\frac{\partial p}{\partial z}+\frac{\partial}{\partial x}\left(\mu\frac{\partial w}{\partial x}\right)$$
$$+\frac{\partial}{\partial y}\left(\mu\frac{\partial w}{\partial y}\right)+\frac{\partial}{\partial z}\left(\mu\frac{\partial w}{\partial z}\right)+\frac{\partial}{\partial z}\left(\frac{1}{3}\mu\frac{\partial w}{\partial z}\right)-\frac{\partial}{\partial z}\left(\frac{2}{3}\mu\frac{\partial u}{\partial x}\right) \quad (4.42)$$
$$-\frac{\partial}{\partial z}\left(\frac{2}{3}\mu\frac{\partial v}{\partial y}\right)+\frac{\partial}{\partial z}\left(\mu\frac{\partial u}{\partial x}\right)+\frac{\partial}{\partial z}\left(\mu\frac{\partial v}{\partial y}\right)$$

Further, simplification yields:

$$\left(\frac{\partial}{\partial x}\rho uw+\frac{\partial}{\partial y}\rho vw+\frac{\partial}{\partial z}\rho ww\right)=-\frac{\partial p}{\partial z}+\frac{\partial}{\partial x}\left(\mu\frac{\partial w}{\partial x}\right)$$
$$+\frac{\partial}{\partial y}\left(\mu\frac{\partial w}{\partial y}\right)+\frac{\partial}{\partial z}\left(\mu\frac{\partial w}{\partial z}\right) \quad (4.43)$$
$$+\frac{\partial}{\partial z}\left[\left(\frac{1}{3}\mu\frac{\partial u}{\partial x}\right)-\left(\frac{2}{3}\mu\frac{\partial v}{\partial y}\right)-\left(\frac{2}{3}\mu\frac{\partial w}{\partial z}\right)+\left(\mu\frac{\partial v}{\partial y}\right)+\left(\mu\frac{\partial w}{\partial z}\right)\right]$$

Simplifying:

$$\left(\frac{\partial}{\partial x}\rho uw+\frac{\partial}{\partial y}\rho vw+\frac{\partial}{\partial z}\rho ww\right)=-\frac{\partial p}{\partial z}+\frac{\partial}{\partial x}\left(\mu\frac{\partial w}{\partial x}\right)$$
$$+\frac{\partial}{\partial y}\left(\mu\frac{\partial w}{\partial y}\right)+\frac{\partial}{\partial z}\left(\mu\frac{\partial w}{\partial z}\right) \quad (4.44)$$
$$+\frac{\partial}{\partial z}\left[\left(\frac{1}{3}\mu\frac{\partial v}{\partial y}\right)+\left(\frac{1}{3}\mu\frac{\partial u}{\partial x}\right)+\left(\frac{1}{3}\mu\frac{\partial w}{\partial z}\right)\right]$$

Combining terms of viscosity:

$$\left(\frac{\partial}{\partial x}\rho uw+\frac{\partial}{\partial y}\rho vw+\frac{\partial}{\partial z}\rho ww\right)=-\frac{\partial p}{\partial z}+\frac{\partial}{\partial x}\left(\mu\frac{\partial w}{\partial x}\right)$$
$$+\frac{\partial}{\partial y}\left(\mu\frac{\partial w}{\partial y}\right)+\frac{\partial}{\partial z}\left(\mu\frac{\partial w}{\partial z}\right)+\frac{\partial}{\partial z}\left[\frac{1}{3}\mu\left(\frac{\partial v}{\partial y}+\frac{\partial u}{\partial x}+\frac{\partial w}{\partial z}\right)\right] \quad (4.45)$$

Further, combining terms together we get:

$$\left(\frac{\partial}{\partial x}\rho uw+\frac{\partial}{\partial y}\rho vw+\frac{\partial}{\partial z}\rho ww\right)=-\frac{\partial p}{\partial z}+\frac{\partial}{\partial x}\left(\mu\frac{\partial w}{\partial x}\right)$$
$$+\frac{\partial}{\partial y}\left(\mu\frac{\partial w}{\partial y}\right)+\frac{\partial}{\partial z}\left(\mu\frac{\partial w}{\partial z}\right)+\frac{\partial}{\partial z}\left(\frac{1}{3}\mu\nabla.\vec{V}\right) \quad (4.46)$$

Equation, is the simplified Z-momentum Navier-stokes equation.

4.5.3.1 Non dimensionalization of Navier-Stokes Z-momentum equation

We non-dimensionalize the simplified three dimensional Z-momentum Navier-Stokes equation to carry out a scaling analysis. The scaling analysis is carried out in order to reduce the three dimensional Z-momentum Navier-Stokes equation into a simplified thin film three dimensional Z-momentum Navier-Stokes equation. The simplified three dimensional Z-momentum Navier-Stokes equation is given by:

$$\begin{aligned}\left(\frac{\partial}{\partial x}\rho uw+\frac{\partial}{\partial y}\rho vw+\frac{\partial}{\partial z}\rho ww\right)&=-\frac{\partial p}{\partial z}+\frac{\partial}{\partial x}\left(\mu\frac{\partial w}{\partial x}\right)\\&+\frac{\partial}{\partial y}\left(\mu\frac{\partial w}{\partial y}\right)+\frac{\partial}{\partial z}\left(\mu\frac{\partial w}{\partial z}\right)+\frac{\partial}{\partial z}\left(\frac{1}{3}\mu\nabla.\vec{V}\right)\end{aligned} \tag{4.47}$$

We apply the same non-dimensional lubrication scaling as applied to X-Momentum and Y-Momentum Navier-stokes equations . This gives:

$$\begin{aligned}&\frac{\partial}{\partial(\bar{x}L)}\left(\bar{\rho}\rho_0\bar{u}u_0\bar{w}u_0\right)+\frac{\partial}{\partial(\bar{y}C)}\left(\bar{\rho}\rho_0\bar{v}u_0\left(\frac{C}{L}\right)\bar{w}u_0\right)\\&+\frac{\partial}{\partial(\bar{z}R)}\left(\bar{\rho}\rho_0\bar{w}u_0\bar{w}u_0\right)=-\frac{\partial(\bar{p}P_a)}{\partial(\bar{z}R)}+\frac{\partial}{\partial(\bar{x}L)}\left(\bar{\mu}\mu_0\frac{\partial(\bar{w}u_0)}{(\bar{x}L)}\right)\\&+\frac{\partial}{\partial(\bar{y}C)}\left(\bar{\mu}\mu_0\frac{\partial(\bar{w}u_0)}{(\bar{y}C)}\right)+\frac{\partial}{\partial(\bar{z}R)}\left(\bar{\mu}\mu_0\frac{\partial(\bar{w}u_0)}{(\bar{z}R)}\right)\\&+\frac{\partial}{\partial(\bar{z}R)}\left(\frac{1}{3}\bar{\mu}\mu_0\left(\frac{\partial\bar{U}U_0}{\partial\bar{X}L}+\frac{\partial\bar{v}u_0\left(\frac{C}{L}\right)}{\partial(\bar{y}C)}+\frac{\partial\bar{w}u_0}{\partial\bar{z}R}\right)\right)\end{aligned} \tag{4.48}$$

Taking constants out of derivatives we get:

$$
\begin{aligned}
&(\frac{\rho_0 u_0 u_0}{L}) * \frac{\partial(\bar{\rho}\bar{u}\bar{w})}{\partial\bar{x}} + \left(\frac{\rho_0 u_0 u_0}{L}\right) * \frac{\partial(\bar{\rho}\bar{v}\bar{w})}{\partial\bar{y}} + \left(\frac{\rho_0 u_0 u_0}{R}\right) * \frac{\partial(\bar{\rho}\bar{w}\bar{w})}{\partial\bar{z}} \\
&= -\left(\frac{P_a}{R}\right) * \frac{\partial\bar{p}}{\partial\bar{z}} + \left(\frac{\mu_0 u_0}{L*L}\right) * \frac{\partial}{\partial\bar{x}}\left(\bar{\mu}\frac{\partial\bar{w}}{\partial\bar{x}}\right) + \left(\frac{\mu_0 u_0}{C*C}\right) * \frac{\partial}{\partial\bar{y}}\left(\bar{\mu}\frac{\partial\bar{w}}{\partial\bar{y}}\right) \\
&+ \left(\frac{\mu_0 u_0}{R*R}\right) * \frac{\partial}{\partial\bar{z}}\left(\bar{\mu}\frac{\partial\bar{w}}{\partial\bar{z}}\right) \\
&+ \frac{1}{3}\left(\frac{\mu_0 u_0}{R*L}\right)\frac{\partial}{\partial\bar{z}}\left\{\bar{\mu}\left[\left(\frac{\partial\bar{u}}{\partial\bar{x}}\right) + \left(\frac{\partial\bar{v}}{\partial\bar{y}}\right) + \left(\frac{L}{R}\right)\left(\frac{\partial\bar{w}}{\partial\bar{z}}\right)\right]\right\}
\end{aligned}
\tag{4.49}
$$

Dividing equation (4.49) throughout by $(\frac{\rho_0 u_0 u_0}{L})$ i.e. coefficient of derivative of 'x' term. We get:

$$
\begin{aligned}
&\frac{\partial(\bar{\rho}\bar{u}\bar{w})}{\partial\bar{x}} + \frac{\partial(\bar{\rho}\bar{v}\bar{w})}{\partial\bar{y}} + \left(\frac{L}{R}\right) * \frac{\partial(\bar{\rho}\bar{w}\bar{w})}{\partial\bar{z}} = -\left(\frac{P_a}{\rho_0 u_0 u_0}\right) * \frac{\partial\bar{p}}{\partial\bar{x}} \\
&+ \left(\frac{\mu_0}{\rho_0 u_0 L}\right) * \frac{\partial}{\partial\bar{x}}\left(\bar{\mu}\frac{\partial\bar{u}}{\partial\bar{x}}\right) + \left(\frac{\mu_0 L}{\rho_0 u_0 C*C}\right) * \frac{\partial}{\partial\bar{y}}\left(\bar{\mu}\frac{\partial\bar{u}}{\partial\bar{y}}\right) \\
&+ \left(\frac{\mu_0 L}{\rho_0 u_0 R*R}\right) * \frac{\partial}{\partial\bar{z}}\left(\bar{\mu}\frac{\partial\bar{u}}{\partial\bar{z}}\right) \\
&+ \frac{1}{3}\left(\frac{\mu_0}{\rho_0 u_0 L}\right)\frac{\partial}{\partial\bar{x}}\left\{\bar{\mu}\left[\left(\frac{\partial\bar{u}}{\partial\bar{x}}\right) + \left(\frac{\partial\bar{v}}{\partial\bar{y}}\right) + \left(\frac{L}{R}\right)\left(\frac{\partial\bar{w}}{\partial\bar{z}}\right)\right]\right\}
\end{aligned}
\tag{4.50}
$$

From the above equation it can be observed that similar terms appear as coefficients in X-momentum and Y-momentum Navier-Stokes equations. The magnitude of the terms $\frac{\mu_0}{\rho_0 u_0 L}$, $\frac{\mu_0 L}{\rho_0 u_0 R*R}$ are quite small thus, the terms appearing as coefficients with these terms can be neglected.

These assumptions reduce the Z-momentum Navier-Stokes equation to :

$$\frac{\partial\left(\bar{\rho}\bar{u}\bar{w}\right)}{\partial\bar{x}}+\frac{\partial\left(\bar{\rho}\bar{v}\bar{w}\right)}{\partial\bar{y}}+\left(\frac{L}{R}\right)*\frac{\partial\left(\bar{\rho}\bar{w}\bar{w}\right)}{\partial\bar{z}}=\frac{\mu_0 L}{\rho_0 u_0 *C*C}*\frac{\partial}{\partial\bar{y}}\left(\bar{\mu}\frac{\partial\bar{w}}{\partial\bar{y}}\right)$$
$$-\left(\frac{L}{\rho_0 u_0 u_0}\right)*\left(\frac{P_a}{R}\right)*\frac{\partial\bar{p}}{\partial\bar{z}} \tag{4.51}$$

This is the thin film z-momentum Navier-stokes equation.

4.6 The Continuity Equation For Compressible Flow

The continuity equation is essentially a mass conservation equation that results from the concept of fluid mass balance across control volumes. In describing the momentum of a fluid, we should note that in the case of a solid body, its mass is readily defined. However, in the case of a fluid, we are dealing with a continuum and the only way to define mass at any given location is in terms of mass flux, i.e. mass transport rate per unit cross sectional area through which flow occurs. This quantity is equal to the product of density of the fluid times its velocity 'ρu' .The velocity fields need to satisfy the continuity equation in order to obtain a correct density field. The density based solver adopted in this thesis solves continuity equation for density field, based on the velocities from the solutions of Navier-stokes momentum equations in order to calculate corrected pressure. Density and pressure are coupled by the equation of state. The density is used to calculate the corrected pressure by the ideal gas law which has been assumed as the equation of state. The three dimensional compressible continuity equation is given by:

$$\left(\frac{\partial}{\partial x}\rho u+\frac{\partial}{\partial y}\rho v+\frac{\partial}{\partial z}\rho w\right)=0 \tag{4.52}$$

4.6.1 Non Dimensionalization Of Continuity Equation

The conventional non-dimensional lubrication scaling discussed in section 4.4.1 is applied to the continuity equation in the same manner as applied to the Reynolds equation and Navier-Stokes equation discussed in sections 4.4 and 4.5. The non-dimensional lubrication scaling applied to the continuity equation gives:

$$\frac{\partial}{\partial(\bar{x}L)}(\bar{\rho}\rho_0\bar{u}u_0)+\frac{\partial}{\partial(\bar{y}C)}\left(\bar{\rho}\rho_0\bar{v}u_0\left(\frac{C}{L}\right)\right)+\frac{\partial}{\partial(\bar{z}R)}(\bar{\rho}\rho_0\bar{w}u_0)=0 \qquad (4.53)$$

Taking constants out of the derivatives simplifies the equation as:

$$(\frac{\rho_0 u_0}{L})*\frac{\partial(\bar{\rho}\bar{u})}{\partial\bar{x}}+\left(\frac{\rho_0 u_0}{L}\right)*\frac{\partial(\bar{\rho}\bar{v})}{\partial\bar{y}}+\left(\frac{\rho_0 u_0}{R}\right)*\frac{\partial(\bar{\rho}\bar{w})}{\partial\bar{z}}=0 \qquad (4.54)$$

The above equation is divided by $\frac{\rho_0 u_0}{L}$ i.e. coefficient of derivative of 'x' term this reduces the continuity equation as:

$$\frac{\partial(\bar{\rho}\bar{u})}{\partial\bar{x}}+\frac{\partial(\bar{\rho}\bar{v})}{\partial\bar{y}}+\left(\frac{L}{R}\right)*\frac{\partial(\bar{\rho}\bar{w})}{\partial\bar{z}}=0 \qquad (4.55)$$

The constant coefficient appearing along with the '$\bar{\rho}\bar{w}$' term can be expressed as:

$$\frac{\partial(\bar{\rho}\bar{u})}{\partial\bar{x}}+\frac{\partial(\bar{\rho}\bar{v})}{\partial\bar{y}}+\left(\frac{1}{c1}\right)*\frac{\partial(\bar{\rho}\bar{w})}{\partial\bar{z}}=0 \qquad (4.56)$$

4.7 Convection Diffusion Schemes For The Governing Equations

Finite Volume discretization requires the governing equations to be expressed in a convection diffusion form as discussed in section 4.3. The convection diffusion form of the governing equations consists of combinations of convection and diffusion terms within the equation, as well as a source term. The convection Term has an in-separable

connection with the diffusion term, and therefore, the two terms are handled in the Finite Volume Discretization scheme as one unit [13].

4.7.1 Convection-Diffusion Form Of Compressible Reynolds Equation

The Non dimensionalized Reynolds equation in section 4.4.1 can be easily converted into a convection diffusion form or a flux form by a minor transformation.

Consider the non-dimensionalized Reynolds equation in section 4.4.1 given as:

$$\frac{\partial}{\partial \bar{x}}\left(\frac{\bar{p}\bar{H}^3}{\bar{\mu}}\frac{\partial \bar{p}}{\partial \bar{x}}\right)+\frac{\partial}{\partial \bar{z}}\left(\frac{\bar{p}\bar{H}^3L^2}{\bar{\mu}R^2}\frac{\partial \bar{p}}{\partial \bar{z}}\right)=\Delta\frac{\partial}{\partial(\bar{x})}\left(\bar{p}\bar{H}\right)$$

Transferring the term on right hand side of the equation to the left hand side and combining with its related diffusive term along ‘x’ direction, we get:

$$\frac{\partial}{\partial \bar{x}}\left(\frac{\bar{p}\bar{H}^3}{\bar{\mu}}\left(\frac{\partial \bar{p}}{\partial \bar{x}}\right)-\Delta\bar{p}\bar{H}\right)+\frac{\partial}{\partial \bar{z}}\left(\frac{\bar{p}\bar{H}^3L^2}{\bar{\mu}R^2}\frac{\partial \bar{p}}{\partial \bar{z}}\right)=0 \qquad (4.57)$$

The above mentioned equation is a convection diffusion form of the Reynolds equation.

4.7.2. Convection-Diffusion Form Of Thin Film Navier-Stokes X-Momentum Equation

the thin film Navier-Stokes x-momentum equation derived in section 4.5.1.1 is given as:

$$\frac{\partial\left(\bar{\rho}\overline{uu}\right)}{\partial \bar{x}}+\frac{\partial\left(\bar{\rho}\overline{vu}\right)}{\partial \bar{y}}+\left(\frac{L}{R}\right)*\frac{\partial\left(\bar{\rho}\overline{wu}\right)}{\partial \bar{z}}=\frac{\mu_0 L}{\rho_0 u_0 * C * C}*\frac{\partial}{\partial \bar{y}}\left(\bar{\mu}\frac{\partial \bar{u}}{\partial \bar{y}}\right)-\frac{P_a}{\rho_0 u_0 u_0}*\frac{\partial \bar{p}}{\partial \bar{x}} \qquad (4.58)$$

This equation can be converted into the convection diffusion scheme with minor simplification as follows:

$$\frac{\partial\left(\bar{\rho}\bar{u}\bar{u}\right)}{\partial\bar{x}}+\frac{\partial\left(\bar{\rho}\bar{v}\bar{u}\right)}{\partial\bar{y}}+\frac{1}{\left(\frac{R}{L}\right)}*\frac{\partial\left(\bar{\rho}\bar{w}\bar{u}\right)}{\partial\bar{z}}=\frac{1}{\left(\frac{\rho_0 u_0 *C*C}{\mu_0 L}\right)}*\frac{\partial}{\partial\bar{y}}\left(\bar{\mu}\frac{\partial\bar{u}}{\partial\bar{y}}\right)$$
$$-\left(\frac{P_a}{\rho_0 u_0 u_0}\right)\frac{\partial\bar{p}}{\partial\bar{x}} \quad (4.59)$$

For simplicity of expression, we express certain quantities appearing as coefficients with the derivatives as constants. These constants are denoted as:

$$C1=\left(\frac{R}{L}\right),\ C2=\left(\frac{\rho_0 u_0 *C*C}{\mu_0 L}\right)\ \text{and},\ C3=\left(\frac{P_a}{\rho_0 u_0 u_0}\right)$$

This allows expression of the thin film X-Momentum Navier-stokes equation as:

$$\frac{\partial\left(\bar{\rho}\bar{u}\bar{u}\right)}{\partial\bar{x}}+\frac{\partial\left(\bar{\rho}\bar{v}\bar{u}\right)}{\partial\bar{y}}+\frac{1}{c1}*\frac{\partial\left(\bar{\rho}\bar{w}\bar{u}\right)}{\partial\bar{z}}=\frac{1}{c2}*\frac{\partial}{\partial\bar{y}}\left(\bar{\mu}\frac{\partial\bar{u}}{\partial\bar{y}}\right)-\mathrm{C3}*\frac{\partial\bar{p}}{\partial\bar{x}} \quad (4.60)$$

This can be further simplified as:

$$\frac{\partial\left(\bar{\rho}\bar{u}\bar{u}\right)}{\partial\bar{x}}+\frac{\partial\left(\bar{\rho}\bar{v}\bar{u}\right)}{\partial\bar{y}}+\frac{\partial\left(\frac{\bar{\rho}\bar{w}\bar{u}}{c1}\right)}{\partial\bar{z}}=\frac{\partial}{\partial\bar{y}}\left(\frac{\bar{\mu}}{c2}\frac{\partial\bar{u}}{\partial\bar{y}}\right)-\mathrm{C3}*\frac{\partial\left(\bar{p}\right)}{\partial\left(\bar{x}\right)} \quad (4.61)$$

By Including diffusive coefficients from the right hand side within convective derivatives on the left hand side we get the convection diffusion form of the thin film X momentum Navier-Stokes equation as:

$$\frac{\partial\left(\bar{\rho}\bar{u}\bar{u}\right)}{\partial\bar{x}}+\frac{\partial}{\partial\bar{y}}\left(\bar{\rho}\bar{v}\bar{u}-\frac{\bar{\mu}}{c2}\frac{\partial\bar{u}}{\partial\bar{y}}\right)+\frac{\partial}{\partial\bar{z}}\left(\frac{\bar{\rho}\bar{w}\bar{u}}{c1}\right)=-\mathrm{c3}\frac{\partial\left(\bar{p}\right)}{\partial\left(\bar{x}\right)} \quad (4.62)$$

The above equation is the convection diffusion form of the thin film X momentum Navier-Stokes equation. The equation calculates the velocity field '$\bar{u}$' by employing an iterative algorithm. Gauss-Seidel is a promising iterative method to solve iterative algebraic equations. The unknown velocity field '$\bar{u}$' is calculated by starting with a guess velocity field and iterating with substitution of latest calculate velocity field '$\bar{u}$' till convergence is achieved.

4.7.3. Convection-Diffusion Form Of Thin Film Navier-Stokes Y-Momentum Equation

The thin film Navier-Stokes y-momentum equation derived in section 4.5.2.1 is given as:

$$\frac{\partial\left(\bar{\rho}\bar{u}\bar{v}\right)}{\partial\bar{x}}+\frac{\partial\left(\bar{\rho}\bar{v}\bar{v}\right)}{\partial\bar{y}}+\left(\frac{L}{R}\right)*\frac{\partial\left(\bar{\rho}\bar{w}\bar{v}\right)}{\partial\bar{z}}=\frac{\mu_0 L}{\rho_0 u_0 *C*C}*\frac{\partial}{\partial\bar{y}}\left(\bar{\mu}\frac{\partial\bar{v}}{\partial\bar{y}}\right)+\frac{1}{3}\left(\frac{\mu_0 L}{\rho_0 u_0 C*C}\right)\frac{\partial}{\partial\bar{y}}\left\{\bar{\mu}\left[\left(\frac{\partial\bar{u}}{\partial\bar{x}}\right)+\left(\frac{\partial\bar{v}}{\partial\bar{y}}\right)+\frac{L}{R}\left(\frac{\partial\bar{w}}{\partial\bar{z}}\right)\right]\right\} \tag{4.63}$$

This equation can be converted into the convection diffusion scheme similar to the X-Momentum equation with minor simplification as follows:

$$\frac{\partial\left(\bar{\rho}\bar{u}\bar{v}\right)}{\partial\bar{x}}+\frac{\partial\left(\bar{\rho}\bar{v}\bar{v}\right)}{\partial\bar{y}}+\frac{1}{\left(\frac{R}{L}\right)}*\frac{\partial\left(\bar{\rho}\bar{w}\bar{v}\right)}{\partial\bar{z}}=\frac{1}{\left(\frac{\rho_0 u_0 *C*C}{\mu_0 L}\right)}*\frac{\partial}{\partial\bar{y}}\left(\bar{\mu}\frac{\partial\bar{v}}{\partial\bar{y}}\right)+\frac{1}{3}\frac{1}{\left(\frac{\rho_0 u_0 *C*C}{\mu_0 L}\right)}\frac{\partial}{\partial\bar{y}}\left\{\bar{\mu}\left[\left(\frac{\partial\bar{u}}{\partial\bar{x}}\right)+\left(\frac{\partial\bar{v}}{\partial\bar{y}}\right)+\frac{1}{\left(\frac{R}{L}\right)}\left(\frac{\partial\bar{w}}{\partial\bar{z}}\right)\right]\right\} \tag{4.64}$$

With reference to the constants defined in section 4.5.1.1 for x-momentum equation, the y-momentum equation can be expressed with similar coefficients. This allows ease of expression of the y-momentum equation into the convection diffusion scheme.

This simplifies the y-momentum equation as:

$$\frac{\partial\left(\bar{\rho}\overline{uv}\right)}{\partial\bar{x}}+\frac{\partial\left(\bar{\rho}\overline{vv}\right)}{\partial\bar{y}}+\frac{1}{c1}*\frac{\partial\left(\bar{\rho}\overline{wv}\right)}{\partial\bar{z}}=\frac{1}{c2}*\frac{\partial}{\partial\bar{y}}\left(\bar{\mu}\frac{\partial\bar{v}}{\partial\bar{y}}\right)$$
$$+\frac{1}{3}*\frac{1}{c2}*\frac{\partial}{\partial\bar{y}}\left\{\bar{\mu}\left[\left(\frac{\partial\bar{u}}{\partial\bar{x}}\right)+\left(\frac{\partial\bar{v}}{\partial\bar{y}}\right)+\frac{1}{c1}\left(\frac{\partial\bar{w}}{\partial\bar{z}}\right)\right]\right\} \quad (4.65)$$

Similar to the x-momentum equation, By Including diffusive coefficients from the right hand side within convective derivatives on the left hand side we get the convection diffusion form of the thin film Y momentum Navier-Stokes equation as:

$$\frac{\partial\left(\bar{\rho}\overline{uv}\right)}{\partial\bar{x}}+\frac{\partial}{\partial\bar{y}}\left(\bar{\rho}\overline{vv}-\frac{\bar{\mu}}{c2}\frac{\partial\bar{v}}{\partial\bar{y}}\right)+\frac{\partial}{\partial\bar{z}}\left(\frac{\bar{\rho}\overline{wv}}{c1}\right)$$
$$=\frac{1}{c2}*\frac{1}{3}*\frac{\partial}{\partial\bar{y}}\left\{\bar{\mu}\left[\left(\frac{\partial\bar{u}}{\partial\bar{x}}\right)+\left(\frac{\partial\bar{v}}{\partial\bar{y}}\right)+\frac{1}{c1}\left(\frac{\partial\bar{w}}{\partial\bar{z}}\right)\right]\right\} \quad (4.66)$$

The above equation is the convection diffusion form of the thin film Y momentum Navier-Stokes equation. It is interesting to note that the thin film Navier-stokes X and Y momentum equations have a very similar behavior. The Left hand terms in the two momentum equations are similar with exception to the fundamental velocity variable field which is different for the three momentum equations. The source terms Right hand side terms in the two equations are fundamentally different. The X momentum equation derives its source from pressure gradient along X direction i.e. in the direction of $'\bar{u}'$ velocity. The greater this pressure gradient the stronger the magnitude of the source

term. The pressure gradient is mainly along the direction of Runner motion. This forms the source for driving velocity field within the fluid domain.

The Y momentum has a different nature of source. The source for driving $'\bar{v}'$ velocity originates from the product of gradient of viscosity and the divergence of velocity term i.e. dilatation term given as: $\frac{1}{c2}*\frac{1}{3}*\frac{\partial}{\partial\bar{y}}\left\{\bar{\mu}\left[\left(\frac{\partial\bar{u}}{\partial\bar{x}}\right)+\left(\frac{\partial\bar{v}}{\partial\bar{y}}\right)+\frac{1}{c1}\left(\frac{\partial\bar{w}}{\partial\bar{z}}\right)\right]\right\}$. Physically, due to a strongly convection dominated flow, The relative contribution of this term as a source is much lower compared to the source terms for X and Z momentum equations.

Similar to the X-momentum equation, The Y momentum equation calculates the velocity field $'\bar{v}'$ by employing the same iterative algorithm. The unknown velocity field $'\bar{v}'$ is calculated by starting with a guess velocity field and iterating with substitution of latest calculate velocity field $'\bar{v}'$ till convergence is achieved.

4.7.4. Convection-Diffusion Form Of Thin Film Navier-Stokes Z-Momentum Equation

The thin film z-momentum Navier-Stokes equation derived in section 4.5.3.1 is repeated in this section for conversion into a convection diffusion form. This is similar to the convection diffusion forms of thin film Navier-stokes X and Y momentum equations discussed in sections 4.5.1 and 4.5.2.

The thin film z-momentum Navier-Stokes equation is given as:

$$\frac{\partial\left(\bar{\rho}\bar{u}\bar{w}\right)}{\partial\bar{x}}+\frac{\partial\left(\bar{\rho}\bar{v}\bar{w}\right)}{\partial\bar{y}}+\left(\frac{L}{R}\right)*\frac{\partial\left(\bar{\rho}\bar{w}\bar{w}\right)}{\partial\bar{z}}= \frac{\mu_0 L}{\rho_0 u_0 * C * C}*\frac{\partial}{\partial\bar{y}}\left(\bar{\mu}\frac{\partial\bar{w}}{\partial\bar{y}}\right)-\left(\frac{L}{\rho_0 u_0 u_0}\right)*\left(\frac{P_a}{R}\right)*\frac{\partial\bar{p}}{\partial\bar{z}} \tag{4.67}$$

This equation can be converted into the convection diffusion scheme similar to the X-Momentum and Y-Momentum equations with minor simplification as follows:

$$\frac{\partial\left(\bar{\rho}\bar{u}\bar{w}\right)}{\partial\bar{x}}+\frac{\partial\left(\bar{\rho}\bar{v}\bar{w}\right)}{\partial\bar{y}}+\frac{1}{\left(\frac{R}{L}\right)}*\frac{\partial\left(\bar{\rho}\bar{w}\bar{w}\right)}{\partial\bar{z}}=\frac{1}{\left(\frac{\rho_0 u_0 * C * C}{\mu_0 L}\right)}*\frac{\partial}{\partial\bar{y}}\left(\bar{\mu}\frac{\partial\bar{w}}{\partial\bar{y}}\right)$$
$$-\left(\frac{P_a}{\rho_0 u_0 u_0}\right)*\frac{1}{\left(\frac{R}{L}\right)}*\frac{\partial\bar{p}}{\partial\bar{z}} \quad (4.68)$$

Expressing coefficients as constants, simplifies the thin film z-momentum Navier-Stokes equation as:

$$\frac{\partial\left(\bar{\rho}\bar{u}\bar{w}\right)}{\partial\bar{x}}+\frac{\partial\left(\bar{\rho}\bar{v}\bar{w}\right)}{\partial\bar{y}}+\frac{1}{c1}*\frac{\partial\left(\bar{\rho}\bar{w}\bar{w}\right)}{\partial\bar{z}}=\frac{1}{c2}*\frac{\partial}{\partial\bar{y}}\left(\bar{\mu}\frac{\partial\bar{w}}{\partial\bar{y}}\right)-\mathrm{C3}*\left(\frac{1}{\mathrm{c1}}\right)*\frac{\partial\bar{p}}{\partial z} \quad (4.69)$$

Similar methodology is adapted for the Z-Momentum equation as for X and Y momentum equations discussed in section 4.5.1 and 4.5.2. The Diffusive term is transferred to the left side and included within the convective term to produce a more suitable form for numerical modelling i.e. convection diffusion form. The pressure gradient term along Z direction appears as source and is retained on the right hand side of the Z-Momentum equation. Similar to the X momentum equation the pressure gradient term along 'Z' direction drives the velocity field $'\bar{w}$'. This simplification gives:

$$\frac{\partial\left(\bar{\rho}\bar{u}\bar{w}\right)}{\partial\bar{x}}+\frac{\partial}{\partial\bar{y}}\left(\overline{\rho v w}-\frac{\bar{\mu}}{c2}\frac{\partial\bar{w}}{\partial\bar{y}}\right)+\frac{\partial}{\partial\bar{z}}\left(\frac{\bar{\rho}\bar{w}\bar{w}}{c1}\right)=-\left(\frac{\mathrm{C3}}{\mathrm{c1}}\right)*\frac{\partial\bar{p}}{\partial z} \quad (4.70)$$

The above equation is the convection diffusion form of the thin film Z-Momentum Navier-Stokes equation.

4.7.5 Convection-Diffusion Form Of Compressible Continuity Equation

The continuity equation is a purely convection driven equation. While the form of continuity equation looks fairly simple compared to non-linearity of Momentum equations, the solution to continuity equation is not straight forward. An approach has been undertaken in this thesis to solve density field from continuity using momentum velocities. This has been made possible by converting the continuity equation into a convection diffusion form where diffusion is zero. To aid in conversion of the continuity equation into convection diffusion scheme an artificial diffusion coefficient has been added to the right hand side of the continuity equation however, this diffusion coefficient is physically assigned a value equal to zero during the computational process. The convection diffusion scheme of continuity is derived and expressed as shown below.

Consider the continuity equation discussed in section 4.6. repeated here:

$$\left(\frac{\partial}{\partial x} \rho u + \frac{\partial}{\partial y} \rho v + \frac{\partial}{\partial z} \rho w \right) = 0$$

The original form of continuity is recast into a form similar to that of Thin film Navier-stokes momentum equations. This is achieved by addition of the term '$\hat{\rho}$' that has a unit magnitude, on the left hand side of the equation. A diffusion coefficient 'γ_0' is added to the right hand side along with artificial diffusion terms of density. The diffusion coefficient is assigned as zero during computational method therefore, this retains the original undisturbed nature of continuity equation while in a convection diffusion form.
This addition makes the continuity to take up a form given as:

$$\left(\frac{\partial}{\partial \overline{x}} \hat{\rho} u \rho + \frac{\partial}{\partial \overline{y}} \hat{\rho} v \rho + \frac{\partial}{\partial \overline{z}} \hat{\rho} w \rho \right) = \gamma_0 \left[\frac{\partial}{\partial x} \left(\frac{\partial \rho}{\partial x} \right) + \frac{\partial}{\partial y} \left(\frac{\partial \rho}{\partial y} \right) + \frac{\partial}{\partial z} \left(\frac{\partial \rho}{\partial z} \right) \right] \quad (4.71)$$

Where, $\hat{\rho} = 1 \ \ and, \ \ \gamma_0 = 0$

Substituting the conventional lubrication scaling non dimensional quantities in the above equation we get:

$$\begin{aligned} &\frac{\partial}{\partial(\bar{x}L)}\left(\hat{\rho}\bar{\rho}\rho_0\bar{u}u_0\right)+\frac{\partial}{\partial(\bar{y}C)}\left(\hat{\rho}\bar{\rho}\rho_0\bar{v}u_0\left(\frac{C}{L}\right)\right)+\frac{\partial}{\partial(\bar{z}R)}\left(\hat{\rho}\bar{\rho}\rho_0\bar{w}u_0\right) \\ &=\gamma_0\left[\frac{\partial}{\partial\bar{x}L}\left(\frac{\partial\bar{\rho}\rho_0}{\partial\bar{x}L}\right)+\frac{\partial}{\partial\bar{y}C}\left(\frac{\partial\bar{\rho}\rho_0}{\partial\bar{y}C}\right)+\frac{\partial}{\partial\bar{z}R}\left(\frac{\partial\bar{\rho}\rho_0}{\partial\bar{z}R}\right)\right] \end{aligned} \tag{4.72}$$

This can be further simplified as:

$$\begin{aligned} &(\frac{\rho_0u_0}{L})*\frac{\partial}{\partial\bar{x}}\left(\hat{\rho}\bar{\rho}\bar{u}\right)+\left(\frac{\rho_0u_0}{L}\right)*\frac{\partial}{\partial\bar{y}}\left(\hat{\rho}\bar{\rho}\bar{v}\right)+\left(\frac{\rho_0u_0}{R}\right)*\frac{\partial}{\partial\bar{z}}\left(\hat{\rho}\bar{\rho}\bar{w}\right) \\ &=\gamma_0\left[\frac{\rho_0}{L^2}\left(\frac{\partial}{\partial\bar{x}}\left(\frac{\partial\bar{\rho}}{\partial\bar{x}}\right)\right)+\frac{\rho_0}{C^2}\left(\frac{\partial}{\partial\bar{y}}\left(\frac{\partial\bar{\rho}}{\partial\bar{y}}\right)\right)+\frac{\rho_0}{R^2}\left(\frac{\partial}{\partial\bar{z}}\left(\frac{\partial\bar{\rho}}{\partial\bar{z}}\right)\right)\right] \end{aligned} \tag{4.73}$$

Further simplification gives:

$$\begin{aligned} &(\frac{\rho_0u_0}{L})*\frac{\partial}{\partial\bar{x}}\left(\hat{\rho}\bar{\rho}\bar{u}\right)+\left(\frac{\rho_0u_0}{L}\right)*\frac{\partial}{\partial\bar{y}}\left(\hat{\rho}\bar{\rho}\bar{v}\right)+\left(\frac{\rho_0u_0}{R}\right)*\frac{\partial}{\partial\bar{z}}\left(\hat{\rho}\bar{\rho}\bar{w}\right) \\ &=\frac{\gamma_0\rho_0}{L^2}\left(\frac{\partial}{\partial\bar{x}}\left(\frac{\partial\bar{\rho}}{\partial\bar{x}}\right)\right)+\frac{\gamma_0\rho_0}{C^2}\left(\frac{\partial}{\partial\bar{y}}\left(\frac{\partial\bar{\rho}}{\partial\bar{y}}\right)\right)+\frac{\gamma_0\rho_0}{R^2}\left(\frac{\partial}{\partial\bar{z}}\left(\frac{\partial\bar{\rho}}{\partial\bar{z}}\right)\right) \end{aligned} \tag{4.74}$$

Dividing the above equation throughout by $(\frac{\rho_0u_0}{L})$ i.e. coefficient of derivative of 'x' term. We get:

$$\frac{\partial}{\partial \bar{x}}\left(\hat{\rho}\bar{\rho}\bar{u}\right)+\frac{\partial}{\partial \bar{y}}\left(\hat{\rho}\bar{\rho}\bar{v}\right)+\left(\frac{L}{R}\right)*\frac{\partial}{\partial \bar{z}}\left(\hat{\rho}\bar{\rho}\bar{w}\right)$$
$$=\frac{\gamma_0}{u_0 L}\left(\frac{\partial}{\partial \bar{x}}\left(\frac{\partial \bar{\rho}}{\partial \bar{x}}\right)\right)+\frac{\gamma_0}{\left(\frac{u_0 C^2}{L}\right)}\left(\frac{\partial}{\partial \bar{y}}\left(\frac{\partial \bar{\rho}}{\partial \bar{y}}\right)\right)+\frac{\gamma_0}{\left(\frac{u_0 R^2}{L}\right)}\left(\frac{\partial}{\partial \bar{z}}\left(\frac{\partial \bar{\rho}}{\partial \bar{z}}\right)\right) \quad (4.75)$$

The above form can be expressed into a more compact form by denoting certain coefficients as constants:

$$\frac{\partial}{\partial \bar{x}}\left(\hat{\rho}\bar{\rho}\bar{u}\right)+\frac{\partial}{\partial \bar{y}}\left(\hat{\rho}\bar{\rho}\bar{v}\right)+\frac{\partial}{\partial \bar{z}}\left(\frac{\hat{\rho}\bar{\rho}\bar{w}}{c1}\right)$$
$$=\frac{\partial}{\partial \bar{x}}\left(\frac{\gamma_0}{a1}\left(\frac{\partial \bar{\rho}}{\partial \bar{x}}\right)\right)+\frac{\partial}{\partial \bar{y}}\left(\frac{\gamma_0}{a2}\left(\frac{\partial \bar{\rho}}{\partial \bar{y}}\right)\right)+\frac{\partial}{\partial \bar{z}}\left(\frac{\gamma_0}{a3}\left(\frac{\partial \bar{\rho}}{\partial \bar{z}}\right)\right) \quad (4.76)$$

Where, $c1=\frac{R}{L}$, $a1=u_0 L$, $a2=\frac{u_0 C^2}{L}$ and $a3=\frac{u_0 R^2}{L}$

The above form can be recast into a convection diffusion scheme by transferring diffusion terms on the right hand side of the equation into convection terms on the left hand side. By converting to Standard convection diffusion form we get:

$$\frac{\partial}{\partial \bar{x}}\left(\hat{\rho}\bar{\rho}\bar{u}-\frac{\gamma_0}{a1}\left(\frac{\partial \bar{\rho}}{\partial \bar{x}}\right)\right)+\frac{\partial}{\partial \bar{y}}\left(\hat{\rho}\bar{\rho}\bar{v}-\frac{\gamma_0}{a2}\left(\frac{\partial \bar{\rho}}{\partial \bar{y}}\right)\right)$$
$$+\frac{\partial}{\partial \bar{z}}\left(\frac{\hat{\rho}\bar{\rho}\bar{w}}{c1}-\frac{\gamma_0}{a3}\left(\frac{\partial \bar{\rho}}{\partial \bar{z}}\right)\right)=0 \quad (4.77)$$

The form of the left hand side of the above continuity equation is very similar to the left hand side of the convection diffusion form of momentum equations. This helps in computational ease.

It is interesting to note that the diffusion coefficient 'γ_0' is added to the right hand side along with artificial diffusion terms of density have negligible or no effect on the solution of continuity owing to the zero or extremely low magnitude of the diffusion coefficient 'γ_0'. This further allows simplification of the convection diffusion form of continuity equation into the general convection diffusion form of the momentum equations discussed in sections 4.7.2, 4.7.3 and 4.7.4.The diffusion along x and Z directions is ignored to ease in expressibility. This form of the compressible continuity equation is represented as:

$$\frac{\partial}{\partial \bar{x}}\left(\hat{\rho}\bar{\rho}\bar{u}\right)+\frac{\partial}{\partial \bar{y}}\left(\hat{\rho}\bar{\rho}\bar{v}-\frac{\gamma_0}{a2}\left(\frac{\partial \bar{\rho}}{\partial \bar{y}}\right)\right)+\frac{\partial}{\partial \bar{z}}\left(\frac{\hat{\rho}\bar{\rho}\bar{w}}{c1}\right)=0 \qquad (4.78)$$

4.8 Finite Volume Discretization Of The Convection Diffusion Form Of Governing Equations

4.8.1 Finite Volume Discretization Of Reynolds Equation

The convection diffusion form of Reynolds equation derived in section 4.6.1. Can be discretized using the Finite Volume method. Consider the convection diffusion form of Reynolds equation presented in section 4.7.1 given as:

$$\frac{\partial}{\partial \bar{x}}\left(\frac{\bar{p}\bar{H}^3}{\bar{\mu}}\left(\frac{\partial \bar{p}}{\partial \bar{x}}\right)-\Delta\bar{p}\bar{H}\right)+\frac{\partial}{\partial \bar{z}}\left(\frac{\bar{p}\bar{H}^3L^2}{\bar{\mu}R^2}\frac{\partial \bar{p}}{\partial \bar{z}}\right)=0$$

This Is Equivalent To The Flux Form:

$$\frac{\partial}{\partial \bar{x}}\left\{\dot{J}_x\right\}+\frac{\partial}{\partial \bar{z}}\left(\dot{J}_z\right)=0 \qquad (4.79)$$

Where,

$$\dot{J}_x = \frac{\bar{p}\bar{H}^3}{\bar{\mu}}\left(\frac{\partial \bar{p}}{\partial \bar{x}}\right) - \Delta\bar{p}\bar{H} \tag{4.80}$$

$\dot{J}_x$ is the flux entering and leaving along x direction and $\dot{J}_z$ is the flux entering and leaving along z direction

Therefore,

$$\dot{J}_z = \frac{\bar{p}\bar{H}^3 L^2}{\bar{\mu}R^2}\frac{\partial \bar{p}}{\partial \bar{z}} \tag{4.81}$$

The flux form of equation can also be written as $\nabla.\dot{q} = 0$

Where,

$$\dot{q} = \left(\frac{\bar{p}\bar{H}^3}{\bar{\mu}}\left(\frac{\partial \bar{p}}{\partial \bar{x}}\right) - \Delta\bar{p}\bar{H}\right)i_x + \left(\frac{\bar{p}\bar{H}^3 L^2}{\bar{\mu}R^2}\frac{\partial \bar{p}}{\partial \bar{z}}\right)i_z$$

Integrating Equation (4.79) over the control surface as shaded in Figure 13, gives:

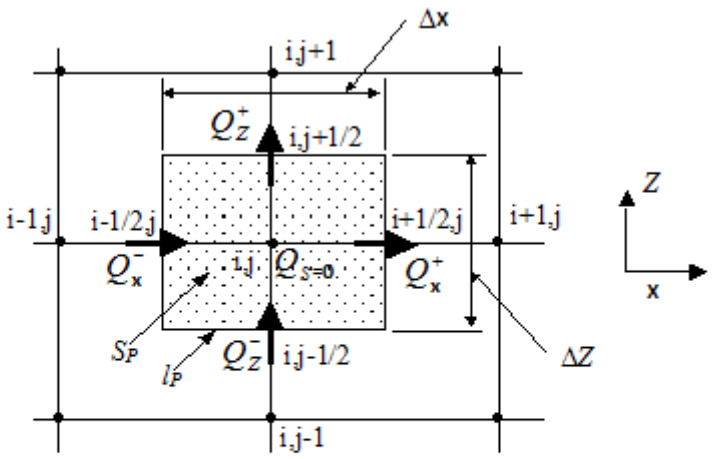

Figure 14, Grid scheme for Reynolds equation control volume method.

$$\iint_{Sp} \nabla . J \, dS_p = 0 \tag{4.82}$$

By, applying the divergence theorem to the left-hand side of the above equation we get:

$$\iint_{Sp} \nabla . J \, dS_p = \int_{lp} \dot{J} . n dl_p \tag{4.83}$$

Where,

$$\int_{lp} \dot{J} . n dl_p = \dot{J}_X^+ - \dot{J}_X^- + \dot{J}_Z^+ - \dot{J}_Z^- \tag{4.84}$$

$\dot{J}_X^+, \dot{J}_X^-, , \dot{J}_Z^+ \; and \; \dot{J}_Z^-$ are line integrals of fluxes along positive and negative x and z directions respectively. Substituting the value of flux terms in the above equation we get:

$$\int_{lp} \dot{J}.ndl_p = \left(\frac{\bar{p}\bar{H}^3}{\bar{\mu}} \left(\frac{\partial \bar{p}}{\partial \bar{x}} \right) - \Delta \bar{p} \bar{H} \right)_{i+\frac{1}{2},j} \Delta z$$
$$- \left(\frac{\bar{p}\bar{H}^3}{\bar{\mu}} \left(\frac{\partial \bar{p}}{\partial \bar{x}} \right) - \Delta \bar{p} \bar{H} \right)_{i-\frac{1}{2},j} \Delta z + \left(\frac{\bar{p}\bar{H}^3 L^2}{\bar{\mu} R^2} \frac{\partial \bar{p}}{\partial \bar{z}} \right)_{i,j+\frac{1}{2}} \Delta x \quad (4.85)$$
$$- \left(\frac{\bar{p}\bar{H}^3 L^2}{\bar{\mu} R^2} \frac{\partial \bar{p}}{\partial \bar{z}} \right)_{i,j-\frac{1}{2}} \Delta x$$

Now, from equations (4.84) and (4.82) we know,

$$\dot{J}_X^+ - \dot{J}_X^- + \dot{J}_Z^+ - \dot{J}_Z^- = 0 \quad (4.86)$$

Now, $consider\ \dot{J}_X^+$

$$\dot{J}_X^+ = \left(\frac{\bar{p}\bar{H}^3}{\bar{\mu}} \left(\frac{\partial \bar{p}}{\partial \bar{x}} \right) - \Delta \bar{p} \bar{H} \right)_{i+\frac{1}{2},j} \Delta z \quad (4.87)$$

Discretizing at east face we get :

$$\dot{J}_X^+ = \left(\frac{\bar{p}_{i+\frac{1}{2},j} \bar{H}_{i+\frac{1}{2},j}^{\ 3}}{\bar{\mu}_{i+\frac{1}{2},j}} \frac{(\bar{p}_{i+1,j} - \bar{p}_{i,j})}{\Delta x} .\Delta z \right) - \left(\Delta \frac{(\bar{p}_{i+1,j} + \bar{p}_{i,j})}{2} \bar{H}_{i+\frac{1}{2},j} \Delta z \right) \quad (4.88)$$

Expressing in terms of convection and diffusion terms we get:

$$\dot{J}_X^+ = \left(D_{i+\frac{1}{2},j}^{\ x+} - \frac{F_{i+\frac{1}{2},j}}{2} \right) (\bar{p}_{i+1,j}) - \left(-D_{i+\frac{1}{2},j}^{\ x+} - \frac{F_{i+\frac{1}{2},j}}{2} \right) (\bar{p}_{i,j}) \quad (4.89)$$

Where,

$$D_{east}{}^{x+} = \frac{\bar{p}_{i+\frac{1}{2},j}\bar{H}_{i+\frac{1}{2},j}{}^{3}}{\bar{\mu}_{i+\frac{1}{2},j}}\frac{\Delta z}{\Delta x} \tag{4.90}$$

And,

$$F_{east}{}^{x} = \Delta\bar{H}_{i+\frac{1}{2},j}\Delta z \tag{4.91}$$

Now, $consider\ \dot{J}_{\bar{X}}$ from equation (4.84)

$$\dot{J}_{\bar{X}} = \left(\frac{\bar{p}\bar{H}^{3}}{\bar{\mu}}\left(\frac{\partial\bar{p}}{\partial\bar{x}}\right) - \Delta\bar{p}\bar{H}\right)_{i-\frac{1}{2},j}\Delta z \tag{4.92}$$

Discretizing at east face we get:

$$\dot{J}_{\bar{X}} = \left(\frac{\bar{p}_{i-\frac{1}{2},j}\bar{H}_{i-\frac{1}{2},j}{}^{3}}{\bar{\mu}_{i-\frac{1}{2},j}}\frac{(\bar{p}_{i,j}-\bar{p}_{i-1,j})}{\Delta x}.\Delta z\right) - \left(\Delta\frac{(\bar{p}_{i,j}+\bar{p}_{i-1,j})}{2}\bar{H}_{i+\frac{1}{2},j}\Delta z\right) \tag{4.93}$$

Expressing in terms of convection and diffusion terms we get:

$$\dot{J}_{\bar{X}} = \left(D_{i-\frac{1}{2},j}{}^{x-} - \frac{F_{i-\frac{1}{2},j}}{2}\right)(\bar{p}_{i,j}) - \left(-D_{i-\frac{1}{2},j}{}^{x-} - \frac{F_{i-\frac{1}{2},j}}{2}\right)(\bar{p}_{i-1,j}) \tag{4.94}$$

Where,

$$D_{west}^{x-} = \frac{\bar{p}_{i-\frac{1}{2},j}\bar{H}_{i-\frac{1}{2},j}^{3}}{\bar{\mu}_{i-\frac{1}{2},j}}\frac{\Delta z}{\Delta x} \tag{4.95}$$

$$F_{west}^{x} = \Delta\bar{H}_{i-\frac{1}{2},j}\Delta z \tag{4.96}$$

Now, $consider\ j_z^+$ from equation (4.84)

$$\dot{J}_z^+ = \left(\frac{\bar{p}\bar{H}^3L^2}{\bar{\mu}R^2}\frac{\partial\bar{p}}{\partial\bar{z}}\right)_{i,j+\frac{1}{2}}\Delta x \tag{4.97}$$

Discretizing at north face we get:

$$\dot{J}_z^+ = \left(\frac{\bar{p}_{i,j+\frac{1}{2}}\bar{H}_{i,j+\frac{1}{2}}^{3}L^2}{\bar{\mu}_{i,j+\frac{1}{2}}R^2}\frac{(\bar{p}_{i,j+1}-\bar{p}_{i,j})}{\Delta z}.\Delta x\right) \tag{4.98}$$

$$\dot{J}_z^+ = \frac{\bar{p}_{i,j+\frac{1}{2}}\bar{H}_{i,j+\frac{1}{2}}^{3}L^2\Delta x}{\bar{\mu}_{i,j+\frac{1}{2}}R^2\Delta z}(\bar{p}_{i,j+1}-\bar{p}_{i,j}) \tag{4.99}$$

Thus, expressing in form of diffusion coefficients we get:

$$\dot{J}_z^+ = \left(D_{i,j+\frac{1}{2}}^{z+}\right)(\bar{p}_{i,j+1}) - \left(D_{i,j+\frac{1}{2}}^{z+}\right)(\bar{p}_{i,j}) \tag{4.100}$$

Thus,

$$\dot{J}_z^+ = \left(D_{north}{}^{z+}\right)(\bar{p}_{i,j+1}) - \left(D_{north}{}^{z+}\right)(\bar{p}_{i,j}) \tag{4.101}$$

Where,

$$D_{north}{}^{z+} = \frac{\bar{p}_{i,j+\frac{1}{2}} \bar{H}_{i,j+\frac{1}{2}}{}^{3} L^2 \Delta x}{\bar{\mu}_{i,j-\frac{1}{2}} R^2 \Delta z} \tag{4.102}$$

Now, $consider\ \dot{J}_z^-$ from equation (4.84)

$$\dot{J}_z^- = \left(\frac{\bar{p}\bar{H}^3 L^2}{\bar{\mu} R^2} \frac{\partial \bar{p}}{\partial z} \right)_{i,j-\frac{1}{2}} \Delta x \tag{4.103}$$

Discretizing at south face we get :

$$\dot{J}_z^- = \left(\frac{\bar{p}_{i,j-\frac{1}{2}} \bar{H}_{i,j-\frac{1}{2}}{}^{3} L^2}{\bar{\mu}_{i,j-\frac{1}{2}} R^2} \frac{(\bar{p}_{i,j} - \bar{p}_{i,j-1})}{\Delta z} . \Delta x \right) \tag{4.104}$$

Further, simplifying:

$$\dot{J}_z^- = \frac{\bar{p}_{i,j-\frac{1}{2}} \bar{H}_{i,j-\frac{1}{2}}{}^{3} L^2 \Delta x}{\bar{\mu}_{i,j-\frac{1}{2}} R^2 \Delta z} (\bar{p}_{i,j} - \bar{p}_{i,j-1}) \tag{4.105}$$

Expressing in terms of diffusive coefficients, we get:

$$\dot{J}_z^- = \left(D_{i,j-\frac{1}{2}}{}^{z-} \right)(\bar{p}_{i,j}) - \left(D_{i,j+\frac{1}{2}}{}^{z-} \right)(\bar{p}_{i,j-1}) \tag{4.106}$$

Thus,

$$\dot{J}_z^- = \left(D_{south}{}^{z-}\right)(\bar{p}_{i,j}) - \left(D_{south}{}^{z-}\right)(\bar{p}_{i,j-1}) \tag{4.107}$$

Where,

$$D_{south}{}^{z-} = \frac{\bar{p}_{i,j-\frac{1}{2}} \bar{\bar{H}}_{i,j-\frac{1}{2}}{}^{3} L^2 \Delta x}{\bar{\mu}_{i,j-\frac{1}{2}} R^2 \Delta z} \tag{4.108}$$

Substituting all fluxes in $\dot{J}_X^+ - \dot{J}_X^- + \dot{J}_Z^+ - \dot{J}_Z^- = 0$ we get:

$$\begin{aligned}
&\left(D_{east}{}^{x+} - \frac{F_{east}{}^{x}}{2}\right)(\bar{p}_{i+1,j}) + \left(-D_{east}{}^{x+} - \frac{F_{east}{}^{x}}{2}\right)(\bar{p}_{i,j}) \\
&-\left(D_{west}{}^{x-} - \frac{F_{west}{}^{x}}{2}\right)(\bar{p}_{i,j}) - \left(-D_{west}{}^{x-} - \frac{F_{west}{}^{x}}{2}\right)(\bar{p}_{i-1,j}) \\
&+\left(D_{north}{}^{z+}\right)(\bar{p}_{i,j+1}) - \left(D_{north}{}^{z+}\right)(\bar{p}_{i,j}) - \left(D_{south}{}^{z-}\right)(\bar{p}_{i,j}) \\
&+\left(D_{south}{}^{z-}\right)(\bar{p}_{i,j-1}) = 0
\end{aligned} \tag{4.109}$$

Simplifying by getting $(\bar{p}_{i,j})$ terms together. We have:

$$\begin{aligned}
&\left(D_{east}{}^{x+} - \frac{F_{east}{}^{x}}{2}\right)(\bar{p}_{i+1,j}) + \left(D_{west}{}^{x-} + \frac{F_{west}{}^{x}}{2}\right)(\bar{p}_{i-1,j}) \\
&+\left(D_{north}{}^{z+}\right)(\bar{p}_{i,j+1}) + \left(D_{south}{}^{z-}\right)(\bar{p}_{i,j-1}) \\
&+\left(-D_{east}{}^{x+} - \frac{F_{east}{}^{x}}{2}\right)(\bar{p}_{i,j}) - \left(D_{west}{}^{x-} - \frac{F_{west}{}^{x}}{2}\right)(\bar{p}_{i,j}) \\
&-\left(D_{north}{}^{z+}\right)(\bar{p}_{i,j}) - \left(D_{south}{}^{z-}\right)(\bar{p}_{i,j}) = 0
\end{aligned} \tag{4.110}$$

Converting to the standard Finite Volume Discretization form :-

$$a_P\phi_P = a_E\phi_E + a_W\phi_W + a_N\phi_N + a_S\phi_S + b \tag{4.111}$$

where, $\phi_P = \bar{p}_{i,j}$ we get:

$$\begin{aligned}
&\left(D_{east}{}^{x+} - \frac{F_{east}{}^{x}}{2}\right)(\bar{p}_{i+1,j}) + \left(D_{west}{}^{x-} + \frac{F_{west}{}^{x}}{2}\right)(\bar{p}_{i-1,j}) \\
&+\left(D_{north}{}^{z+}\right)(\bar{p}_{i,j+1}) + \left(D_{south}{}^{z-}\right)(\bar{p}_{i,j-1}) \\
&= \left[\left(D_{east}{}^{x+} + \frac{F_{east}{}^{x}}{2}\right) + \left(D_{west}{}^{x-} - \frac{F_{west}{}^{x}}{2}\right) + \left(D_{north}{}^{z+}\right) + \left(D_{south}{}^{z-}\right)\right](\bar{p}_{i,j})
\end{aligned} \tag{4.112}$$

Therefore, we get the discretized Finite volume coefficients of the standard discretized equations as:

$$a_E = \left(D_{east}{}^{x+} - \frac{F_{east}{}^{x}}{2}\right) \tag{4.113}$$

$$a_W = \left(D_{west}{}^{x-} + \frac{F_{west}{}^{x}}{2}\right) \tag{4.114}$$

$$a_N = \left(D_{north}{}^{z+}\right) \tag{4.115}$$

$$a_S = \left(D_{south}{}^{z-}\right) \tag{4.116}$$

$$a_P = \left[\left(D_{east}{}^{x+} + \frac{F_{east}{}^{x}}{2}\right) + \left(D_{west}{}^{x-} - \frac{F_{west}{}^{x}}{2}\right) + \left(D_{north}{}^{z+}\right) + \left(D_{south}{}^{z-}\right)\right] \tag{4.117}$$

We now use power Law discussed in section 4.3.1 for Numerical stability of this discretized equation when equation is solved iteratively for ϕ_P .

Peclet number is defined as the ratio of convection factor to diffusion factor. It is a dimensionless number that governs whether it is the physics of convection or diffusion that dominates the problem. The larger the value of peclet number more is the convection dominant physics. The lesser the value of peclet number more is the diffusion dominant physics.[30]

$$P_e = \frac{F}{D} \tag{4.118}$$

Therefore,

$$a_E = D_{east}{}^{x}\left(1 - \frac{P_{eeast}{}^{x}}{2}\right) \tag{4.119}$$

By, power law scheme for stability we get :-

$$a_E = D_{east}{}^{x} A(|P_{eeast}|) + 0, -F_{east}{}^{x} \tag{4.120}$$

Where, $A(|P_{e\,east}|) = Max\left(0, (1 - 0.1|P_{e\,east}|)^5\right)$ by powerlaw scheme

Similarly,

$$a_W = D_{west}{}^{x}\left(1 + \frac{P_{e\,west}{}^{x}}{2}\right) \tag{4.121}$$

Or,

$$a_W = D_{west}{}^{x}\left(1+\frac{P_{ewest}{}^{x}}{2}\right) \tag{4.122}$$

$$a_W = D_{west}{}^{x}\left[A(|P_{ewest}|)+P_{ewest}\right] \tag{4.123}$$

Where, $A(|P_{e_{west}}|) = Max\left(0,(1-0.1|P_{e_{west}}|)^5\right)$ by powerlaw scheme

$$a_N = \left(D_{north}{}^{z+}\right) \tag{4.124}$$

And,

$$a_S = \left(D_{south}{}^{z-}\right) \tag{4.125}$$

Thus, a_P becomes:

$$a_P = \left[a_E + a_W + a_N + a_S + Max\left(0, F_{east}{}^{x} - F_{west}{}^{x}\right)\right] \tag{4.126}$$

And, source term 'b' becomes:

$$b = Max\left(0, F_{east}{}^{x} - F_{west}{}^{x}\right)(\bar{p}_{i,j}) \tag{4.127}$$

The new coefficients are substituted into equation (4.111) and we solve for ϕ_P by using iterative methods.

4.8.2 A Generic Finite Volume Discretization For Momentum And Continuity Equations

The unique behaviour of the thin film Navier-stokes equations is its ability to be expressed into a generic form for computational ease. The convection diffusion scheme of the thin film Navier-stokes momentum equation derived and discussed in sections 4.7.2, 4.7.3 and 4.7.4 shows that the left hand side of the three momentum equations are

identical if the velocity field considered for calculation is the velocity in the direction of the momentum transport represented by the equation. Consider the x-momentum Navier-Stokes equation as derived in section 4.7.2. This is represented as:

$$\frac{\partial\left(\bar{\rho}\bar{u}\bar{u}\right)}{\partial\bar{x}}+\frac{\partial}{\partial\bar{y}}\left(\bar{\rho}\bar{v}\bar{u}-\frac{\bar{\mu}}{c2}\frac{\partial\bar{u}}{\partial\bar{y}}\right)+\frac{\partial}{\partial\bar{z}}\left(\frac{\bar{\rho}\bar{w}\bar{u}}{c1}\right)=-\mathrm{c3}\frac{\partial\left(\bar{p}\right)}{\partial\left(\bar{x}\right)}$$

the field variable to be calculated from the thin film x-momentum Navier-Stokes equation is the velocity field $'\bar{u}'$. The general form of Advection-Diffusion equation expresses velocity as the transported quantity. This when applied to the Convection-Diffusion form of the governing momentum equation allows the left hand side of the thin film x-momentum Navier-Stokes equation to be represented by the equation of the form:

$$\frac{\partial\left(\bar{\rho}\bar{u}\bar{\phi}\right)}{\partial\bar{x}}+\frac{\partial}{\partial\bar{y}}\left(\bar{\rho}\bar{v}\bar{\phi}-\frac{\bar{\mu}}{c2}\frac{\partial\bar{\phi}}{\partial\bar{y}}\right)+\frac{\partial}{\partial\bar{z}}\left(\frac{\bar{\rho}\bar{w}\bar{\phi}}{c1}\right)=-\mathrm{c3}\frac{\partial\left(\bar{p}\right)}{\partial\left(\bar{x}\right)} \qquad (4.128)$$

Where 'ϕ' is the transported quantity. The right hand side term represents the source term. Essentially in the finite volume discretization that follows, the source term for X- Momentum is taken as $-\mathrm{c3}\frac{\partial(\bar{p})}{\partial(\bar{x})}$. It is interesting to know that the left hand sides of the thin film y-momentum Navier-Stokes equation and the thin film z-momentum Navier-Stokes equations can be expressed in the same form if the transported quantity is considered as $'\bar{v}'$ velocity field and $'\bar{w}'$ respectively.

Consider the thin film Y-momentum Navier-Stokes equation derived in sections 4.7.3. This is given as:

$$\frac{\partial\left(\bar{\rho}\overline{uv}\right)}{\partial\bar{x}}+\frac{\partial}{\partial\bar{y}}\left(\bar{\rho}\overline{vv}-\frac{\bar{\mu}}{c2}\frac{\partial\bar{v}}{\partial\bar{y}}\right)+\frac{\partial}{\partial\bar{z}}\left(\frac{\bar{\rho}\overline{wv}}{c1}\right)=\frac{1}{c2}*\frac{1}{3}*\frac{\partial}{\partial\bar{y}}\left\{\bar{\mu}\left[\left(\frac{\partial\bar{u}}{\partial\bar{x}}\right)+\left(\frac{\partial\bar{v}}{\partial\bar{y}}\right)+\frac{1}{c1}\left(\frac{\partial\bar{w}}{\partial\bar{z}}\right)\right]\right\}$$

By considering the transported quantity as $'\bar{v}'$ velocity field. The left hand side of the thin film Y-Momentum equation can be represented in the form Similar to the x momentum equation which is given as:

$$\begin{aligned}&\frac{\partial\left(\bar{\rho}\bar{u}\phi\right)}{\partial\bar{x}}+\frac{\partial}{\partial\bar{y}}\left(\bar{\rho}\bar{v}\phi-\frac{\bar{\mu}}{c2}\frac{\partial\phi}{\partial\bar{y}}\right)+\frac{\partial}{\partial\bar{z}}\left(\frac{\bar{\rho}\bar{w}\phi}{c1}\right)\\&=\frac{1}{c2}*\frac{1}{3}*\frac{\partial}{\partial\bar{y}}\left\{\bar{\mu}\left[\left(\frac{\partial\bar{u}}{\partial\bar{x}}\right)+\left(\frac{\partial\bar{v}}{\partial\bar{y}}\right)+\frac{1}{c1}\left(\frac{\partial\bar{w}}{\partial\bar{z}}\right)\right]\right\}\end{aligned}\qquad(4.129)$$

The right hand side of the above equation forms the source term for the y-momentum equation.

The thin film Z-Momentum equation from section 4.7.4 can be recast into the same form of the transported quantity $'\emptyset'$ as x and y momentum equations. Consider the Thin film Convection-diffusion form of Z momentum equation from 4.7.4. Given as:

$$\frac{\partial\left(\bar{\rho}\overline{uw}\right)}{\partial\bar{x}}+\frac{\partial}{\partial\bar{y}}\left(\bar{\rho}\overline{vw}-\frac{\bar{\mu}}{c2}\frac{\partial\bar{w}}{\partial\bar{y}}\right)+\frac{\partial}{\partial\bar{z}}\left(\frac{\bar{\rho}\overline{ww}}{c1}\right)=-\left(\frac{c3}{c1}\right)*\frac{\partial\bar{p}}{\partial z}$$

A similar approach in regard to the X and Y momentum equations is applied. By considering the transported quantity as $'\bar{w}'$ velocity field. The left hand side of the thin film Z-Momentum equation can be represented in the form Similar to the x and Y momentum equation which is given as:

$$\frac{\partial\left(\bar{\rho}\bar{u}\phi\right)}{\partial\bar{x}}+\frac{\partial}{\partial\bar{y}}\left(\bar{\rho}\bar{v}\phi-\frac{\bar{\mu}}{c2}\frac{\partial\phi}{\partial\bar{y}}\right)+\frac{\partial}{\partial\bar{z}}\left(\frac{\bar{\rho}\bar{w}\phi}{c1}\right)=-\left(\frac{C3}{c1}\right)*\frac{\partial\bar{p}}{\partial z} \qquad (4.130)$$

The source term for the Z momentum equation is taken as the pressure gradient term along Z direction i.e. $-(\frac{C3}{c1})*\frac{\partial\bar{p}}{\partial z}$ which appears as a right hand side term in the Z momentum equation.

We extend similar expressibility to the convection diffusion form of the continuity equation discussed in section 4.7.5.

The continuity equation in its convection diffusion form is given as:

$$\frac{\partial}{\partial\bar{x}}\left(\hat{\rho}\bar{\rho}\bar{u}-\frac{\gamma_0}{a1}\left(\frac{\partial\bar{\rho}}{\partial\bar{x}}\right)\right)+\frac{\partial}{\partial\bar{y}}\left(\hat{\rho}\bar{\rho}\bar{v}-\frac{\gamma_0}{a2}\left(\frac{\partial\bar{\rho}}{\partial\bar{y}}\right)\right)+\frac{\partial}{\partial\bar{z}}\left(\frac{\hat{\rho}\bar{\rho}\bar{w}}{c1}-\frac{\gamma_0}{a3}\left(\frac{\partial\bar{\rho}}{\partial\bar{z}}\right)\right)=0$$

The convection-diffusion form of the continuity equation can be expressed in the advection-diffusion form in terms of transported quantity ∅ i.e. $'\bar{\rho}'$ in case of continuity. This is similar to the approach adopted for the three momentum equations discussed previously. The general advection-diffusion form applied to the three momentum equations when extended to the continuity equation takes up the form as:

$$\frac{\partial}{\partial\bar{x}}\left(\hat{\rho}\bar{u}\phi\right)+\frac{\partial}{\partial\bar{y}}\left(\hat{\rho}\bar{v}\phi-\frac{\gamma_0}{a2}\left(\frac{\partial\phi}{\partial\bar{y}}\right)\right)+\frac{\partial}{\partial\bar{z}}\left(\frac{\hat{\rho}\bar{w}\phi}{c1}\right)=0 \qquad (4.131)$$

The source term for the continuity equation is essentially zero. This is a challenge in solving the convection-diffusion form of the continuity equation using the finite volume discretization. Suitable numerical adjustments are required to be added to aid in the solution of the density field from the continuity equation. These numerical adjustments are added in such a manner that they do not affect the principal mass conservation in the Finite Volume discretization scheme.

4.8.2.1 Finite volume discretization of the general form of Advection-Diffusion equation applicable to The Thin film Momentum and Continuity equations.

In this section a finite volume discretization scheme is presented to discretize the standard form of convection-diffusion equation discussed in section 4.8.2. applicable to the thin film momentum and continuity equations. Consider the general form of the momentum equations discussed in section 4.8.2. It can be expressed as:

$$\frac{\partial\left(\bar{\rho}\bar{u}\phi\right)}{\partial\bar{x}}+\frac{\partial}{\partial\bar{y}}\left(\bar{\rho}\bar{v}\phi-\frac{\bar{\mu}}{c2}\frac{\partial\phi}{\partial\bar{y}}\right)+\frac{\partial}{\partial\bar{z}}\left(\frac{\bar{\rho}\bar{w}\phi}{c1}\right)=S \qquad (4.132)$$

Where $S=-c3\frac{\partial\left(\bar{p}\right)}{\partial\left(\bar{x}\right)}$, for x momentum equation

Or, $S=\frac{1}{c2}*\frac{1}{3}*\frac{\partial}{\partial\bar{y}}\left\{\bar{\mu}\left[\left(\frac{\partial\bar{u}}{\partial\bar{x}}\right)+\left(\frac{\partial\bar{v}}{\partial\bar{y}}\right)+\frac{1}{c1}\left(\frac{\partial\bar{w}}{\partial\bar{z}}\right)\right]\right\}$, for Y- Momentum equation

Or, $S=-\left(\frac{C3}{c1}\right)*\frac{\partial\bar{p}}{\partial z}$, for Z momentum equation

Further, the general advection-diffusion form of continuity equation can be expressed as:

$$\frac{\partial}{\partial\bar{x}}\left(\hat{\rho}\bar{u}\phi\right)+\frac{\partial}{\partial\bar{y}}\left(\hat{\rho}\bar{v}\phi-\frac{\gamma_0}{a2}\left(\frac{\partial\phi}{\partial\bar{y}}\right)\right)+\frac{\partial}{\partial\bar{z}}\left(\frac{\hat{\rho}\bar{w}\phi}{c1}\right)=0$$

Where, $S=0$

The above two general advection-diffusion equations can also be expressed in a flux form similar to the one applied for Reynolds equation in section 4.8.1, this gives:

$$\frac{\partial}{\partial \overline{x}}\left\{\dot{J}_x\right\}+\frac{\partial}{\partial \overline{y}}\left\{\dot{J}_y\right\}+\frac{\partial}{\partial \overline{z}}\left(\dot{J}_z\right)=S \tag{4.133}$$

Which can also be expressed as short hand flux form as:

$$\nabla.\overline{J}=S \tag{4.134}$$

The above equation is essentially an expression of divergence of flux flow along the three directions. Integrating the above equation over the finite control volume shown below we get:

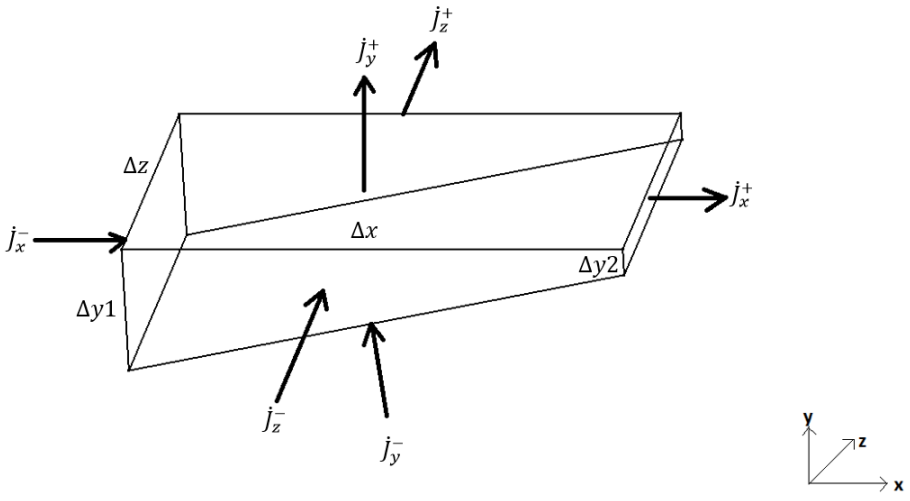

Figure 15 Finite control volume cell for thin film momentum and continuity equations

$$\int_{cv} \frac{\partial\left(\bar{\rho}\bar{u}\phi\right)}{\partial\bar{x}} dV + \int_{cv} \frac{\partial}{\partial\bar{y}}\left(\bar{\rho}\bar{v}\phi - \frac{\bar{\mu}}{c2}\frac{\partial\phi}{\partial\bar{y}}\right) dV + \int_{cv} \frac{\partial}{\partial\bar{z}}\left(\frac{\bar{\rho}\bar{w}\phi}{c1}\right) dV = \int_{cv} \left(S\right) dV \tag{4.135}$$

Where, $dV = dx * dy * dz$

Equation (4.135) can be also represented in short form divergence notation as:

$$\int_{cv} \left(\nabla.\bar{J}\right) dV = \int_{cv} \left(S\right) dV \tag{4.136}$$

By, applying the gauss divergence theorem over the volume integral and converting it into a surface integral with unit vectors, we get:

$$\int_{cv} \left(\nabla.\bar{J}\right) dV = \int_{cs} \left(\bar{J}.\bar{n}\right) dS \tag{4.137}$$

Here onwards, all quantities do not have an accent included. However, are the quantities are dimensionless on account of Lubrication scaling Non dimensionalization applied from sections 4.4.1.1, 4.4.2.1, 4.4.3.1 and 4.5.1

The right hand side of the equation (4.137) gives flux flow by divergence theorem into and from control faces of the control volume. This can be written as:

$$\int_{cs} \left(\bar{J}.\bar{n}\right) dS = \dot{J}_X^+ - \dot{J}_X^- + \dot{J}_y^+ - \dot{J}_y^- + \dot{J}_z^+ - \dot{J}_z^- \tag{4.138}$$

The terms $\dot{J}_X^+, \dot{J}_X^-, \dot{J}_y^+, \dot{J}_y^-, \dot{J}_z^+, \dot{J}_z^-$ express the flux flow into and out of the control faces of the control volume along x,y and z directions. The positive and negative signs originate due to presence of unit vector from divergence theorem. The positive fluxes are

flux flowing out of the control volume and the negative fluxes indicate the flux entering the control volume.

Essentially, from the integration of the general advection-diffusion equation the integrated flux term along x direction on the east face is given by:

$$\dot{J}_X^+ = \overline{\rho}\overline{u}\phi.\Delta y2.\Delta z \tag{4.139}$$

Thus, the flux flow out of the east face is:

$$\dot{J}_X^+ = \rho_{i+\frac{1}{2},j,k}\, u_{i+\frac{1}{2},j,k}\, \frac{(\phi_{i+1,j,k} + \phi_{i,j,k})}{2} \Delta y2.\Delta z \tag{4.140}$$

The property ∅ is linearly interpolated at the east face by averaging its values at cell centered nodes at $i+1, j, k$ and i, j, k respectively. $\Delta y2.\Delta z$ represents the area through which the flux flows.

$\Delta y2$ is the value of Δy at east face. This is smaller than $\Delta y1$ which is the value of Δy at west face. This is on account of the constant wedge shaped taper of the thin film.

Thus, we get:

$$\dot{J}_X^+ = \frac{\rho_{i+\frac{1}{2},j,k}\, u_{i+\frac{1}{2},j,k}}{2}.(\phi_{i+1,j,k} + \phi_{i,j,k}).\Delta y2.\Delta z \tag{4.141}$$

We now identify convection flux in the east term. This allows expression of the flux along east face to be expressed as:

$$\dot{J}_X^+ = \frac{F_{east}}{2}(\phi_{i+1,j,k} + \phi_{i,j,k}) \tag{4.142}$$

Where, $F_{east} = \rho_{i+\frac{1}{2},j,k}\, u_{i+\frac{1}{2},j,k}.\Delta y2.\Delta z$ (4.143)

F_{east} represents the convective flux term along east face of the control volume.

Further, expressing the flux term along east face in terms of convection terms and transported property ∅ we get:

$$\dot{J}_X^+ = \frac{F_{east}}{2}(\phi_{i+1,j,k}) + \frac{F_{east}}{2}\left(\phi_{i,j,k}\right) \tag{4.144}$$

The flux term along west face is expressed in a similar fashion as the east face. Consider the flux term along west face of the control volume, we have:

$$\dot{J}_X^- = \bar{\rho}\bar{u}\phi.\Delta y1.\Delta z \tag{4.145}$$

The property ∅ is linearly interpolated at the west face by averaging its values at cell centered nodes at $i-1, j, k$ and i, j, k respectively. This gives:

$$\dot{J}_X^- = \rho_{i-\frac{1}{2},j,k}\, u_{i-\frac{1}{2},j,k}\, \frac{(\phi_{i-1,j,k} + \phi_{i,j,k})}{2}.\Delta y1\Delta z \tag{4.146}$$

Further, simplifying we get:

$$\dot{J}_X^- = \frac{\rho_{i-\frac{1}{2},j,k}\, u_{i-\frac{1}{2},j,k}}{2}.\Delta y1\Delta z.(\phi_{i-1,j,k} + \phi_{i,j,k}) \tag{4.147}$$

A Convection flux term F_{west} is defined as:

$$F_{west} = \rho_{i-\frac{1}{2},j,k}\, u_{i-\frac{1}{2},j,k}.\Delta y1\Delta z \tag{4.148}$$

This substitution simplifies the flux term along west face as:

$$\dot{J}_X^- = \frac{F_{west}}{2}(\phi_{i-1,j,k}) + \frac{F_{west}}{2}\left(\phi_{i,j,k}\right) \tag{4.149}$$

Similarly, consider the Flux term along north face of the control volume, which is given as:

$$\dot{J}_z^+ = \bar{\rho}\bar{w}\phi.\Delta x.\Delta y \tag{4.150}$$

By, interpolating face value of transported quantity we have:

$$\dot{J}_Z^+ = \frac{\rho_{i,j+\frac{1}{2},k}\, w_{i,j+\frac{1}{2},k}}{c1}\frac{(\phi_{i,j+1,k}+\phi_{i,j,k})}{2}.\Delta x.\Delta y \tag{4.151}$$

Further simplification yields:

$$\dot{J}_z^+ = \frac{\rho_{i,j+\frac{1}{2},k}\, w_{i,j+\frac{1}{2},k}}{2*c1}.\Delta x.\Delta y.(\phi_{i,j+1,k}+\phi_{i,j,k}) \tag{4.152}$$

A Convection flux term F_{north} is defined as:

$$F_{north} = \frac{\rho_{i,j+\frac{1}{2},k}\, w_{i,j+\frac{1}{2},k}}{c1}.\Delta x.\Delta y \tag{4.153}$$

We express the flux $\dot{J}_z^+$ along north face in terms of convection terms along north face as:

$$\dot{J}_z^+ = \frac{F_{north}}{2}(\phi_{i,j+1,k}) + \frac{F_{north}}{2}\left(\phi_{i,j,k}\right) \tag{4.154}$$

The flux term at the south face of the control volume is given by:

$$\dot{J}_z^- = \bar{\rho}\bar{w}\phi.\Delta x.\Delta y \tag{4.155}$$

Interpolating face value of transported property we get:

(4.156)

(4.157)

$$\dot{J}_Z^- = \frac{\rho_{i,j-\frac{1}{2},k} w_{i,j-\frac{1}{2},k}}{c1} \frac{(\phi_{i,j-1,k} + \phi_{i,j,k})}{2} .\Delta x.\Delta y$$

On further simplification, we have:

$$\dot{J}_z^- = \frac{\rho_{i,j-\frac{1}{2},k} w_{i,j-\frac{1}{2},k}}{2*c1} .\Delta x.\Delta y.(\phi_{i,j-1,k} + \phi_{i,j,k}) \quad (4.158)$$

Convection flux at the south face is defined as:

$$F_{south} = \frac{\rho_{i,j-\frac{1}{2},k} w_{i,j-\frac{1}{2},k}}{c1} .\Delta x.\Delta y \quad (4.159)$$

The flux term at the south face is expressed in terms of the convection flux at the south face. This yields:

$$\dot{J}_z^- = \frac{F_{south}}{2}(\phi_{i,j-1,k}) + \frac{F_{south}}{2}(\phi_{i,j,k}) \quad (4.160)$$

The top and bottom flux terms are now considered. The nature of thin film advection-diffusion equations generalized for momentum and continuity exhibit presence of both convection and diffusion phenomenon along top and bottom faces of the control volume. Consider the flux term at the top face. This is given by:

$$\dot{J}_y^+ = \left(\bar{\rho}\bar{v}\varnothing - \frac{\bar{\mu}}{c2}\frac{\partial \phi}{\partial \bar{y}} \right)_{i,j,k+\frac{1}{2}} \Delta x \Delta z \quad (4.161)$$

Linear, Interpolation is applied for the transported property ∅ by averaging it in between $i, j, k+1$ and i, j, k nodes. The face derivative of the transported

property ∅ is calculated by taking central difference of property across the control face. i.e. in case of top face of the control volume the derivative is calculated as difference of property variation at top node and at the point node itself. This approach simplifies the flux term along top direction as:

$$\dot{J}_y^+ = \left(\rho_{i,j,k+\frac{1}{2}} v_{i,j,k+\frac{1}{2}} \frac{(\phi_{i,j,k+1} + \phi_{i,j,k})}{2} .\Delta x.\Delta z \right) - \left(\frac{\mu_{i,j,k+\frac{1}{2}}}{c2} \frac{\partial \phi}{\partial y}_{i,j,k+\frac{1}{2}} .\Delta x.\Delta z \right) \quad (4.162)$$

Taking the derivative of the property at the top face, we get:

$$\dot{J}_y^+ = (\rho_{i,j,k+\frac{1}{2}} v_{i,j,k+\frac{1}{2}} \frac{(\phi_{i,j,k+1} + \phi_{i,j,k})}{2} .\Delta x.\Delta z) - \left(\frac{\mu_{i,j,k+\frac{1}{2}}}{c2} \frac{(\phi_{i,j,k+1} - \phi_{i,j,k)}}{\Delta y} .\Delta x.\Delta z \right) \quad (4.163)$$

A convective flux term F_{top} is defined at the top face of the control volume. Which is given as:

$$F_{top} = (\rho_{i,j,k+\frac{1}{2}} v_{i,j,k+\frac{1}{2}}).\Delta x.\Delta z \quad (4.164)$$

A diffusion flux term D_{top} is also defined at the top face. Which is given as:

$$D_{top} = \frac{\mu_{i,j,k+\frac{1}{2}}}{c2} \frac{.\Delta x.\Delta z}{\Delta y} \quad (4.165)$$

We express the flux term along top face in a similar manner as the other faces. The flux term is expressed in terms of convective and diffusive terms along top faces. This gives:

$$\dot{J}_y^+ = \left\{ \frac{F_{top}}{2}(\phi_{i,j,k+1}) - D_{top}(\phi_{i,j,k+1}) \right\} + \left\{ \frac{F_{top}}{2}(\phi_{i,j,k}) + D_{top}(\phi_{i,j,k}) \right\} \qquad (4.166)$$

The same principle applies to the flux term at the bottom face. This is given as:

$$\dot{J}_y = \left(\bar{\rho}\bar{v}\phi - \frac{\bar{\mu}}{c2}\frac{\partial \phi}{\partial \bar{y}} \right)_{i,j,k-\frac{1}{2}} \Delta x.\Delta z \qquad (4.167)$$

Applying similar approach to interpolate face value and derivative of transported property ∅ we have:

$$\dot{J}_y = (\rho_{i,j,k-\frac{1}{2}} v_{i,j,k-\frac{1}{2}} \frac{(\phi_{i,j,k-1} + \phi_{i,j,k})}{2}.\Delta x.\Delta z) - \left(\frac{\mu_{i,j,k-\frac{1}{2}}}{c2}\frac{\partial \phi}{\partial y}_{i,j,k-\frac{1}{2}}.\Delta x.\Delta z \right) \qquad (4.168)$$

$$\dot{J}_y = \left(\rho_{i,j,k-\frac{1}{2}} v_{i,j,k-\frac{1}{2}} \frac{(\phi_{i,j,k-1} + \phi_{i,j,k})}{2}.\Delta x.\Delta z \right) - \left(\frac{\mu_{i,j,k-\frac{1}{2}}}{c2}\frac{(\phi_{i,j,k} - \phi_{i,j,k-1)}}{\Delta y}.\Delta x.\Delta z \right) \qquad (4.169)$$

Convective flux terms and diffusive flux terms at the bottom face are defined as:

$$F_{bottom} = \rho_{i,j,k-\frac{1}{2}} v_{i,j,k-\frac{1}{2}}.\Delta x.\Delta z \qquad (4.170)$$

And,

$$D_{bottom} = \frac{\mu_{i,j,k-\frac{1}{2}}}{c2} \frac{.\Delta x.\Delta z}{\Delta y} \tag{4.171}$$

Expressing the flux term at the bottom face in terms of the convection and diffusion fluxes at the bottom face of the control volume, we have:

$$\begin{aligned} \dot{J}_y^- &= \left\{ \frac{F_{bottom}}{2} (\phi_{i,j,k-1}) + D_{bottom} \left(\phi_{i,j,k-1} \right) \right\} \\ &+ \left\{ \frac{F_{bottom}}{2} \left(\phi_{i,j,k} \right) - D_{bottom} (\phi_{i,j,k}) \right\} \end{aligned} \tag{4.172}$$

We, now have all the flux terms from the integrated convection diffusion scheme over the finite volume.

We substitute the flux terms into the integrated equation with gauss divergence theorem application given as:

$$\int_{cv} \left(\nabla . \bar{J} \right) dV = \int_{cs} \left(\bar{J} . \bar{n} \right) dS = \dot{J}_X^+ - \dot{J}_X^- + \dot{J}_y^+ - \dot{J}_y^- + \dot{J}_z^+ - \dot{J}_z^- = S.dV$$

This substitution of flux terms into the integrated equation yields:

$$\frac{F_{east}}{2}(\phi_{i+1,j,k}+\phi_{i,j,k})-\left\{\frac{F_{west}}{2}(\phi_{i-1,j,k}+\phi_{i,j,k})\right\}$$
$$+\frac{F_{top}}{2}(\phi_{i,j,k+1}+\phi_{i,j,k})-D_{top}(\phi_{i,j,k+1}-\phi_{i,j,k})$$
$$-\left\{\frac{F_{bottom}}{2}(\phi_{i,j,k-1}+\phi_{i,j,k})-D_{bottom}(\phi_{i,j,k}-\phi_{i,j,k-1})\right\} \quad (4.173)$$
$$+\frac{F_{north}}{2}(\phi_{i,j+1,k}+\phi_{i,j,k})-\left\{\frac{F_{south}}{2}(\phi_{i,j-1,k}+\phi_{i,j,k})\right\}$$
$$=S*dx*dy*dz$$

By, combining convective and diffusive term coefficients of transported property 'ø' at the finite volume node i,j,k together we get:

$$\frac{F_{east}}{2}(\phi_{i+1,j,k})-\frac{F_{west}}{2}(\phi_{i-1,j,k})+\frac{F_{top}}{2}(\phi_{i,j,k+1})-D_{top}(\phi_{i,j,k+1})$$
$$-\frac{F_{bottom}}{2}(\phi_{i,j,k-1})-D_{bottom}\left(\phi_{i,j,k-1}\right)+\frac{F_{north}}{2}(\phi_{i,j+1,k})-\frac{F_{south}}{2}(\phi_{i,j-1,k})$$
$$+\left\{\frac{F_{east}}{2}-\frac{F_{west}}{2}+\left(\frac{F_{top}}{2}+D_{top}\right)-\left(\frac{F_{bottom}}{2}-D_{bottom}\right)+\frac{F_{north}}{2}-\frac{F_{south}}{2}\right\}\phi_{i,j,k}$$
$$=S*dx*dy*dz$$

(4.174)

The above equation is expressed into the Finite Volume Discretized form where 'b' term represents source term.

$$a_P\phi_P=a_E\phi_E+a_W\phi_W+a_N\phi_N+a_S\phi_S+a_T\phi_T+a_B\phi_B+b \quad (4.175)$$

Arrangement of the equation into the Finite Volume discretized form gives:

$$\left\{\frac{F_{east}}{2}-\frac{F_{west}}{2}+\left(\frac{F_{top}}{2}+D_{top}\right)-\left(\frac{F_{bottom}}{2}-D_{bottom}\right)+\frac{F_{north}}{2}-\frac{F_{south}}{2}\right\}\phi_{i,j,k}$$

$$=-\frac{F_{east}}{2}(\phi_{i+1,j,k})+\frac{F_{west}}{2}(\phi_{i-1,j,k})-\frac{F_{top}}{2}(\phi_{i,j,k+1})+D_{top}(\phi_{i,j,k+1}) \quad (4.176)$$

$$+\frac{F_{bottom}}{2}(\phi_{i,j,k-1})+D_{bottom}\left(\phi_{i,j,k-1}\right)-\frac{F_{north}}{2}(\phi_{i,j+1,k})+\frac{F_{south}}{2}(\phi_{i,j-1,k})+b$$

Where,

$a_E=-\frac{F_{east}}{2}$, $a_W=+\frac{F_{west}}{2}$, $a_T=D_{top}-\frac{F_{top}}{2}$, $a_B=\frac{F_{bottom}}{2}+D_{bottom}$, $a_N=-\frac{F_{north}}{2}$,

$a_s=\frac{F_{south}}{2}$ and b=$S*\ dx*dy*dz$

Similar to the scheme for stability applied to Finite Volume discretized Reynolds equation, we apply the power law scheme for numerical stability to the general convection diffusion form of momentum and continuity equations.

We now use the definition of peclet number P_e, given as :

$$P_e=\frac{F}{D}$$

peclet number is defined as the ratio of convection factor to diffusion factor. It is a dimensionless number that governs whether it is the physics of convection or diffusion that dominates the problem. The larger the value of peclet number more is the convection dominant physics. The lesser the value of peclet number more is the diffusion dominant physics. [30]

We now apply power law in various coefficients of the discretized finite volume equation. We have coefficients of the equation (4.175) given as:

$$a_E=-\frac{F_{east}}{2}$$

And,

$$a_W = + \frac{F_{west}}{2}$$

And,

$$a_N = - \left(\frac{F_{north}}{2} \right)$$

And,

$$a_s = + \left(\frac{F_{south}}{2} \right)$$

By power law we have for top and bottom coefficients:

$$a_T = D_{TOP}(1 - \frac{P_{eTOP}}{2}) = D_{i, j+\frac{1}{2}} A(|P_{eTOP}|)$$

$$where, A(|P_{eTOP}|) = Max\left(0, (1 - 0.1|P_{eTOP}|)^5\right)$$

And,

$$a_B = D_{i, j-\frac{1}{2}}(1 + \frac{P_{eBOTTOM}}{2}) = D_{i, j-\frac{1}{2}}(A(|P_{eBOTTOM}|) + P_{eBOTTOM})$$

$$where, A(|P_{eBOTTOM}|) = Max\left(0, (1 - 0.1|P_{eBOTTOM}|)^5\right)$$

Thus, the term a_P becomes:

$$a_P = a_E + a_W + a_N + a_S + a_t + a_b + MAX\left(0, F_{EAST} - F_{WEST}\right)$$
$$+MAX\left(0, F_{NORTH} - F_{SOUTH}\right) + MAX\left(0, F_{top} - F_{bottom}\right)$$

The new coefficients are substituted into equation (4.175) and we solve for ϕ_P by using iterative methods.

Chapter 5

RESULTS AND DISCUSSIONS

This chapter presents the results from the solutions of Reynolds equation versus results from thin film Navier-Stokes momentum and continuity equations for combination of different subsonic mach numbers i.e. runner velocities, Reynolds numbers, maximum and minimum film thickness ratios. Profiles of pressure, velocities and density for each case are presented in this section.

5.1 Grid Independence Test

The grid Independence Test is a vital CFD analysis practice which is carried out to ensure that the grid resolution does not have any effect on the solution accuracy. The grid independence test helps in selecting a suitable grid size that reduces discretization error significantly so that it can be considered negligible in its effect on solution accuracy.

The choice of grid selection for the simulation is made on the basis of the outcome from grid independence test as well as keeping in mind the balance between the choice of best grid size and time for its computation. For the grid independence test The Reynolds equation solver was chosen. The computational time taken by the Reynolds equation solver to converge is much lesser than the time taken by any of the three thin film momentum equations. This is on account of the discretization complexity as well as the complexity of the fundamental nature of thin film momentum equations. 3 grid configurations were tested to see the percentage deviation with the most refined version of the mesh i.e. grid configuration 1 with 512,000 number of nodes. The parameter compared was the maximum non dimensional pressure from Reynolds equation. The deviation in value of maximum pressure has been considered as a criteria for

The grid configuration chosen are given in table 1 below:

Table 1 grid independence test details

Grid configuration	Resolution	Number of Nodes along X direction	Number of Nodes along Y direction	Number of Nodes along Z direction	Total number of Nodes	Time for computation (Hrs)	Relative Deviation from finest grid configuration (%)
1.	Finest	80	80	80	512,000	96 to 120	0%
2.	fine	60	60	60	216,000	50 to 80	0.11 %
3.	medium	28	28	28	21,952	8 to12	0.3%
4.	Low	20	20	20	8,000	4 to 6	0.82%

A plot of maximum non dimensional pressure versus No. of nodes in each direction is shown below. From the results of the grid independence test it was found that grid configuration 2 has a relative percentage deviation of about 0.11 percent from grid configuration 1. Grid configuration 3 has a relative percentage deviation of about 0.3 percent from grid configuration 1. And grid configuration 4 has a relative percentage deviation of about 0.82 percent from grid configuration 1. Therefore, by keeping

computational time requirement and relative percentage deviation from finest configuration in mind, Grid configuration 3 with 21,952 total number of nodes was selected as the best grid configuration for simulation.

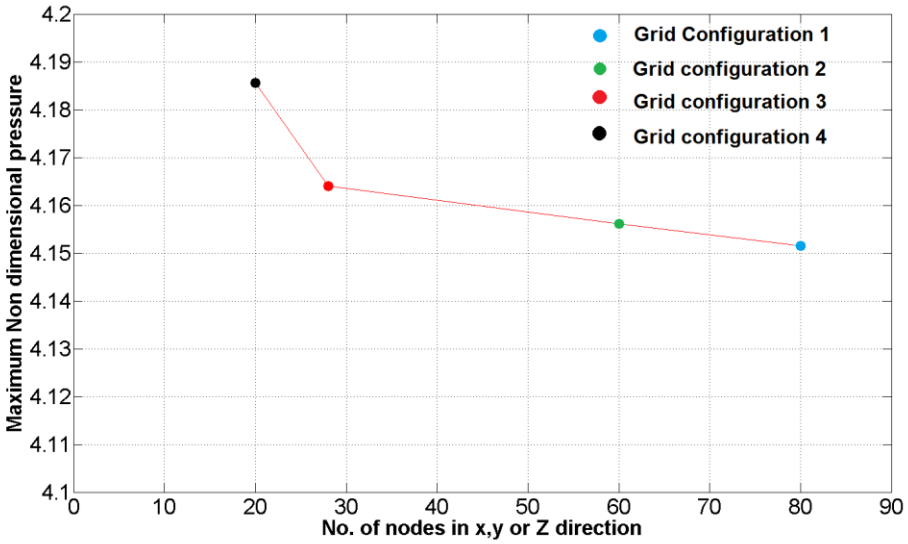

Figure 16 plot of Grid independence test results

5.2 Reference Fluid Domain And Conditions For Simulation

The reference fluid domain for simulation is a fluid domain representation of a thin film formed between a runner and a top foil. For the purpose of computational ease and modelling the fluid domain has been assumed to be of rectangular shape. The width along the direction of leakage flow is 60 mm. The length of the thin film is fixed to 60 mm. several combinations of maximum and minimum film thickness and velocities are compared. These values are summarized in the table 2

Table 2: details of cases considered for simulation

Case number	Minimum Film thickness (μm)	Maximum Film thickness (μm)	clearance (μm)	Runner Velocity (m/s)	Pressure boundaries (bar)	Reynolds number	Mach number	Length of Taper (mm)	Length of Flat (mm)
1	10	40	25	300	1.0	512.556	0.882	50	10
2	10	50	30	300	1.0	615.068	0.882	50	10
3	10	30	20	300	3.0	1230.14	0.882	50	10

5.3. Boundary Conditions

In this section the boundary conditions applicable to the physical system are discussed. The 3D thin film geometry requires careful consideration and handling of boundary conditions to make sure that the problem is adequately defined. Over defining or under defining boundary conditions will lead to incorrect solutions from the solver. The boundary conditions have been discussed for all faces of the thin film which are shown in figure 17. The isothermal Boundary and temperature field within thin film has been assumed. Thus, temperature has been assumed throughout all simulations to be as:

$T = 298K$

1) Thin Film Inlet:

The inlet of the thin film is defined with a total pressure boundary condition. This is the most realistic representation of the phenomenon encountered in thin films at inlet. Inlet of thin film is directly exposed to the surrounding ambient pressure as inlet is unbounded and simply exists at the beginning of the thin film between the runner and

beginning of top foil. This allows definition of pressure boundary at the inlet as equal to surrounding pressure. Considering the system is located within earth's atmosphere, this allows specification of boundary pressure to be equal to atmospheric pressure. The velocities at inlet face are unknown hence, these are extrapolated from within the domain.

2) Thin Film Outlet:

The outlet of the thin film is specified as total pressure boundary condition. This is again a direct consequence of pressure condition at outlet boundary which has an interface with surrounding atmosphere. The outlet is specified as an atmospheric boundary condition. The velocities at outlet face are unknown, these are extrapolated from within the domain.

3) Runner Moving Wall:

The Runner wall is defined as a no-slip boundary condition for the three velocities. Owing to the high speed translational velocity of the runner 'U' velocity is defined at the runner surface. The boundary condition for 'V' velocity is defined as: $U\frac{\partial H}{dx}$ at the runner surface. This boundary condition follows from the fact that the runner velocity along with slope generates a vertical component of velocity i.e. 'V' velocity. The height of the film is only a function of X direction i.e. the height does not vary in the direction of leakage flow. 'W' velocity is assigned zero at the runner wall.

4) The Bearing Surface:

The bearing wall is defined as a no-slip boundary condition for the three velocities. All three velocities i.e. U, V, W are set to zero at the bearing surface.

5) Leakage Flow Walls:

The wall at the inner diameter of the bearing and the outer diameter of the bearing along the direction of leakage flow are assigned with total pressure boundaries similar to inlet and outlet. The velocities at these walls are unknown. Hence, these are extrapolated from within the domain.

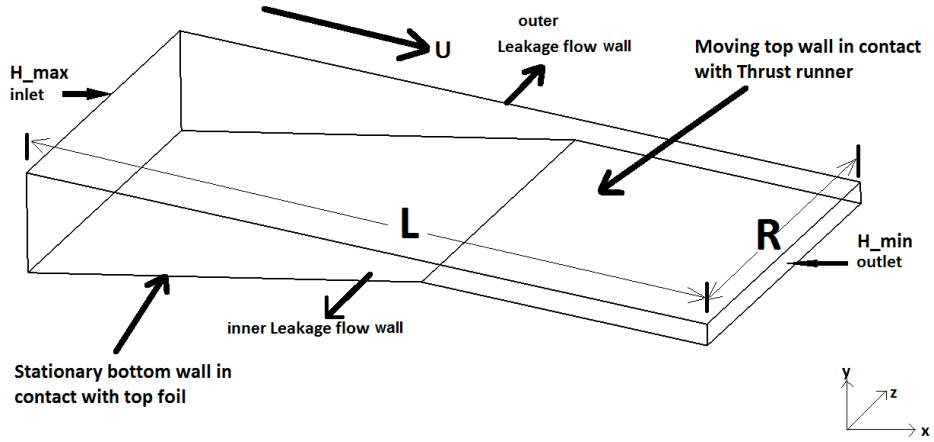

Figure 17 boundary face nomenclature for thin film

5.4 Results

The cases discussed in section 5.2 were simulated by the solver and the results from the simulations of the cases discussed in section 5.2. Are presented in this section. The criteria for convergence is set based on the residuals of the governing equations. Convergence is accepted if the value of residuals for all governing equations become less than or equal to $10^{-5.}$

Monitoring and accepting residuals to be sole basis of convergence is not a good CFD practice hence, a quantity has been monitored for stability in value at any given point within the grid. Convergence is said to have reached once the variation of this

monitored quantity becomes negligible. For this purpose, Mass flow rate has been monitored at the same grid point in all cases. From the plots presented it is clear that convergence can be said to have reached. 'V' velocity field has not been discussed in the results as its magnitude and behaviour has been found to be not of a very significant interest to performance prediction of the thin film. Several remarks can be made concerning rest of the results.

5.4.1 Case 1 Results

Case 1 was simulated with the parameters shown in table 3. This is the lowest Reynolds number (R_e= 512.556) case simulated in this thesis.

Table 3: case 1 simulation parameters

Minimum Film thickness (μm)	Maximum Film thickness (μm)	clearance (μm)	Runner Velocity (m/s)	Pressure boundaries (bar)	Reynolds Number(R_e)	Mach number	Length of Taper (mm)	Length of Flat (mm)
10	40	25	300	1.0	512.556	0.882	50	10

The case converges well within 100 iterations the converged residuals are shown in figure 18. Although mass flow flux from figure 19 seems to have stabilized at about 40 iterations, Convergence of all equations is achieved at about 90 iterations.

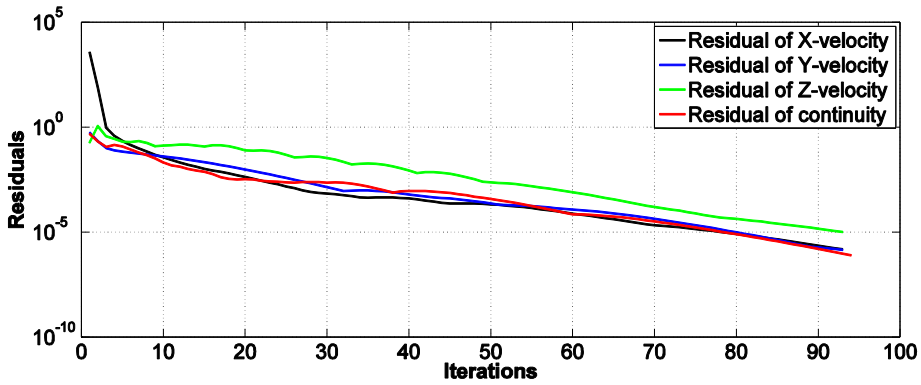

Figure 18 Plot of Residuals for case 1

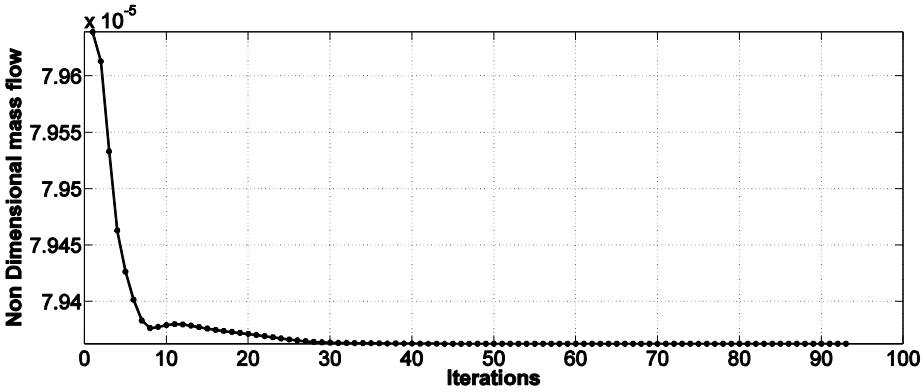

Figure 19 Plot of Non dimensional mass flow for case 1

The solution of Non dimensional pressure from Reynolds equation for case 1 is shown in figure 20. The profile is smooth and dome shaped. This is characteristic of pressure profile generated by Reynolds equation. The peak pressure reached by Reynolds equation solution is about 3.6 bar.

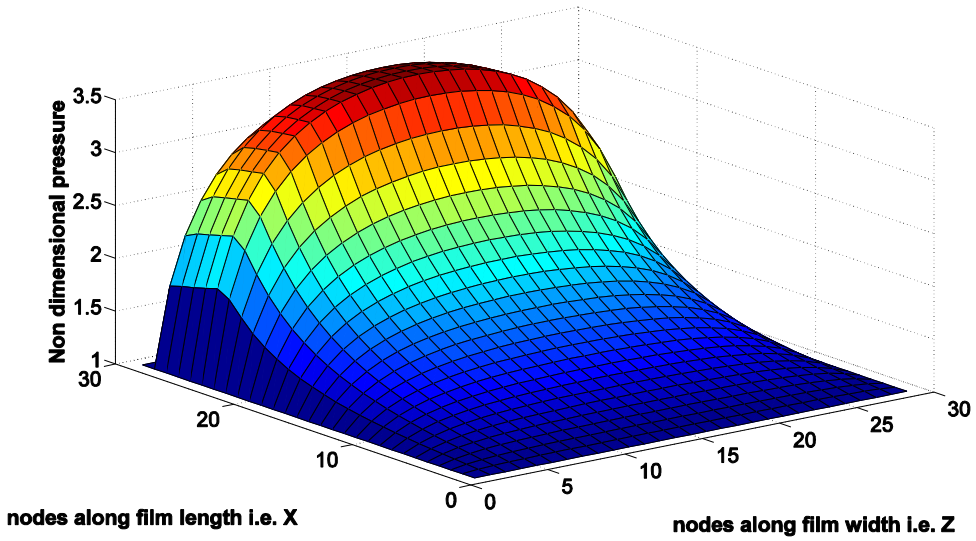

Figure 20 surface profile of Non dimensional pressure from Reynolds equation for case 1

Figure 21 shows the pressure profile from CFD solution using isothermal temperature and density calculated from continuity equation. The density is calculated from the continuity equations based on the solutions of three velocities from momentum equations. The pressure surface profile from CFD solution is slightly different than Reynolds equation. The pressure is found to be higher than what Reynolds equation predicts. The gradient of density calculated from continuity equation is found to be negligible. This is an expected consequence on account of extremely small clearance to length ratio for the cases analysed in this thesis.

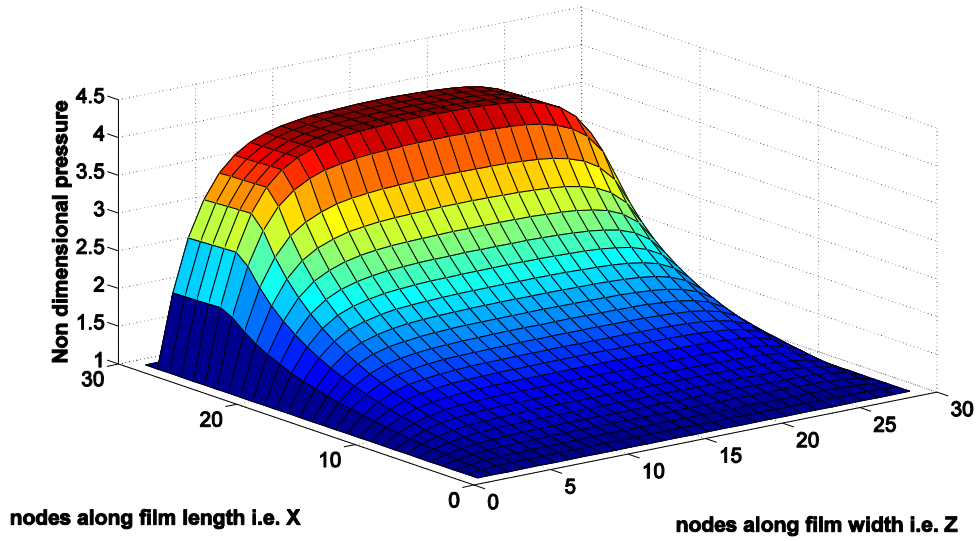

Figure 21 surface profile of Non dimensional pressure from CFD solution for case 1

Figure 22 shows comparison of pressure calculated from CFD solution of momentum equations, continuity and ideal gas solver with pressure calculated from Reynolds equation. It can be observed that the pressure calculated from CFD solution is higher than what is predicted by Reynolds equation. Inertia has a significant effect at this high value of Mach number i.e. M=0.882 and Reynolds number=512.556.

The peak pressure predicted by Reynolds equation which is about 3.6 bar is found to be lower than actual pressure in the high speed operation, which is about 3.9 bar. Thus inertia can be seen to have added 0.3 bar to the prediction of classical lubrication theory for this case.

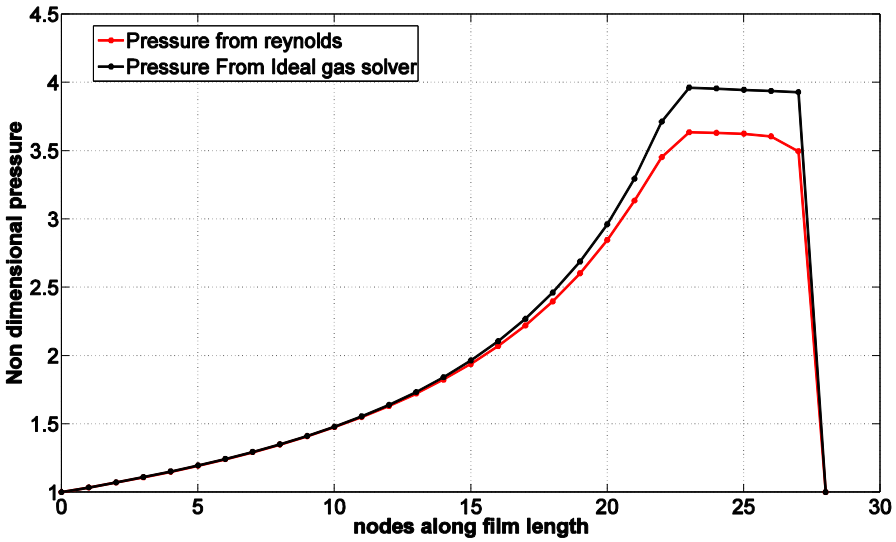

Figure 22 comparison of non-dimensional pressure from Reynolds equation vs CFD solution for case 1

. Figure 23 and figure 24 show plots of 'U' velocities from Analytical solution of 'U' velocity from Reynolds equation and X momentum Navier-stokes thin film equation respectively. The velocity profiles are plotted at mid-section i.e. in the middle of the film along leakage flow direction. The plots are at inlet, middle of the film length and at the outlet of the film. The plots describe behaviour of 'U' velocity which is driven by pressure gradient along film length. The nature of fluid flow in the thin film is a combination of poiseuille flow and couette flow. While couette flow will have significance at locations where pressure gradient is zero and the flow is completely shear driven, most of the flow in thin films have a combined couette and poiseuille flow nature. The pressure gradient along x direction is such that it retards the flow at entrance and accelerates the flow at outlet. The positive pressure gradient at the beginning of the film up to length of taper causes the 'U'

velocity to be retarded. However, the negative pressure gradient at the outlet area cause the fluid velocity ‘U’ to be accelerated.

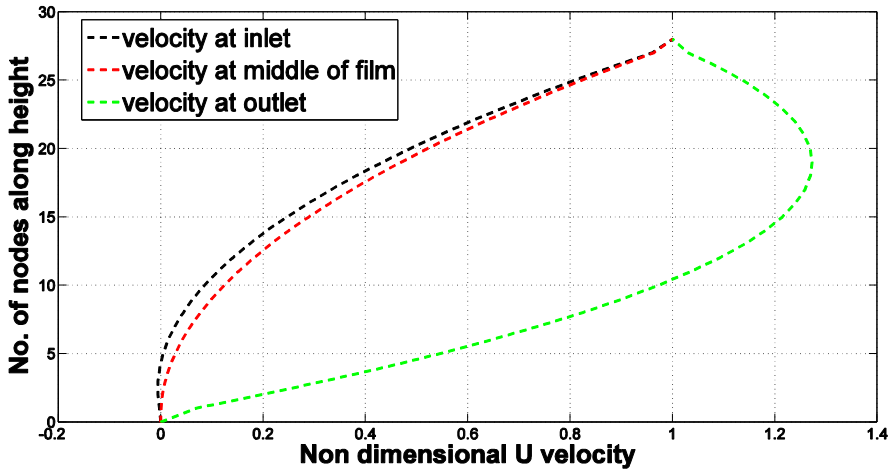

Figure 23 Plot of analytical ‘U’ Velocity profile at inlet, middle and outlet of film from solution of Reynolds equation for case 1

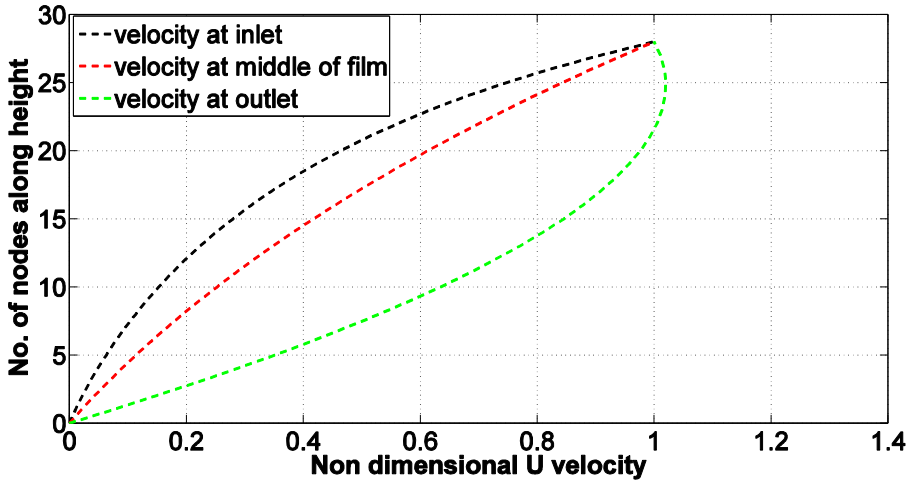

Figure 24 plot of ‘U’ Velocity profile at inlet, middle and outlet of film from solution of X momentum equation for case 1

Figure 25 and figure 26 show surface profiles and magnitude of leakage flow velocities i.e. ‘W’ velocities from analytical solution of leakage flow velocity based on classical lubrication theory. Figure 25 is a surface profile of leakage flow at the inner leakage wall and Figure 26 is a surface profile of leakage flow at the outer leakage wall. The magnitude and nature of leakage flow velocities from these two figures are compared with magnitude and nature of leakage flow velocities from figure 27 and figure 28, which are surface profiles of leakage flow velocity ‘ W’ from solutions of ‘Z’ momentum equation. The magnitude of leakage flow velocity at the outer leakage wall is found to be lower than analytical solution prediction. This indicates that the amount of mass flow leaking out of the outer wall is lower than what is predicted by classical lubrication theory. Inertia is thus reducing the leakage flow velocity magnitude at the outer wall at high speeds. Further, from comparing figures 25 and 27, it can be inferred that classical lubrication theory predicts the magnitude of leakage flow at inner wall to be higher than the actual prediction from the Navier-Stokes Z momentum equation solution. Thus, it seems that at steady state and high speeds inertia creates less leakage flow at the inner wall along the leakage flow direction and allows less leakage at the outer wall. Thus, the design consideration of thrust bearing at high speeds needs to account for effect of inertia on leakage flow which is visible from solutions of Navier-Stokes equations for case 1.

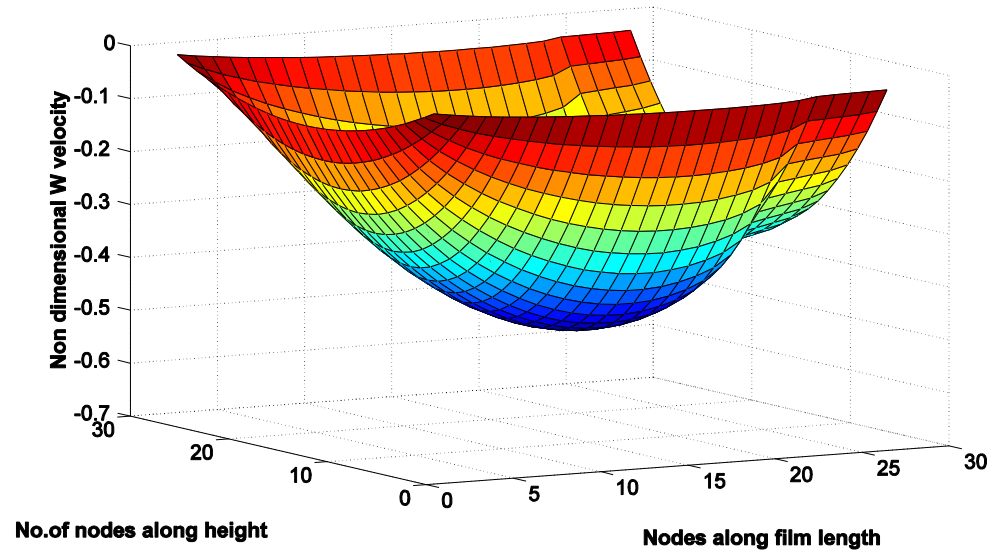

Figure 25 surface profile of Analytical ‘W’ Velocity at inner leakage flow wall from solution of Reynolds equation for case 1

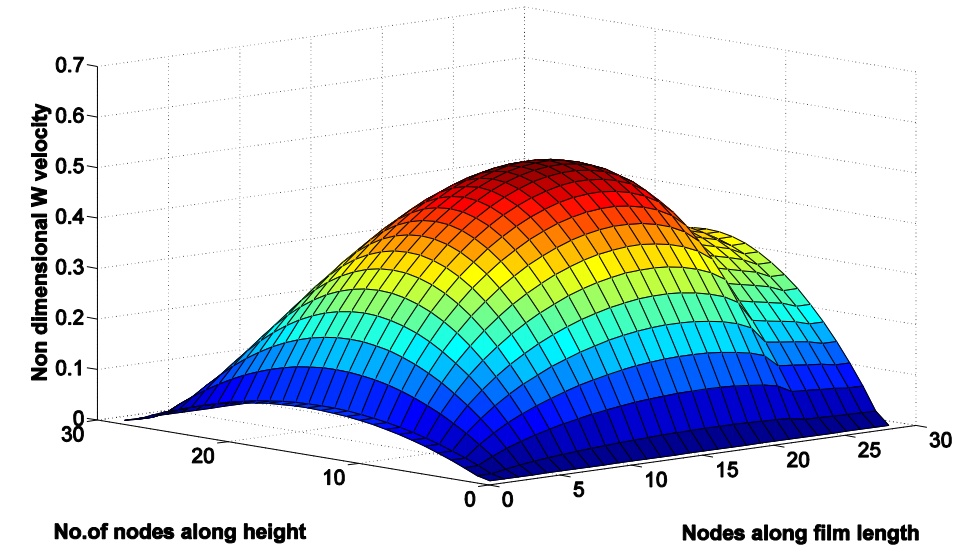

Figure 26 surface profile of Analytical 'W' Velocity at outer leakage flow wall from solution of Reynolds equation for case 1

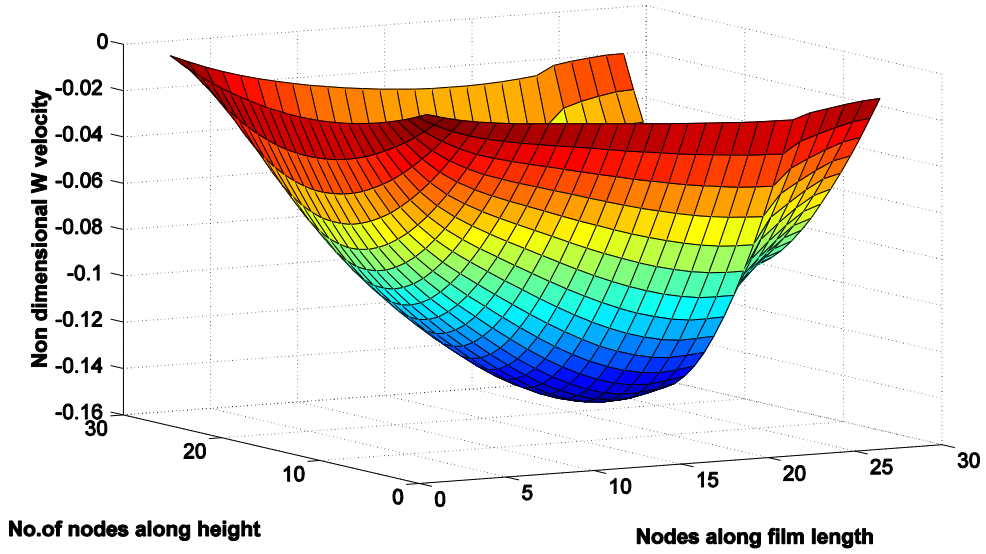

Figure 27 surface profile of 'W' Velocity at inner leakage flow wall from solution of 'Z' momentum equation for case 1

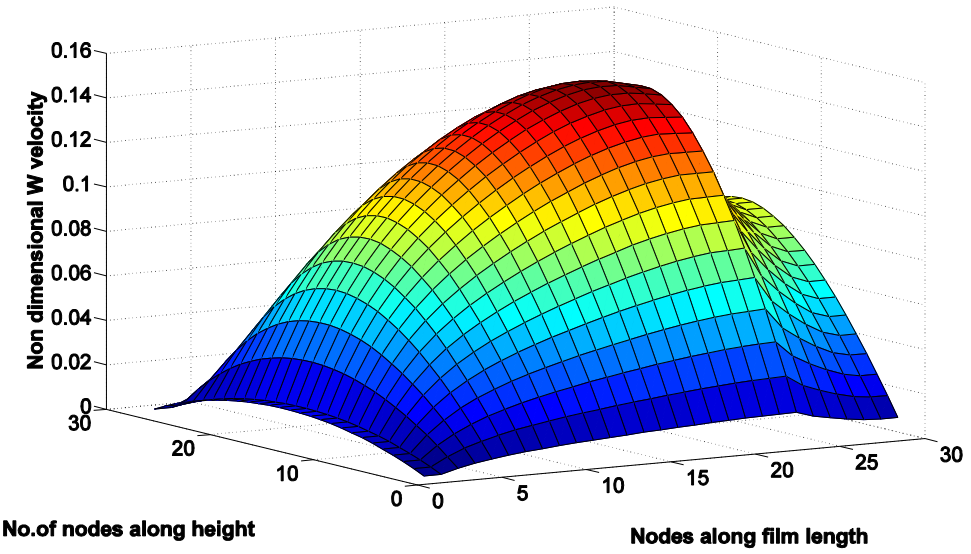

Figure 28 surface profile of 'W' Velocity at outer leakage flow wall from solution of 'Z' momentum equation for case 1

5.4.2 Case 2 Results

Case 2 was simulated with the parameters shown in table 3.

Table 4: case 2 simulation parameters

Minimum Film thickness (μm)	Maximum Film thickness (μm)	clearance (μm)	Runner Velocity (m/s)	Pressure boundaries (bar)	Reynolds number	Mach number	Length of Taper (mm)	Length of Flat (mm)
10	50	30	300	1.0	615.068	0.882	50	10

The case converges well at about 100 iterations the converged residuals are shown in figure 29. Although mass flow flux from figure 30 seems to have stabilized at about 40 iterations, Convergence of all equations is achieved at about 100 iterations. This is about 10 iterations higher than case 1. Reynolds number for this flow is higher

than case 1 therefore, the solver requires more number of iterations to reach a converged solution.

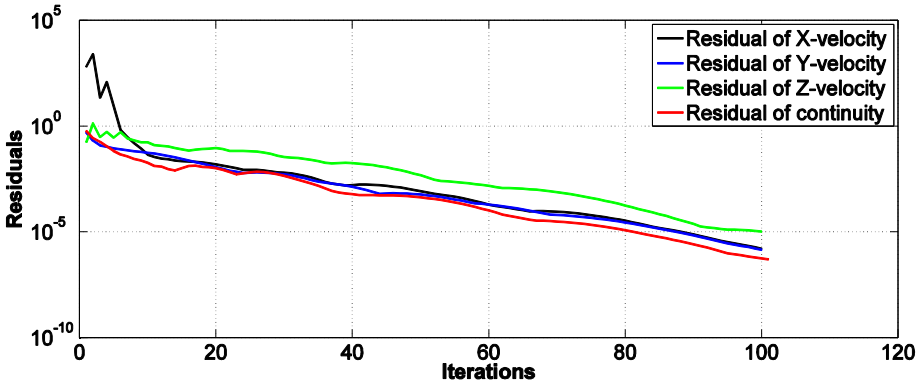

Figure 29 Plot of Residuals for case 2

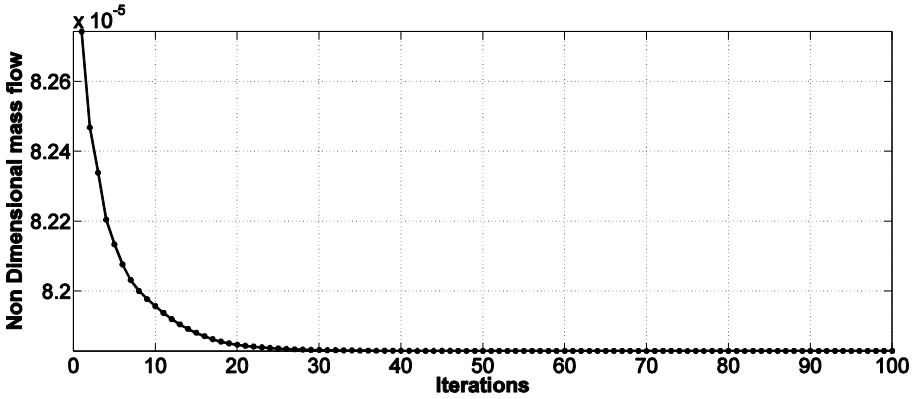

Figure 30 Plot of Non dimensional mass flow for case 2

The solution of Non dimensional pressure from Reynolds equation for case 2 is shown in figure 31. The profile is smooth and dome shaped similar to case 1. The peak pressure reached by Reynolds equation solution is about 4.2 bar.

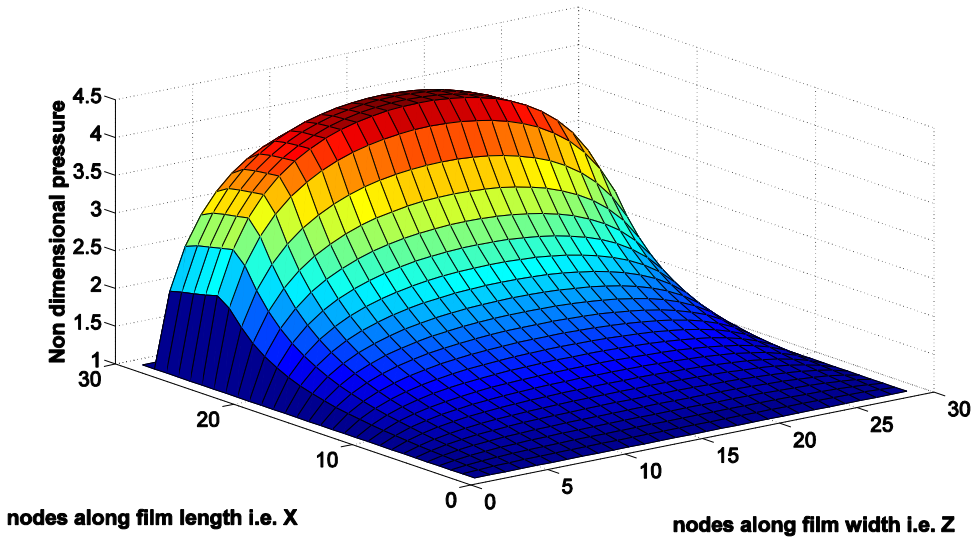

Figure 31 surface profile of Non dimensional pressure from Reynolds equation for case 2

Figure 32 shows the pressure profile from CFD solution using isothermal temperature and density calculated from continuity equation. The pressure surface profile from ideal gas equation of state is slightly different than Reynolds equation. The pressure is found to be higher than what Reynolds equation predicts. This is a similar behaviour as encountered in case 1.

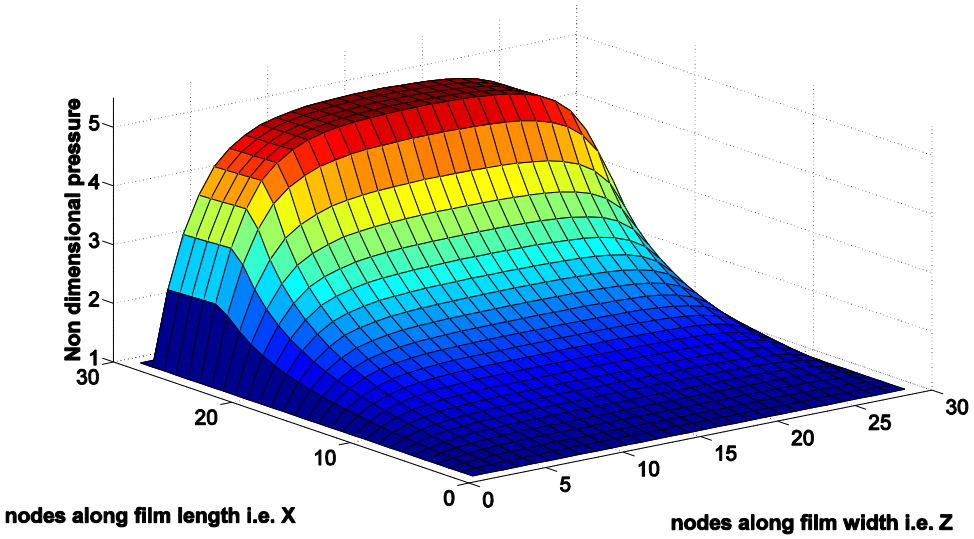

Figure 32 surface profile of Non dimensional pressure from CFD solution for case 2

Inertia can be seen to increase the pressure to about 4.9 bar when compared to about 4.2 bar predicted by classical lubrication theory, This is evident from figure 33. Compared to effect of inertia on pressure increase in case 1, the effect of inertia on increasing pressure in case 2 seems to be higher which is 0.7 bar in this case. This is on account of Higher Reynolds number.

Further, the maximum height has been increased to 50 μm compared to 40 μm from case 1. The minimum film thickness is still maintained at 10 μm. Thus the effect of a steeper slope is also visible on the pressure profiles.

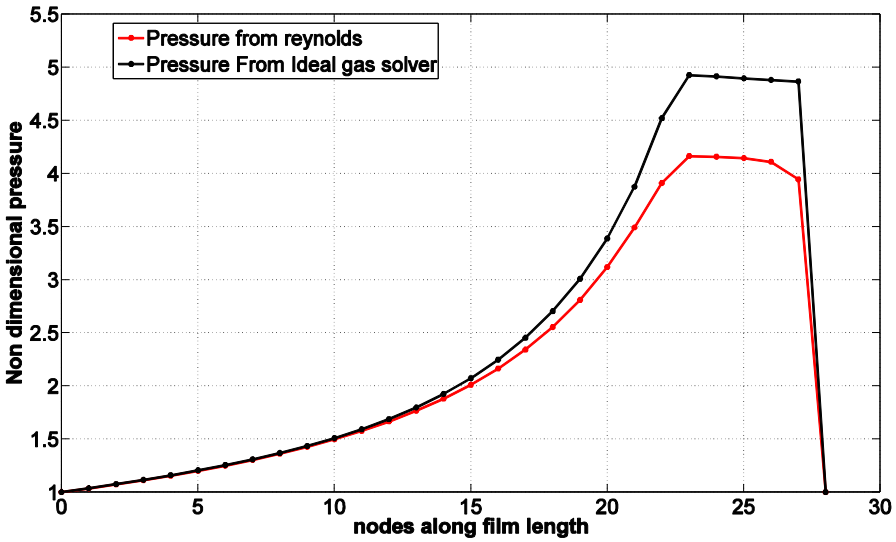

Figure 33 comparison of non-dimensional pressure from Reynolds equation vs Ideal gas solver for case 2

Figure 34 and figure 35 show plots of 'U' velocities from Analytical solution of 'U' velocity from Reynolds equation and X momentum Navier-stokes thin film equation respectively. The velocity profiles are plotted at mid-section i.e. in the middle of the film along leakage flow direction. The plots are at inlet, middle of the film length and at the outlet of the film. The plots describe behaviour of 'U' velocity which is driven by pressure gradient along film length. Similar to case 1, the positive pressure gradient at the beginning of the film up to length of taper causes the 'U' velocity to be retarded. However, the negative pressure gradient at the outlet area cause the fluid velocity 'U' to be accelerated.

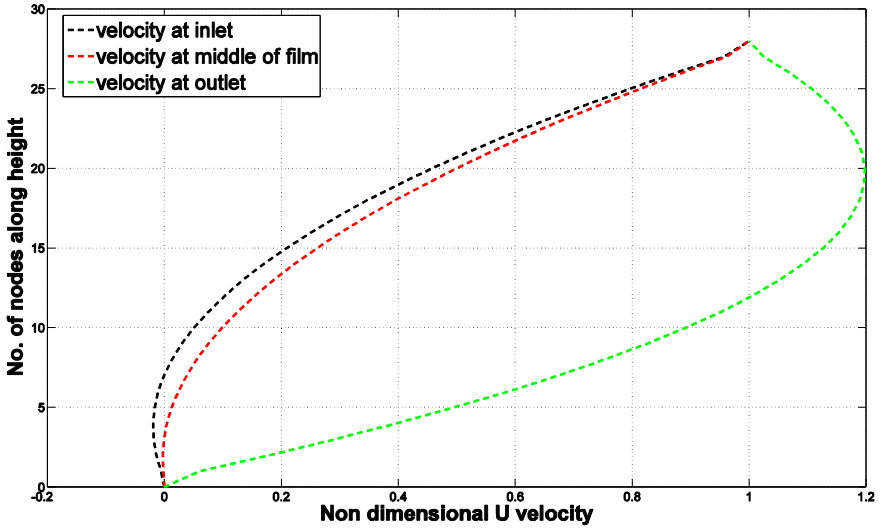

Figure 34 Plot of analytical 'U' Velocity profile at inlet, middle and outlet of film from solution of Reynolds equation for case 2

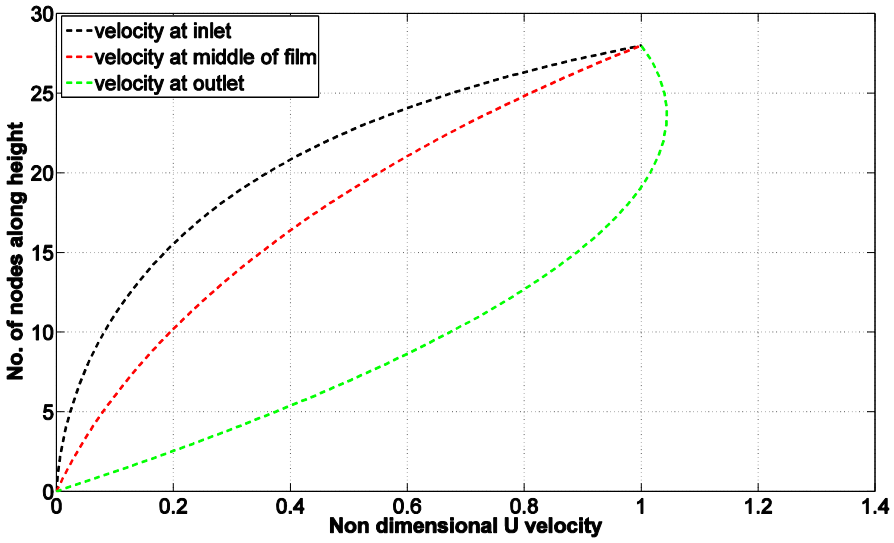

Figure 35 plot of 'U' Velocity profile at inlet, middle and outlet of film from solution of X momentum equation for case 2

Figure 36 and figure 37 show surface profiles and magnitude of leakage flow velocities i.e. 'W' velocities from analytical solution of leakage flow velocity based on classical lubrication theory. Figure 36 is a surface profile of leakage flow at the inner leakage wall and Figure 37 is a surface profile of leakage flow at the outer leakage wall. The magnitude and nature of leakage flow velocities from these two figures are compared with magnitude and nature of leakage flow velocities from figure 38 and figure 39, which are surface profiles of leakage flow velocity ' W' from solutions of 'Z' momentum equation. The magnitude of leakage flow velocity at the outer leakage wall is found to be lower than analytical solution prediction this is similar to prediction in case 1. This indicates that the amount of mass flow leaking out of the outer wall is lower than what is predicted by classical lubrication theory. Inertia is thus reducing the leakage flow velocity magnitude at the outer wall at high speeds. Further, from comparing figures 36 and 38, it can be inferred that classical lubrication theory predicts the magnitude of leakage flow at inner wall to be higher than the actual prediction from the Navier-Stokes Z momentum equation solution. At steady state and high speeds, inertia creates less leakage flow at the inner wall along the leakage flow direction and allows less leakage flow to escape from the outer wall. Thus, similar to case 1 the design consideration of thrust bearing at high speeds needs to account for effect of inertia on leakage flow which is visible from solutions of Navier-Stokes equations for case 2.

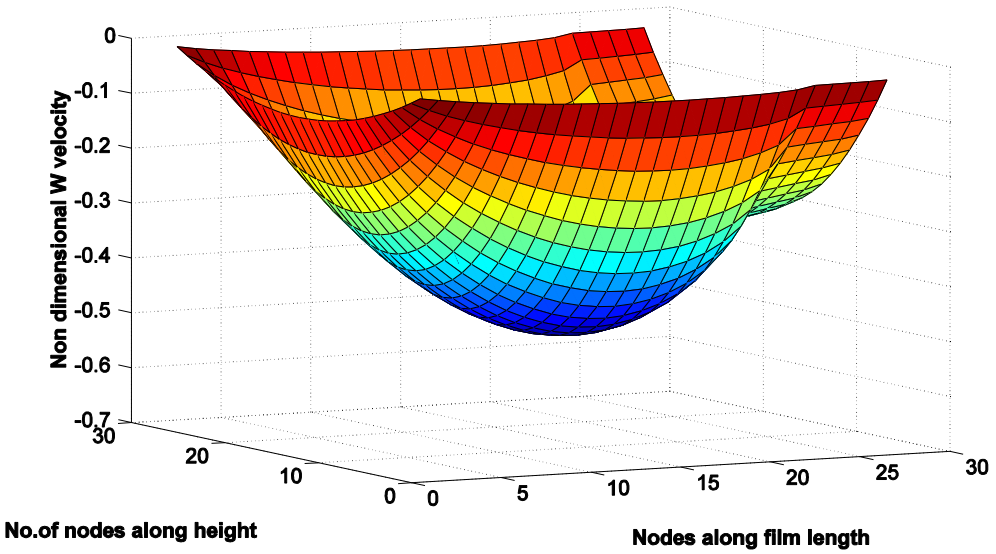

Figure 36 surface profile of Analytical 'W' Velocity at inner leakage flow wall from solution of Reynolds equation for case 2

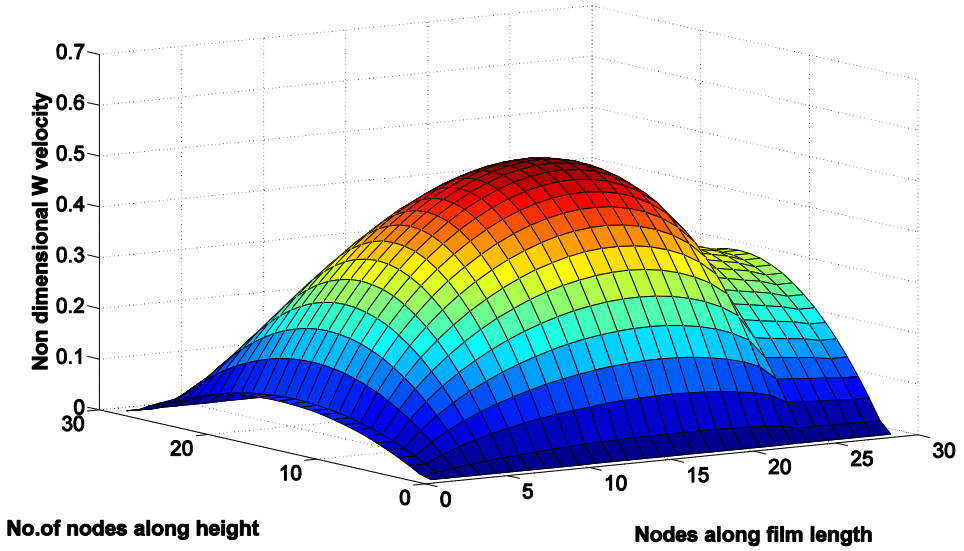

Figure 37 surface profile of Analytical 'W' Velocity at outer leakage flow wall from solution of Reynolds equation for case 2

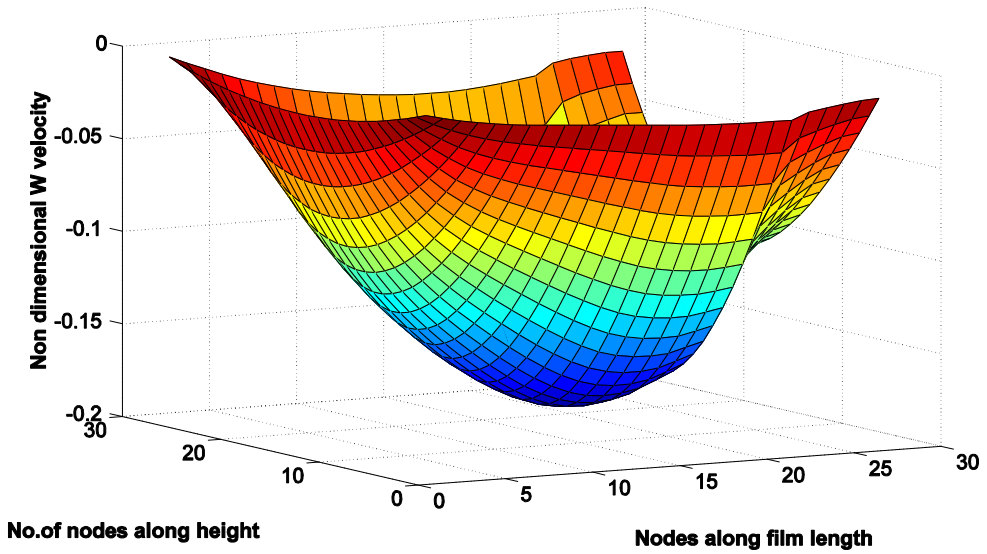

Figure 38 surface profile of 'W' Velocity at inner leakage flow wall from solution of 'Z' momentum equation for case 2

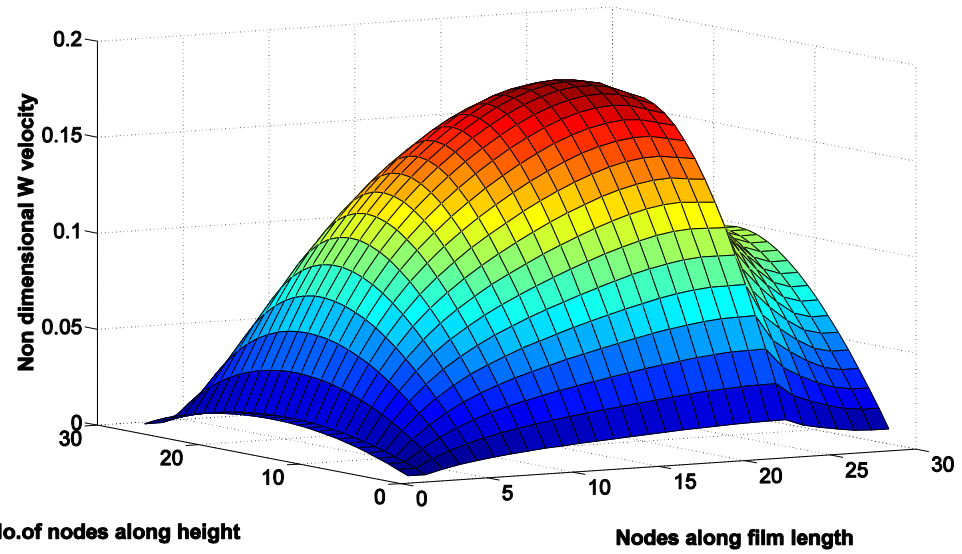

Figure 39 surface profile of 'W' Velocity at outer leakage flow wall from solution of 'Z' momentum equation for case 2

5.4.3 Case 3 Results

Table 5: case 3 simulation parameters

Minimum Film thickness (μm)	Maximum Film thickness (μm)	clearance (μm)	Runner Velocity (m/s)	Pressure boundaries (bar)	Reynolds number	Mach number	Length of Taper (mm)	Length of Flat (mm)
10	30	20	300	3.0	1230.14	0.882	50	10

The case converges well at about 250 iterations the converged residuals are shown in figure 40. Although mass flow flux from figure 41 seems to have stabilized at about 100 iterations, Convergence of all equations is achieved at about 100 iterations. This is about 150 iterations higher than case 2. Reynolds number for this flow is higher than both case 1 and case 2 therefore, the solver requires more number of iterations to

reach a converged solution. Also the boundary pressure has been set to 3.0 bar which is three times higher than boundary pressures of case 1 and case 2. This causes a higher value of flow Reynolds number.

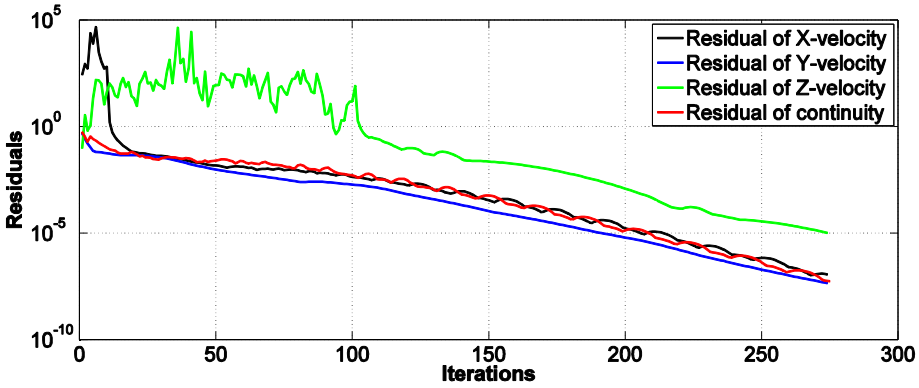

Figure 40 Plot of Residuals for case 3

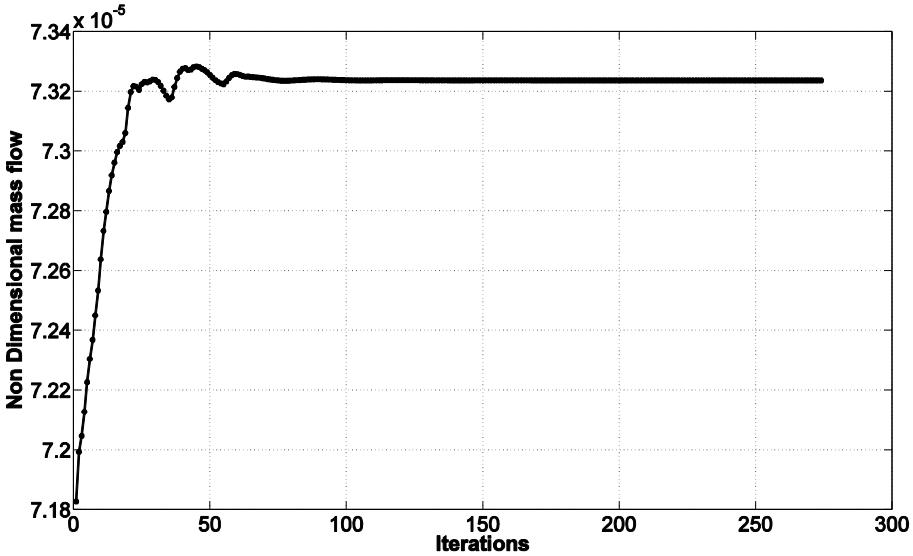

Figure 41 Plot of Non dimensional mass flow for case

The solution of non-dimensional pressure from Reynolds equation for case 3 is shown in figure 42. The profile is smooth and dome shaped similar to case 1 and 2. The peak pressure reached by Reynolds equation solution is about 7.5 bar.

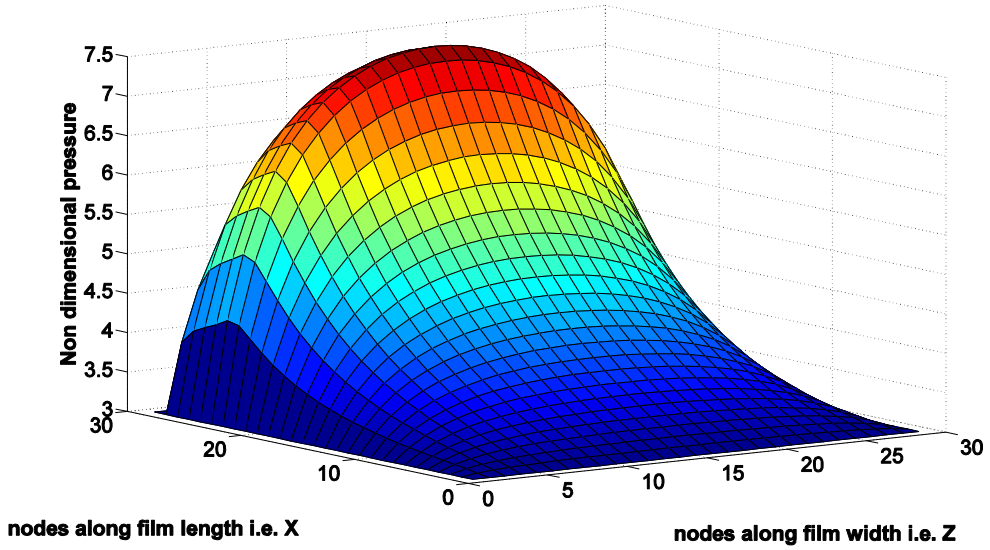

Figure 42 surface profile of Non dimensional pressure from Reynolds equation for case 3

Figure 43 shows the pressure profile from CFD solution using isothermal temperature and density calculated from continuity equation. The pressure surface profile from ideal gas equation of state is slightly different than Reynolds equation. The pressure is found to be higher than what Reynolds equation predicts. This is a similar behaviour as encountered in case 1 and case 2.

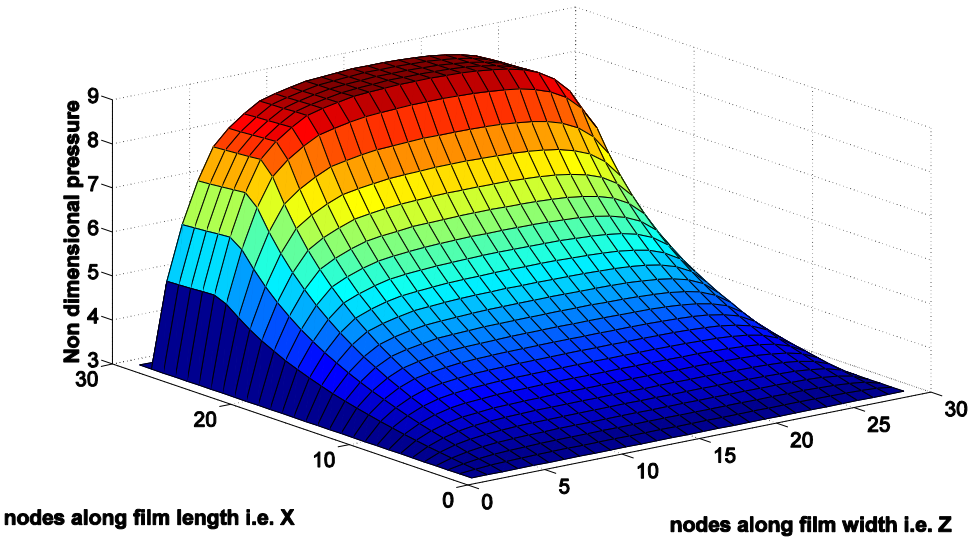

Figure 43 surface profile of Non dimensional pressure from CFD solution for case 3

Inertia can be seen to increase the pressure to about 8.7 bar when compared to about 7.5 bar predicted by classical lubrication theory, This is evident from figure 44. Compared to effect of inertia on pressure increase in case 1 and case 2, the effect of inertia on increasing pressure in case 3 seems to be higher which is about 1.2 bar in this case. This is on account of Higher Reynolds number.

The effect of inertia for high flow Reynolds number in increasing pressure is high for this large value of flow Reynolds number even if the slope of the thin film has been decreased compared to case 1 and 2. The reduction in slope comes from reduction of maximum film thickness to 30 μm while maintaining the inlet film thickness to 10 μm

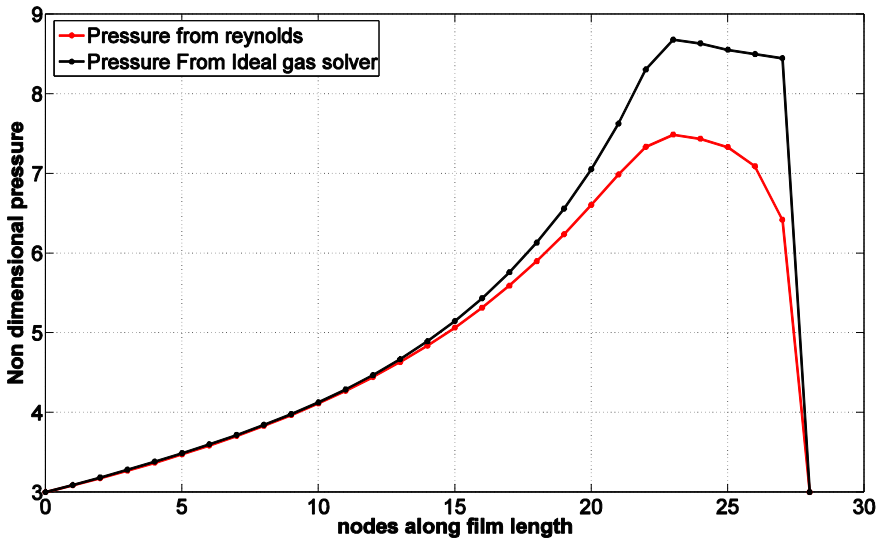

Figure 44 comparison of non-dimensional pressure from Reynolds equation vs Ideal gas solver for case 3

Figure 45 and figure 46 show plots of 'U' velocities from Analytical solution of 'U' velocity from Reynolds equation and X momentum Navier-stokes thin film equation respectively. The velocity profiles are plotted at mid-section i.e. in the middle of the film along leakage flow direction. The plots are at inlet, middle of the film length and at the outlet of the film. The plots describe behaviour of 'U' velocity which is driven by pressure gradient along film length. Similar to case 1 and case 2, the positive pressure gradient at the beginning of the film up to length of taper causes the 'U' velocity to be retarded. However, the negative pressure gradient at the outlet area cause the fluid velocity 'U' to be accelerated. Thus, these results agree well with the theory of pressure driven and shear driven flows.

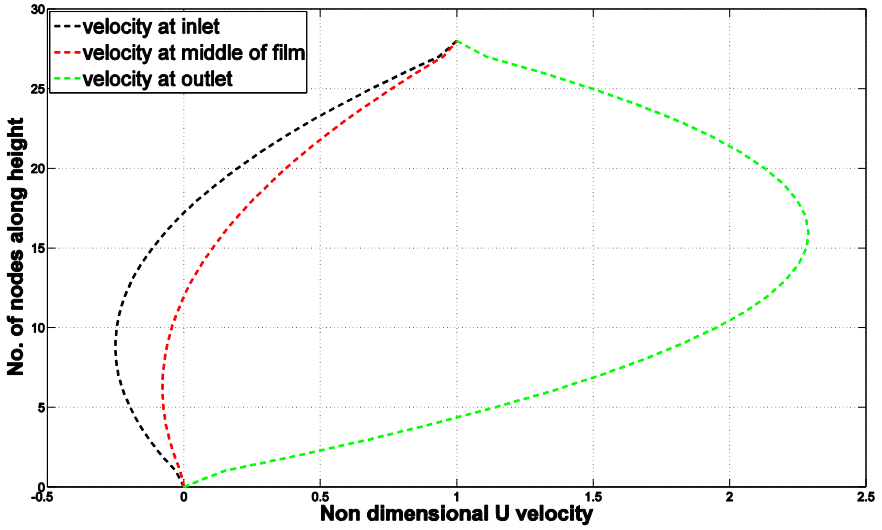

Figure 45 Plot of analytical 'U' Velocity profile at inlet, middle and outlet of film from solution of Reynolds equation for case 3

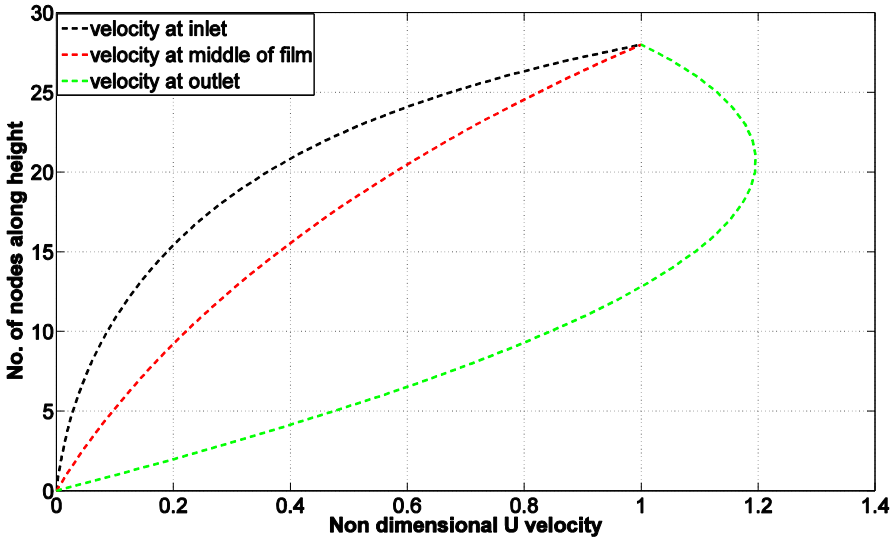

Figure 46 plot of 'U' Velocity profile at inlet, middle and outlet of film from solution of X momentum equation for case 3

Figure 47 and figure 48 show surface profiles and magnitude of leakage flow velocities i.e. 'W' velocities from analytical solution of leakage flow velocity based on classical lubrication theory. The magnitude and nature of leakage flow velocities from these two figures are compared with magnitude and nature of leakage flow velocities from figure 49 and figure 50. The magnitude of leakage flow velocity from Z momentum equation solution at the outer leakage wall is found to be lower than analytical solution prediction this is similar to prediction in case 1 and case 2. This indicates that the amount of mass flow leaking out of the outer wall is lower than what is predicted by classical lubrication theory. Inertia is thus reducing the leakage flow velocity magnitude at the outer wall at high speeds. Further, from comparing figures 47 and 49, it can be inferred that classical lubrication theory predicts the magnitude of leakage flow at inner wall to be higher than the actual prediction from the Navier-Stokes Z momentum equation solution for very high Reynolds numbers. At steady state and high speeds, inertia creates less leakage flow at the inner wall along the leakage flow direction and allows less leakage flow to escape from the outer wall. Thus, the design consideration of thrust bearing at high speeds needs to account for effect of inertia on leakage flow which is visible from solutions of Navier-Stokes equations for case 1, case 2 and case 3.

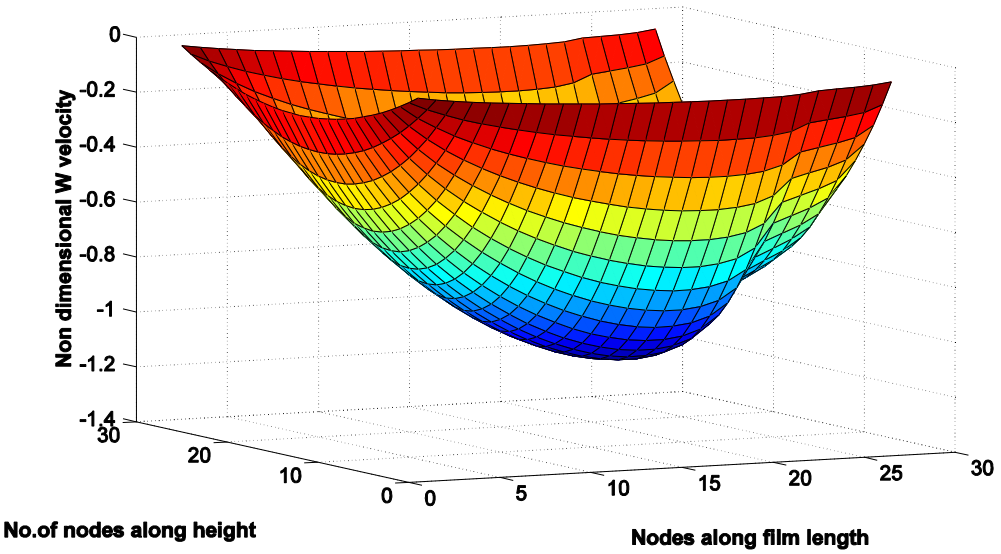

Figure 47 surface profile of Analytical 'W' Velocity at inner leakage flow wall from solution of Reynolds equation for case 3

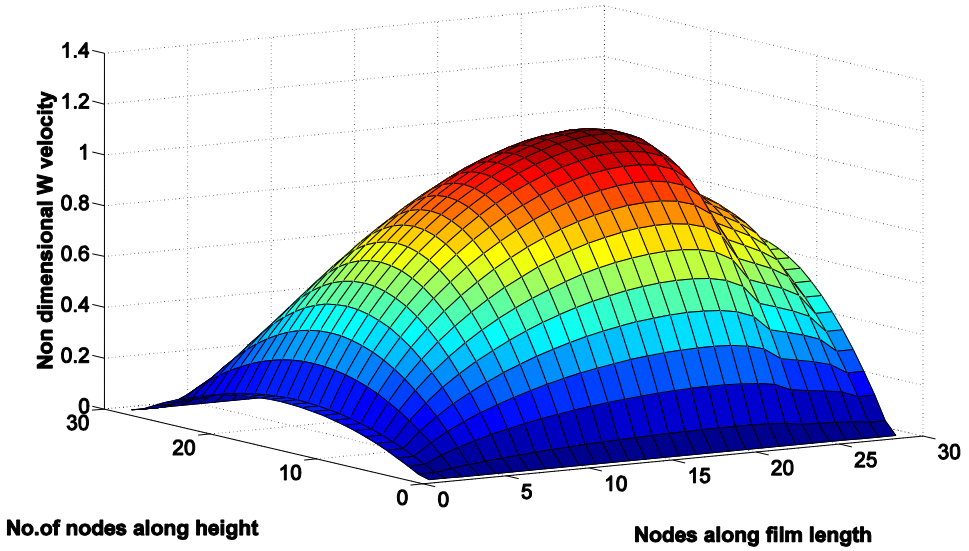

Figure 48 surface profile of Analytical 'W' Velocity at outer leakage flow wall from solution of Reynolds equation for case 3

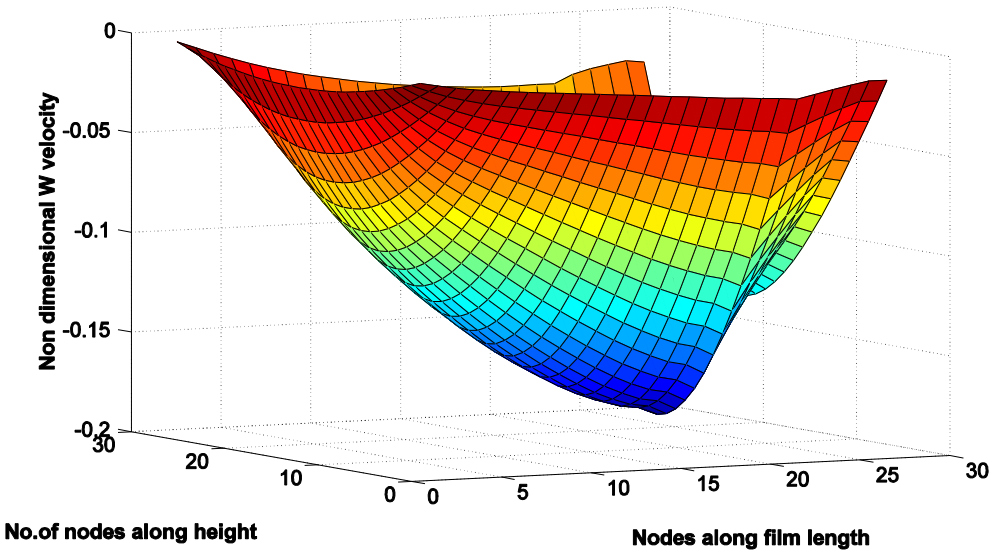

Figure 49 surface profile of 'W' Velocity at inner leakage flow wall from solution of 'Z' momentum equation for case 3

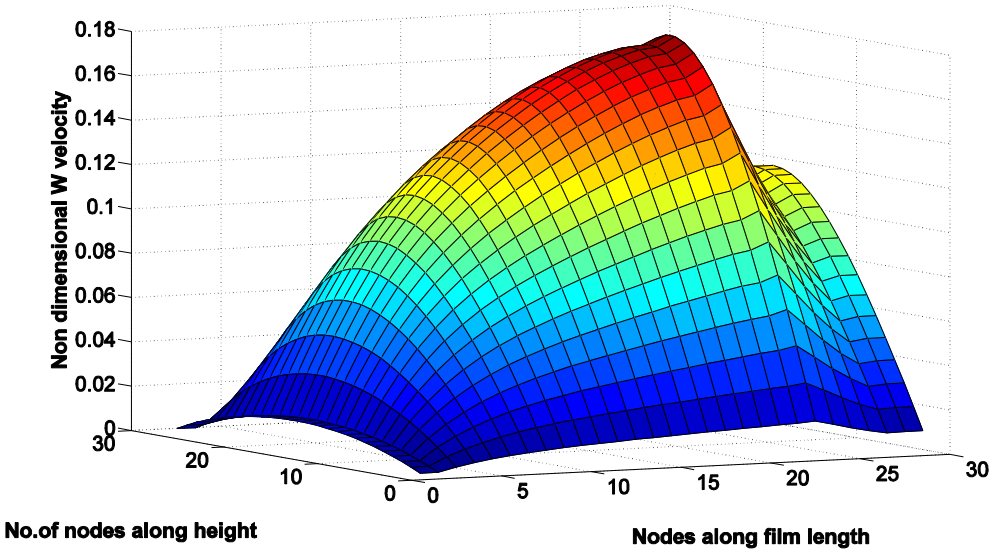

Figure 50 surface profile of 'W' Velocity at outer leakage flow wall from solution of 'Z' momentum equation for case 3

Chapter 6

CONCLUSIONS

A brief introduction to the concept of thin film lubrication and its application to thrust bearings was discussed in chapter 1. Further, the thesis presented discussion on classical lubrication theory and viscous flow theory that govern the fields of lubrication and viscous fluid flow respectively. Chapter 2 was a review of literature pertaining to research work on effects of fluid inertia in bearings. Chapter 3 was a discussion about fundamental governing equations of thin fluid films. Chapter 4 discussed the numerical modeling of governing thin film equations followed by chapter 5 which presented results from three cases simulated for the purpose of this thesis.

A robust computational solver was developed successfully for the purpose of this research thesis to solve the compressible 3D Navier-Stokes equations for thin films. The results from the solver have been compared with available results from Reynolds equation to confirm reasonability of results. The research also sheds light on validity of the use of classical Lubrication theory in modeling performance for high speed bearings.

The solution from the numerical solution of Navier-Stokes equations for thin films suggests that at high speeds inertia has a significant role on leakage flow magnitude and load carrying capacity of the thin film. Thus, The design consideration for thrust bearings operating in high speed subsonic regimes need to account for high speed inertial effects.

Chapter 7

FUTURE AREAS OF RESEARCH

This chapter outlines the scope for future development in this area of research. A discussion about few among many possible areas in which work described in previous chapters can be extended, is presented.

1) The present version of the computational solver uses a segregated Density based solver for calculating density from solution of continuity equation. However, this is not a robust model for accurate density prediction if low flow speeds cause the fluid flow nature to be incompressible. Thus, incorporating a pressure based solver using a pressure correction algorithm (SIMPLE algorithm) would present a robust model capable of handling incompressibility and compressibility due to range of speeds from low to high.

2) The fundamental assumption of the present research in restricting analysis to Non-turbulent fluid regimes may not apply for extremely high Reynolds numbers. Thus, this will require the effort of integrating a suitable turbulence model along with this existing model to understand the effect of turbulence on performance of a three dimensional thin film. Effect of turbulence on performance of thin films has been studied in the past by many authors however, a great deal of study still remains to be completed in this area.

3) The present model can be extended to study non isothermal thin fluid film performance by incorporating the solution of Energy transport within this existing model. Previous research has found that at high speeds effect of energy transport has significant effect on the performance of thin fluid film.

4) The solver can be extended to study performance of thin film in supersonic regimes however, this may require higher resolution schemes such as high order Weighted Essentially non-oscillatory (WENO) scheme to capture effect of shock waves and discontinuities associated with such shocks. The behavior of thin films in supersonic regimes is an area of research where a significant study still remains to be completed.

5) The present study is restricted to thin film performance for a simple rectangular geometry. With suitable modifications the code can be extended to studying nature of fluid flow in cylindrical coordinates for thrust bearings and similar modifications may apply for extension of analysis to journal bearings.

REFERENCES

[1] John Tichy, Florence Dupuy, Benyebka Bou-Sa€ıd, “High-Speed Subsonic Compressible Lubrication” Journal of Tribology | Volume 137 | Issue 4, May 06, 2015

[2] Bauman, S., 2005. An Oil-Free Thrust Foil Bearing Facility Design, Calibration, and Operation. NASA TM 2005-213568, National Aeronautics and Space Administration, Cleveland, OH.

[3] Howard, S. A., Bruckner, R. J., DellaCorte, C., and Radil, K. C., 2008, “Preliminary Analysis for an Optimized Oil-Free Rotorcraft Engine Concept,” Report No. NASA/TM-2008-215064.

[4] Capstone, “Description of Capstone Microturbines,” Capstone Turbine Corporation, Chatsworth, CA, www.capstonemicroturbines.com

[5] Neuros, “Product Line of Turbo Blowers, Turbo Compressors, and Generators,” Neuros Co. Ltd., Daejeon, South Korea, http://www.neuros.com/

[6] Design Space of Foil Bearings for Closed-Loop Supercritical CO2 Power Cycles Based on Three-Dimensional Thermohydrodynamic Analyses.

[7] Tribology , H.G. Phakatkar, R.R. Ghorpade, pg 1.12.

[8] Yu Ping Wang, Experimental Identification Of Force Coefficients Of Hybrid Air Foil Bearings, Pg 14.

[9] Srikanth Honavara-Prasad, “ Scaling Laws For Radial Foil Bearings” The University of Texas at Arlington, December 2014

[10] Dykas, B., Bruckner, R., Dellacorte, C., Edmonds, B., Prahl, J., “Design, Fabrication and Performance of Foil Gas Thrust Bearings for Microturbomachinery Applications,” Journal of Engineering for Gas Turbines and Power, Vol. 131/012301-1, January 2009

[11] Gross, W. A., July 1959, "A Gas Film Lubrication Study, Part 1, some Theoretical Analyses of Slider Bearings," IBM Journal, pp. 237-255.

[12] Navier–Stokes equations.
(https://old.uqu.edu.sa/files2/tiny_mce/plugins/filemanager/files/4282164/Navier.pdf)
[13] Suhas patankar, Numerical heat transfer and fluid flow, pg 80.
[14] The Differential Equations Of Flow
(http://www.columbia.edu/itc/ldeo/lackner/E4900/Themelis5.pdf)
[15] C. Foias, O. Manley, R. Rosa, R. Temam , Navier-Stokes Equations and Turbulence By, pg 83.
[16] Robert J. Bruckner, Performance of Simple Gas Foil Thrust Bearings in Air, National Aeronautics and Space Administration, Glenn Research Center Cleveland, Ohio 44135
[17] Henry A, Putre, Computer Solution Of Unsteady Navier-Stokes Equations For An Infinite Hydrodynamic Step Bearing(1970), NASA TN D-5682
[18] Rayleigh, Lord: Notes on the Theory of Lubrication. Phil. Mag., vol. 35, 1918, pp. 1-12.
[19] Noël Brunetière, Bernard Tournerie, " Finite Element Solution of Inertia Influenced Flow in Thin Fluid Films" Journal of Tribology | Volume 129 | Issue 4, May 30, 2007
[20] Gandjalikhan S. A. Nassab ,Inertia Effect on the Thermohydrodynamic Characteristics of Journal Bearings.
[21] Constantinescu, V., 1970, "On the Influence of Inertia Forces in Turbulent and Laminar Self-Acting Films," ASME J. Tribol., 92(3), pp. 473–480.
[22] Mingfeng Qiu, Brian N. Bailey, Rob Stoll, and Bart Raeymaekers, The accuracy of the compressible Reynolds equation for predicting the local pressure in gas-lubricated textured parallel slider bearings
[23] Hu J, Leutheusser HJ. Micro-inertia effects in laminar thin-film flow past a sinusoidal boundary. J Tribol-T ASME. 1997;119:211–216.

[24] Arghir M, Roucou N, Helene M, Frene J. Theoretical analysis of the incompressible laminar flow in a macro-roughness cell. J Tribol-T ASME. 2003;125:309–318.

[25] S. Acharya, B. R. Baliga, K. Karki, J. Y. Murthy, C. Prakash and S. P. Vanka, Pressure-Based Finite-Volume Methods in Computational Fluid Dynamics, Journal of Heat Transfer | Volume 129 | Issue 4, Jan 07, 2007

[26] T. J. Craft, Density Variation in Finite Volume Schemes.

[27] Robert Eymard, Thierry Gallouët, Raphaèle Herbin, Anthony Michel. Convergence of a finite volume scheme for nonlinear degenerate parabolic equation, Numer. Math. 92, 41-82, 2002.

[28] Salas, M.D. The Curious Events Leading to the Theory of Shock Waves. // NASA Langley Research Center, Invited lecture, 17th Shock Interaction Symposium / Rome, 2006.

[29] Ashford, G. An unstructured grid generation and adaptive solution technique for high-Reynolds-number compressible flows. // Phd thesis / The University of Michigan, 1996.

[30] Ajit Rajesh Desai, Computational Model For Steady State Simulation Of A Plate-Fin Heat Exchanger, The University of Texas at Arlington, December 2015.

[31] Derivation of the Navier–Stokes equations. (https://www.math.ucdavis.edu/~temple/MAT22C/NavierStodesWiki.pdf)

BIOGRAPHICAL INFORMATION

Arvind prabhakar earned his Bachelor in Mechanical Engineering from Manipal Institute of Technology, India, in 2014. He joined University of Texas at Arlington to pursue Masters of Science in Mechanical Engineering in fall 2014. His research interests include numerical modelling of fluid flow, computational fluid dynamics for high speed compressible and viscous flows, heat transfer in turbines and analysis of advanced air cooling schemes (internal channel cooling). During the course of graduate degree at University of Texas at Arlington, he completed an internship at Carollo Engineers.